arXiv:1701.01421v2 [math.GT] 28 Feb 2017

ON THE THE BERGE CONJECTURE FOR TUNNEL NUMBER ONE KNOTS

YOAV MORIAH AND TALI PINSKY

Abstract. In this paper we use an approach based on dynamics to prove that if $K \subset S^3$ is a tunnel number one knot which admits a Dehn filling resulting in a lens space L then K is either a Berge knot, or $K \subset S^3$ is $(1,1)$-knot.

Introduction

One of the main goals of low dimensional topology is to determined which manifolds are obtained by a Dehn filling on knots in the 3-sphere. A major achievement of 3-manifold research in the 80's was the proof by C. Gordon and J. Luecke [13] that if non-trivial surgery on a knot yields S^3 then the knot must be the trivial knot. Just before then was the important positive resolution of the Property R Conjecture by D. Gabai [9], who proved that one can only obtain $S^2 \times S^1$ by 0-surgery on a trivial knot in S^3. That done, a following natural question is:

Question: Which knots in S^3 other than the unknot have non-trivial surgery resulting in a lens space which is not S^3 or $S^2 \times S^1$?

This question was first raised by L. Moser in 1971 in [17]. She determined the surgeries on torus knots yielding lens spaces. Subsequently, Bleiler and Litherland [5], Wang [25] and Wu [27], independently, characterised the surgeries on satellite knots in S^3 which result in lens spaces. The question is still unresolved for hyperbolic knots.

In his celebrated notes, see [24], W. Thurston proved that each hyperbolic knot has only finitely many surgery slopes so that the manifolds obtained by Dehn fillings along these slopes fail to be hyperbolic. (In fact this number is uniformly bounded over all knots.) Since then there was a huge effort by many mathematicians to precisely determine these fillings. As lens spaces are non-hyperbolic, the above question can be viewed as a special case of this huge task.

Date: March 1, 2017.

1991 *Mathematics Subject Classification.* Primary 57M.

Key words and phrases. Berge Conjecture, doubly primitive, Heegaard splittings, lens spaces, genus reducing surgery.

The first author wishes to thank the University of British Columbia UBC for its generous hospitality.

In [3] John Berge compiled a list of twelve families of knots $K \subset S^3$ all of which are tunnel number one knots and all are doubly primitive, (see definitions below). All these knots have surgeries resulting in lens spaces. This list came to be known as the *Berge list* and it includes the known cases of torus and satellite knots. Then, J. Berge asked in 1995 if the list is complete (see [15] Problem 1.78). This question became to be known as *The Berge Conjecture*:

Conjecture 0.0.1 (The Berge conjecture)**.** *Let $K \subset S^3$ be a non-trivial knot which has Dehn surgery resulting in a lens space. Then K belongs to the Berge list.*

A knot $K \subset S^3$ is a *tunnel number one knot* if there is a properly embedded arc (unknotting tunnel) t in $S^3 \setminus \mathcal{N}(K)$ so that $S^3 \setminus \mathcal{N}(K \cup t)$ is a handlebody of genus two.

A knot $K \subset S^3$ is *doubly primitive* if S^3 has a genus two Heegaard splitting (V, W), where V and W are handlebodies, so that K can be isotoped onto the Heegaard surface $\Sigma = \partial V = \partial W$ and there are essential disks $D_1 \subset V$ and $D_2 \subset W$ each of which intersects K in a single point. Such a splitting corresponds to two unknotting tunnels for K. Note that K might have other unknotting tunnels so that K is not doubly primitive in the induced Heegaard splittings of S^3.

Lemma 0.0.2 (Berge)**.** *A knot $K \subset S^3$ is on the Berge list if and only if K is doubly primitive.*

A knot $K \subset M$ is a $(1,1)$-knot if M has a genus one Heegaard surface Σ so that K intersects Σ in two points and the arcs of $K - \Sigma$ are unknotted in the respective solid tori which contain them. A knot $K \subset S^3$ which has surgery giving a lens space L determines a *dual knot* $K^* \subset L$: Namely the core of the surgery solid torus. Berge proves that a knot $K \subset S^3$ is doubly primitive if and only if K^* is a $(1,1)$ in the lens space [3] (see also Williams [26]). Thus, the Berge conjecture can be restated as:

Conjecture 0.0.3. *Let $K \subset S^3$ be a non-trivial knot which has Dehn surgery resulting in a lens space. Then K^* is a $(1,1)$ knot in the lens space.*

The following is the main theorem of this paper:

Theorem 0.0.4. *If $K \subset S^3$ is a tunnel number one knot which admits a Dehn filling resulting in a lens space, then either K or K^* is a $(1,1)$-knot.*

Note that the statement of Theorem 0.0.4 is symmetric with respect to K and K^* unlike the statement in Conjecture 0.0.3.

It is known that many Berge knots cannot be represented as $(1,1)$ knots [7]. Many of them, e.g., the $(-2,3,7)$-pretzel knot, have several unknotting tunnels. A Berge knot can have an unknotting tunnel determining a genus two Heegaard splitting with respect to which it is not doubly primitive. In the proof we assume that K has lens space surgery but is not doubly primitive with respect to some Heegaard splitting. This Heegaard splitting does not change throughout the proof. Thus, the next corollary follows.

Corollary 0.0.5. *A Berge knot K which has an unknotting tunnel yielding a Heegaard splitting of S^3 with respect to which K is not doubly primitive, is a $(1,1)$ knot.*

Strong evidence for the Berge conjecture is J. Green's resolution of the Realization Problem. Namely: If a lens space can be obtained by surgery on a knot in S^3 then such a lens space can be obtained by a knot in the Berge list (see [11, Theorem 1.3]) .

Let $K \subset S^3$ be a knot. We say that K admits *genus reducing surgery* if $S^3 \setminus \mathcal{N}(K)$ has a non-trivial surgery resulting in a manifold M so that $g(M) \leq g(S^3 \setminus \mathcal{N}(K)) - 1$, where $g(X)$ denotes the genus of the manifold X. $\mathcal{N}(\,\cdot\,)$ denotes an *open regular neighborhood* in the appropriate space. It will be called *strongly genus reducing surgery* if $g(M) < g(S^3 \setminus \mathcal{N}(K)) - 1$.

Conjecture 0.0.6 (Strong genus reducing surgery)**.** *The first author conjectures that knots in S^3 do not have strongly genus reducing surgery slopes other than the slope of the meridian.*

If the tunnel number of K is greater than one then $g(S^3 \setminus \mathcal{N}(K)) \geq 3$ and if a lens space M can be obtained by surgery on K then $1 = g(M) < g(S^3 \setminus \mathcal{N}(K)) - 1$. Thus, an affirmative proof of Conjecture 0.0.6 will prove that in order to prove the Berge Conjecture it suffices to prove it for tunnel number one knots.

It is a consequence of the Cyclic Surgery Theorem [8] that if $K \subset S^3$ is a hyperbolic knot only integer slope surgery can yield a lens space. Thus the following weaker conjecture, if true, will show that it is sufficient to prove Conjecture 0.0.1 only for tunnel number one knots:

Conjecture 0.0.7. *No knot $K \subset S^3$ has an integral slope γ, so that γ is a strongly genus reducing surgery slope.*

The Berge conjecture has been studied extensively, e.g., by Berge himself in [3] and [4] also by K. Baker, E. Grigsby, and M. Hedden, see [1], P. Ozsvath and Z. Szabo,

see [19], J. Rasmussen, see [20], T. Saito, see [21], M. Tange, see [22], [23] and others. Connections to $(1,1)$-position have been studied by D. Gabai in [10].

In this paper we take an approach based on dynamics. As the knot $K \subset S^3$ is a tunnel number one knot, the knot space $K \subset S^3$ has a genus two Heegaard splitting. The conditions imposed on the Heegaard splitting because K has a lens space surgery imply that an associated Heegaard diagram of this splitting is too "complicated" to be a Heegaard splitting for S^3 (after trivially filling the knot) unless K is on the Berge list or that K is a $(1,1)$-knot, which proves Theorem 0.0.4. To the best of our knowledge such an approach has not been tried before.

Very little is currently known on either Conjecture 0.0.6 or Conjecture 0.0.7. The only result in this direction was obtained by K. Baker, C. Gordon and J. Luecke who showed in [2, Corollary 1.1] the following:

Corollary:(Baker-Gordon-Luecke) There is a linear function $w : \mathbb{N} \to \mathbb{N}$ with the following property: Let K' be a hyperbolic knot in S^3, $M = K'(p/q)$ where $q \geq 2$, and K is the core of the attached solid torus in M. Let S be a genus g, strongly irreducible Heegaard surface in M. If p/q is not a $(g, 2w(g)-2)$-boundary slope for the exterior of K' then either $brS(K) \leq w(g)$, or M is a Seifert fibered space over the 2-sphere with exactly three exceptional fibers, at least one of which has order 2 or 3.

Here $M = K'(p/q)$ is the manifold obtained by p/q-Dehn surgery on K' and $brS(K)$ denotes the bridge number of K with respect to S. Note that Corollary 1.1 gives a linear bound on the extent to which Heegaard genus can decrease under a non-integral Dehn surgery.

As mentioned above, the situation for non-hyperbolic knots in S^3 is fully understood. For completion we state what is known: The Type I family, in the Berge list, is composed of torus knots and Type II is composed of satellite knots (see [21]). For torus knots L. Moser showed in [17], that an (r,s) surgery on a (p,q)-torus knot results in a lens space if only if $|pqr + s| = 1$, and the lens space obtained is $L(|s|, rq^2)$. The situation for satellite knots was resolved independently by Bleiler and Litherland [5], Wang [25] and Y-Q. Wu [27]. They gave a complete classification of satellite knots with lens space surgery and proved that if a satellite knot K is not a $(2, 2pq \pm 1)$-cable of some (p,q)-torus knot, then nontrivial surgery on K will never yield a manifold with cyclic fundamental group.

Acknowledgements. The authors wish to thank John Berge for important remarks regarding and for pointing out the importance of the papers by T. Homa, M. Ochiai and M. Takahashi [14] and M. Ochiai [18] to the Berge Conjecture. We also wish to thank Dale Rolfsen for his support and Jessica Purcell for helpful remarks.

CHAPTER 1

Preliminaries

In this chapter we describe the setup and the main tools, particularly the theorem by T. Homma, M. Ochiai, and M, Takahashi about Heegaard diagrams for S^3 which we repeatedly use throughout the paper.

1.1. Primitive and doubly primitive

In this section we present some essential definitions and facts:

Definition 1.1.1. Let S be a closed surface. A *compression body* U is a 3-manifold which is the union of $S \times [0,1]$ and a finite collection of 1-handles attached to $S \times \{1\}$. We denote $S \times \{0\}$ by $\partial_- U$ and $\partial U \setminus \partial_- U$ by $\partial_+ U$. We will further assume here that S is connected. The genus of U is the genus of $\partial_+ U$.

Let $K \subset S^3$ be a knot and let (U, W) be a Heegaard splitting for $(S^3 \setminus \mathcal{N}(K))$ with $\partial_- U = \partial(S^3 \setminus \mathcal{N}(K))$. Throughout this paper P will denote an incompressible planar surface which is not a disk in U. We require further that P has a single boundary component on $\partial_+ U$ and $N \geq 1$ boundary components on $\partial_- U$. We denote such a planar surface by P_N or just P if there is no need to specify N.

Definition 1.1.2. For any surface S properly embedded in a compression body U let $\partial_- S$ denote $S \cap \partial_- U$ and $\partial_+ S$ denote $S \cap \partial_+ U \subset \Sigma$. In particular we denote $P_N \cap \Sigma$ by $\partial_+ P$.

The following lemma is well known:

Lemma 1.1.3. *An incompressible planar surface P_N in a compression body U is isotopic into a collection of N vertical annuli, denoted by $\mathfrak{a}_1, \ldots, \mathfrak{a}_N$, which are connected by $N-1$ bands, denoted by $\mathfrak{b}_1, \ldots, \mathfrak{b}_{N-1}$, which are disjoint from $\partial_- U$.*

Proof. Since $\partial_- U$ is connected the compression body U has a structure of a disk sum between a handlebody and $\partial_- U \times I$. Denote the disk by D and consider $P_N \cap D$.

As P_N is incompressible there are no essential simple closed curves in $\{P_N \cap D\}$ and since compression bodies are irreducible we can assume, by choosing D to minimize $|\, P_N \cap D \,|$ that the intersection contains only arcs. An outermost arc of intersection bounds together with ∂D a "bigon" disk in D which is a boundary compression disk for P_N. Successively boundary compressing along all these "bigons" we obtain an incompressible surface in $\partial_- U \times I$ and an incompressible surface in the handlebody component of $U \setminus \mathcal{N}(D)$. Now keep boundary compressing the two surfaces in $\partial_- U \times I$ and the handlebody till we get boundary incompressible surfaces. The only boundary incompressible surfaces in $\partial_- U \times I$ are vertical annuli. As $|\, \partial_- P \,| = N$ the surface in $\partial_- U \times I$ is a collection of N vertical annuli. Now reattach vertical annuli and disks along the boundary compression whenever is possible, and note that the resulting surfaces are still vertical annuli. Given such a compression disk Δ where $\partial\Delta$ is the union of two arcs $\beta \subset P$ and $\sigma \subset \Sigma$. The rectangle $\mathfrak{b} = \beta \times I$ connects two vertical annuli and is therefore a *band*. If a band happens to connect to another band we can slide it till it meets a vertical annulus. Thus boundary compressions correspond to bands connecting the annuli. Since $\partial_+ P$ is a single curve there are exactly $N-1$ boundary compressions corresponding to bands connecting vertical annuli to vertical annuli. □

Denote the $N-1$ boundary compression disks for the bands, by $\{\Delta_1, \ldots, \Delta_{N-1}\}$. We will say that the band $\mathfrak{b}_i$ is *nested* in the band $\mathfrak{b}_j$ if a boundary compression disk Δ_i for $\mathfrak{b}_i$ is contained in a boundary compression disk Δ_j for $\mathfrak{b}_j$. Given a specific embedding of a planar surface $i : P_N \to U$ it is possible that there is more than one such collection of boundary disks and they are perhaps nested. We therefore make the following definition:

Definition 1.1.4. Let P_N, $N \geq 2$ be an embedding of a planar surface in a compression body U. A *band structure* on P_N (or P) is a choice of a spine and $N-1$ boundary compressing disks for P_N in U. Thus, for the rest of the paper by P_N we mean a planar surface with a specific band structure up to isotopy relative to the boundary, unless explicitly said otherwise.

Definition 1.1.5. A knot K in a 3-manifold M is called a:

(i) (P, D)-*knot* if $M^3 \setminus \mathcal{N}(K)$ has a Heegaard splitting (U, W), where U denotes the compression body and W denotes the handlebody, so that U contains a planar surface P with $\partial_+ P$ a single curve which intersects an essential disk $D \subset W$ in a single point.

(ii) (A, D)-*knot* if the conditions in (i) are satisfied and P is an annulus A.

Remark 1.1.6. If one can obtain a lens space by surgery on a non-trivial knot $K \subset S^3$ then K must be a (P, D) knot: We start with a minimal genus Heegaard splitting of genus $g \geq 2$ for $S^3 \setminus \mathcal{N}(K)$ and end up, after surgery, with a lens space which is of genus one. The genus g Heegaard splitting of $S^3 \setminus \mathcal{N}(K)$ induces a genus g Heegaard splitting of the lens space which is reducible by Bonahon-Otal [6]. Since the surgery affects only the compression body in the Heegaard splitting it must contain a planar surface P which becomes part of a reducing pair of disks after the surgery.

We finish this section by proving the following proposition:

Proposition 1.1.7. *Let $K \subset S^3$ be a tunnel number one knot which has lens space surgery. Then K is doubly primitive if and only if K is an (A, D)-knot.*

Proof. If K is doubly primitive then there is a Heegaard splitting (V, W) of S^3 so that K is embedded in $\Sigma = \partial V = \partial W$ and intersects essential disks D_1 in V and D_2 in W in a single point respectively. We can isotope K slightly into the handlebody V where it meets the essential disk D_1 in a single point. So $V \setminus \mathcal{N}(K)$ is a compression body, denoted by U, once $\mathcal{N}(K)$ is removed from V. The isotopy by which K is pushed into V determines an annulus with one boundary component on $\partial_- U$ and the other is the curve K intersecting the disk D_2 in a single point. Thus K has an (A, D)-reducing pair.

Assume that K has an (A, D) reducing pair. Then there is a genus two Heegaard splitting (U, W) of $S^3 \setminus \mathcal{N}(K)$ so that $A \subset U$ is a vertical annulus meeting the disk $D \subset W$ in a single point in $\partial_+ A$. By Dehn filling along the curve $\partial_- A$ we attach the co-core disk of a solid torus J along it's boundary to $\partial_- A$ thus getting a reducing disk pair (D', D). Since K is a tunnel number one knot the resulting manifold is a lens space. By the Cyclic Surgery Theorem (see [8]) only integer surgery on K can yield a lens space. Hence the slope of $\partial_- A \subset \partial(S^3 \setminus \mathcal{N}(K))$ is an integer. Thus we can find an annulus A_1 in $\mathcal{N}(K)$ with one boundary component K, the core of $\mathcal{N}(K)$, and the other $\partial_- A$. Now we can isotope K through the annulus $A \cup A_1$ into $\Sigma = \partial_+ U$. The union $U \cup \mathcal{N}(K)$ is a genus two handlebody V which together with the handlebody W exhibits K as a doubly primitive knot. □

Corollary 1.1.8. *The Berge Conjecture for tunnel number one knots is equivalent to the statement that if $K \subset S^3$ is a tunnel number one knot which has a non-trivial surgery producing a lens space then K is (A, D).*

1.1.1. **Idea of proof.** The intuition behind the proof is as follows: Let $K \subset S^3$ be a tunnel number one knot which has a lens space surgery and let (U, W) be a genus

two Heegaard splitting for $S^3 \setminus \mathcal{N}(K)$, where U is the compression body and W is a handlebody. Doing ∞-surgery (i.e., trivial) on K turns U into a handlebody V and (V, W) is a genus two Heegaard splitting for S^3 (see Figure 1). Since K has lens space surgery, (U, W) contains a (P_N, D)-pair. Where $D \subset W$ is a disk and $P_N \subset V$ is a planar surface. When P_N is not an annulus then the single boundary component $\partial_+ P_N \subset \Sigma$ must be very "complicated". This forces the disk D and the other disjoint meridian disk $E \subset W$, which is also disjoint from $\partial_+ P_N$, to be very "complicated" relative to a meridian system (A, B, C) for V resulting in a "complicated" Heegaard diagram for S^3.

We show that, whenever $N \geq 2$, this "complicated" Heegaard diagram either corresponds to a Berge knot, or, by using a theorem of Homma, Ochiai and Takahashi, [14] about Heegaard diagrams of Heegaard splittings of S^3, is not be a Heegaard diagram of S^3.

More specifically: Operating under the assumption that $N \geq 2$, we consider , in Section 1.2, meridian disks A, B and C for the handlebody V. We show that the disk D must intersect any boundary compressing disk Δ for P_N in at least two points and that any band connecting vertical annuli in P_N must intersect the disk C.

Given a genus two handle body V, a system of meridians $\{v_1, v_2\} \subset V$ and a system of disjoint simple closed curves $\{w_1, w_2\} \subset \Sigma$, where $\Sigma = \partial V$, it is a natural question to ask when such a system determines a Heegaard diagram for S^3? This question was addressed in a fundamental paper by Homma, Ochiai and Takahashi [14]. Their main results are expressed in terms of a Whitedhead graph for a Heegaard splitting. The results of their paper are the stepping stone for present paper.

In Section 1.3, we first recall the definition, of a *Whitehead graph* with respect to the meridional set $\{v_1, v_2\} \subset V$ and a system of meridians $w_1, w_2 \subset W$. We then recall the definition of *waves* as in [14] and quote the Homa-Ochiai-Takahashi result that a genus two Heegaard diagram of S^3 always contains waves with respect to either the meridional system $\{v_1, v_2\}$ or the other set of meridional curves $\{w_1, w_2\} \subset W$ so that after a finite sequence of wave moves on one or the other system we obtain the standard Heegaard diagram for S^3.

By a theorem of Ocihai [18], a Whitehead graph is a graph for a Heegaard diagram of a genus two Heegaard splitting for a 3-manifold M if it is one of the three graphs in Figure 3 satisfying some additional conditions. Corollary 1.3.12 states that the existence of two vertical edges or one horizontal and one diagonal edge in Whitehead graphs with respect to both systems of meridional curves excludes the existence of waves. We refer to these edges as *blocking edges*. Thus the Heegaard diagram in

question cannot be a diagram of S^3 if the total intersection number of $\{v_1, v_2\}$ and $\{w_1, w_2\}$ is greater than two. Corollary 1.3.12, is one of the main technical tools in the paper.

We show that when $N \geq 2$ the curve $\partial_+ P_N$ is "complicated". This implies that the required blocking edges in the Whitehead graphs of the possible Heegaard diagrams, exist and Corollary 1.3.12 can be applied to conclude that the Heegaard diagram is not a Heegaard diagram of S^3 or we have either a Berge knot or a $(1,1)$- knot.

To do this we need to consider all possible planar surfaces $P_N \subset U$ where $N \geq 2$. So in order to build an argument we need some kind of "normal" form for all such planar surfaces.

In Section 2.1 we begin the process of normalizing the planar surface P_N with respect to the meridian systems of curves $\{\alpha = \partial A, \gamma = \partial C\} \subset V$ (see Section 1.2) and $\{\delta = \partial D, \varepsilon = \partial E\} \subset W$.

Cutting the Heegaard surface Σ along $\partial_+ P_N$ results in a twice punctured torus which can always always be described as a union of two annuli connected by two bands emanating from both boundary components of the annuli. We show that one can choose the annuli and bands so that they intersect a complete meridian set, $\{\alpha, \gamma\}$ or $\{\alpha, \beta\}$ for V, in a very particular set of essential arcs only. In Proposition 2.1.6 it is shown that there is a flow on $\Sigma \setminus \partial_+ P$ so that the curves $\{\delta, \varepsilon\}$ are orbits of this flow.

In Sections 2.2 - 2.4 we continue the normalization process and prove that: We can choose a band structure for P_N so that each vertical annulus will be connected to at most two bands. Planar surfaces with such a planar structure will be called *admissible*.

In Section 2.5 we use the fact that P is admissible, proved in Section 2.4, to find a new pair of meridional curves $\{\alpha, \beta\}$ for V with the property that there are no waves with respect to them.

A careful, case by case, analysis in Chapter 3 on the system $\{\delta, \varepsilon\}$ and meridional systems obtained by iterated wave moves on it is done in Sections 3.1, 3.2, 3.3 and 3.4 to finish the proof in Section 3.5.

The reason that this analysis requires so much work is that any time wave moves are done on one of the meridians new waves might appear so one must perform further wave moves till the obtained meridional sets for V and W do not allow waves with respect to each other. If the complexity is higher than two this case results in a contradiction. The only other option left is that $N = 1$ and the proof of Theorem 0.0.4 is complete.

Remark 1.1.9. *We would like to emphasize that throughout the paper the enclosed figures are an essential part of the various proofs and not just schematic illustrations*

for the convenience of the reader. In the figures the δ curve is depicted in red (dark) and the ε curve is depicted in blue (light), throughout.

The complexity of the analysis done in Chapter 3 also provides a heuristic explanation for why this approach to proving the Strong Genus Reducing conjecture seems so difficult at this time. The fundamental obstruction is that unlike the genus two case (as in Theorems 1.3.10 and [18] Theorem 1) we have no idea as to what a genus $g \geq 3$ Heegaard diagram of S^3 looks like. Furthermore, it would require to do the detailed analysis, now done is Sections 2.5, 3.1, 3.2, 3.3 and 3.4 for five curves, to collections of $2g+1$ curves. A daunting task indeed.

1.2. Planar Surfaces in knot complements

In light of the previous section, assume that $K \subset S^3$ is a tunnel number one knot, i.e., $g(S^3 \setminus \mathcal{N}(K)) = 2$. Let Σ be a genus two Heegaard surface for $S^3 \setminus \mathcal{N}(K)$ with (U, W) being the compression body handlebody pair, respectively. Assume further that there is some integer surgery on K which results in a lens space $L = L(p, q)$. Thus $S^3 \setminus \mathcal{N}(K)$ contains a (P, D) reducing pair such that $|\, \partial_- P \,| = N$. Of all such (P, D) pairs choose one which minimizes N. If $N = 1$ the planar surface P is an annulus and K is a Berge knot by Corollary 1.1.8. Hence, from now on and throughout this paper, we assume $N \geq 2$, i.e., K is a (P, D) but not an (A, D) knot.

Let $V \subset S^3$ be the handlebody obtained from U by ∞-Dehn surgery on $\partial_- U$. We next fix a set of three disks in V. Let $C \subset U$ be the unique non separating disk in U. As $K \cap C = \emptyset$ the disk C exists in $V = U(\infty)$. Let $A \subset V$ be a meridional disk intersecting K in a single point depicted in Figure 1. Let $B \subset V$ be an essential non separating disk so that $B \cap K$ is a single point and $B \cap A = \emptyset$. The three disks are shown in Figure 1. By choosing a base point on the disk B the pair of disks $\{A, C\}$ determine a pair $\{x, y\}$ of generators for $F(x, y) = \pi_1(V)$, where A will be a co-core disk for the generator x and C will be a co-core disk for the generator y.

The curves $\alpha = \partial A$, $\beta = \partial B$ and $\gamma = \partial C$ cut the Heegaard surface Σ into two pairs of pants and $V \setminus \{A \cup B \cup C\}$ are two 3-balls $\mathcal{B}^+$, $\mathcal{B}^-$ which we think of as solid pairs of pants. Each of these solid pairs of pants has three distinguished disks on its boundary denoted by$\{A^\pm, B^\pm, C^\pm\}$ respectively. Denote by $\alpha^\pm = \partial A^\pm$, $\beta^\pm = \partial B^\pm$ and $\gamma^\pm = \partial C^\pm$ respectively. There is an additional disk in V denoted by $\beta^\perp$ which is perpendicular to β, intersects it in a single arc and is a separating disk for V.

Claim 1.2.1. *Let $\Delta \in \{\Delta_1, \ldots, \Delta_{N-1}\}$ be a boundary compression disk for $P \subset V$. Then the intersection of ∂D with Δ contains at least two points.*

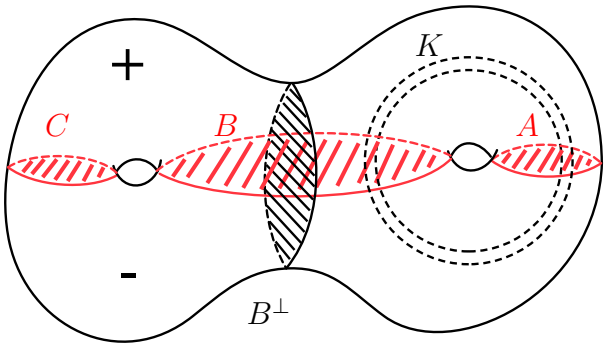

FIGURE 1. The four disks in V

Proof. In light of Lemma 1.1.3 we may think of P as a union of N vertical annuli $\mathfrak{a}_1, \ldots, \mathfrak{a}_N$ and connected by $N-1$ bands $\mathfrak{b}_1, \ldots, \mathfrak{b}_{N-1}$ which are boundary compressible. By the choice of P there is no outermost compression disk that does not meet D. As otherwise we could boundary compress P and choose the component containing the intersection point with D to obtain a planar surface with fewer boundary curves on $\partial_- U$ than N. If there is an outermost disk Δ so that $|\,\Delta \cap D\,| = 1$ then after doing the boundary compression there we obtain two planar surfaces P^1, P^2 each with $|\,\partial_- P^i\,| < N$, $i = 1, 2$, and one of $\partial_+ P^i$ meets D in a single point. □

Definition 1.2.2.
(i) A band $\mathfrak{b}_i$ in P will be called an *interior band* if the boundary compression disk Δ_i, as in Lemma 1.1.3, cannot be isotoped into the disk C.

(ii) A vertical annulus $\mathfrak{a}_i$ will be called an *external annulus* if it is connected to a single band. Note that P_N must have at least two external annuli. A non-external annulus will be called an *internal annulus*.

Lemma 1.2.3. *P has no interior bands.*

Proof. Assume in contradiction that P does have an interior band $\mathfrak{b}_i$. Cut U along the disk C. The result is homeomorphic to $T^2 \times I$. The components of the surface $(P \setminus C) \subset T^2 \times I$ are not all vertical annuli because of the interior band $\mathfrak{b}_i$. Hence we have a vertical annulus $\mathfrak{a}$ (which is not part of P) which meets $P \setminus C$ in trivial arcs on $\mathfrak{a}$ some of which will correspond to boundary compression disks for the internal bands. These trivial arcs all have their boundary on $\partial_+ \mathfrak{a}$. An innermost such arc i.e., the one closest to $\partial_- \mathfrak{a}$, which must correspond to an interior band as well, gives rise to a *compressing* disk Δ for P which meets the corresponding innermost band in two

arcs (see Figure 2). Compressing P along Δ results in a new planar surface P' so that $\partial_+ P' = \partial_+ P$ but $|\partial_- P'| = N - 2$ in contradiction to the choice of P. □

Corollary 1.2.4. *The planar surface P must intersect the disk C.* □

Corollary 1.2.5. *The intersection $C \cap P$ contains only arcs and $C \cap D$ contains at least four points.*

Proof. If $C \cap P$ contains a simple closed curve it must bound a disk on C, then using cut and paste techniques, we either reduce the intersection $C \cap P$ using the fact that compression bodies are irreducible or can obtain a new planar surface P' with the same boundary curve on Σ and smaller $|\partial_- P|$ in contradiction to the choice of P. Any outermost arc of intersection on C defines a boundary compression disk $\Delta \subset C$ for P. As there are at least two boundary compression disks the statement follows now from Claim 1.2.1. □

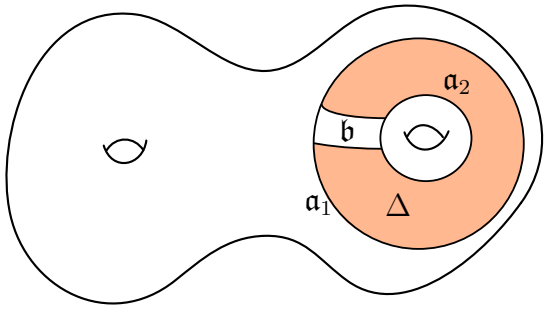

FIGURE 2. The disk Δ intersecting the innermost band b in two arcs. It is a compressing disk for P. The innermost band b connects the vertical annuli $\mathfrak{a}_1$ and $\mathfrak{a}_2$.

1.3. Meridional disks and Whitehead graphs

1.3.1. **Meridional disks.** Given the (P, D) pair we now choose a pair $\{D, E\}$ of disjoint meridional disks for the handlebody W as follows: D is the disk which intersects P in a single point denoted by X. The Heegaard splitting (U, W) of $S^3 \setminus \mathcal{N}(K)$ induces a reducible genus two Heegaard splitting (V', W) of the lens space L after surgery on K. It induces a genus one Heegaard splitting (H_1, H_2) of $L = L(p, q)$ after removing a regular neighborhood $\mathcal{N}(P)' = P' \times [0, 1]$ from V' and attaching it to W. The disk

P' is obtained from the planar surface P by attaching disks to $\partial_- P$. We choose E to be a meridional disk of the obtained solid torus H_2 which is disjoint from $D \cup \partial\mathcal{N}(P')$. The components of $C \setminus \mathcal{N}(P)' = C \setminus \mathcal{N}(P)$ are all isotopic to a meridian disk Q of H_1. We conclude that each component intersects E algebraically the same number of times $p \geq 2$.

Remark 1.3.1. Since we assumed that after Dehn surgery on K we obtained the lens space $L(p,q)$, the integral surgery coefficient must be $p/1$ as can be seen from the homology of the space.

Remark 1.3.2. To simplify the figures throughout the paper we always depict V, the genus two handlebody obtained from U by ∞-surgery on K, as "standardly" embedded in S^3. Cut V along C to obtain a solid torus with two marked disks $C^{\pm}$ on its boundary. Thus the curves $\partial_+ \mathfrak{a}_i$, $i = 1, \ldots, N$, belong to exactly two families of curves up to isotopy rel C^+, C^-. Since the curves $\partial_- \mathfrak{a}_i$, $i = 1, \ldots, N$, correspond to integer slopes we can twist the Heegaard diagram determined by $\{A, C\}$ and $\{D, E\}$ along $\alpha = \partial A$ and $\beta = \partial B$ so that any particular one of the isotopy classes is represented by a "standard" curve embedded in $\partial_+ V$ which is standardly embedded in S^3. In particular we may assume that there is an external annulus standardly embedded. This can be done without changing the fact that these are Heegaard diagrams for S^3.

Lemma 1.3.3. *Let V_1 be a meridian of V which intersects K in a single point. If there is a meridian of W which intersects V_1 either once or not at all then K is a $(1,1)$-knot.*

Proof. If a meridian W_1 of W intersects V_1 once then K is μ-primitive which is equivalent to being $(1,1)$-knot (see e.e. [16]). Assume W_1 does not intersect V_1. Then when we consider W as a standardly embedded genus two handlebody in S^3 the meridian μ of K is isotopic to a curve $\alpha = \partial V_1$ on $\Sigma = \partial V$ which misses the meridian W_1. Adding the disk W_1 to V results in a manifold with torus boundary. The second meridian W_2 in a meridional system of W bounds a curve on this torus hence it is unknotted. Thus α is a (p,q)-torus knot on an unknotted solid torus in S^3. If $p \neq 1$ then after filling in the meridian we obtain a lens space different than S^3 which is a contradiction. If $p = 1$ then $|\, \alpha \cap W_2 \,| = 1$ thus K is μ-primitive. □

Assumption 1.3.4.

(1) From now on we assume that $K \subset S^3$ is *not* a $(1,1)$- knot.

(2) With the above notation, given a minimal N, choose a triplet $\{P_N, D, A\}$ so that the sum of mutual intersections of $\partial_+ P_N, \delta = \partial D, \alpha = \partial A$ and $\gamma = \partial C$

is minimal. Of all possible minimal triplets $\{P_N, D, A\}$ choose a quadruple $\{P_N, D, A, E\}$ so that $\varepsilon = \partial E$ has minimal intersection with α and γ.

Lemma 1.3.5. *Let (V, W) be a Heegaard splitting for S^3 and let $\{A, C\}$ and $\{D, E\}$ be meridional sets for V and W respectively. The pair of free homotopy classes of $\delta = \partial D$ and $\varepsilon = \partial E$ normally generate $F(x, y)$. In particular $\{[\delta], [\varepsilon]\}$ generate $H_1(V)$.*

Proof. Note that (V, W) is a Heegaard splitting for S^3. Hence after adding a neighborhood of D to H we obtain a manifold $N = V \cup \mathcal{N}(D) \subset S^3$ which is a knot space in S^3. Since $\varepsilon = \partial E$ is disjoint from $\delta = \partial D$ it is contained in $\partial N = T^2$. After adding $\mathcal{N}(E)$ to N we obtain a manifold $\widehat{N} = S^3 \setminus B^3$. In particular $\pi_1(\widehat{N})$ is the trivial group and thus $F(x, y) = \pi_1(V)$ is normally generated by δ and ε as required. □

1.3.2. **Whitehead Graphs.** Let (Σ, V, W) be a genus two Heegaard splitting of a 3-manifold M. Let $\hat{V} = \{V_1, V_2\}$ and $\hat{W} = \{W_1, W_2\}$ be *complete meridian sets* respectively. That is, each is a pair of essential disks so that $V \setminus \hat{V}$ and $W \setminus \hat{W}$ are 3-balls. The boundary of the 4-punctured sphere $S = \Sigma \setminus \{v_1 = \partial V_1, v_2 = \partial V_2\}$ consists of four components $\{v_1^+, v_1^-, v_2^+, v_2^-\}$. By cutting Σ along $\widehat{V} = \{v_1, v_2\}$ the curves $\widehat{W} = \{w_1, w_2\}$ are cut into a collection of arcs.

A Heegaard diagram $(\Sigma, \widehat{V}, \widehat{W})$ for some 3-manifold M is said to be *normal* if no domain in $\Sigma \setminus \{\widehat{V} \cup \widehat{W}\}$ is a bigon. We can always assume that the diagram is normal after tightening by an isotopy.

Definition 1.3.6 (Genus two Whitehead graphs)**.** The graph $\Gamma(\{v_1, v_2\})$ obtained, as above, by setting $\{v_1^+, v_1^-, v_2^+, v_2^-\}$ to be vertices and the arcs of $\{w_1, w_2\} \setminus \{v_1, v_2\}$ to be edges is called the *Whitehead graph* corresponding to $\{v_1, v_2\}$. Similarly we have the Whitehead graph $\Gamma(\{w_1, w_2\})$ corresponding to $\{w_1, w_2\}$.

Ochiai states in [18, Theorem 1], that any Whitehead graph of a genus two Heegaard diagram of a 3-manifold is isomorphic as a planar graph to one of the three graphs $(i), (ii)$ or (iii) in Figure 3 below, where the integers $a,\ b, c$ and d represent the number of parallel arcs corresponding to each graph edge.

Definition 1.3.7.
(1) A *standard wave* ζ with respect to a closed curve κ on a surface Σ is a simple arc so that $\zeta \cap \kappa = \partial\zeta$, the arc ζ intersects κ from the same side and ζ is not homotopic into a sub-arc of κ rel $\partial\zeta$.

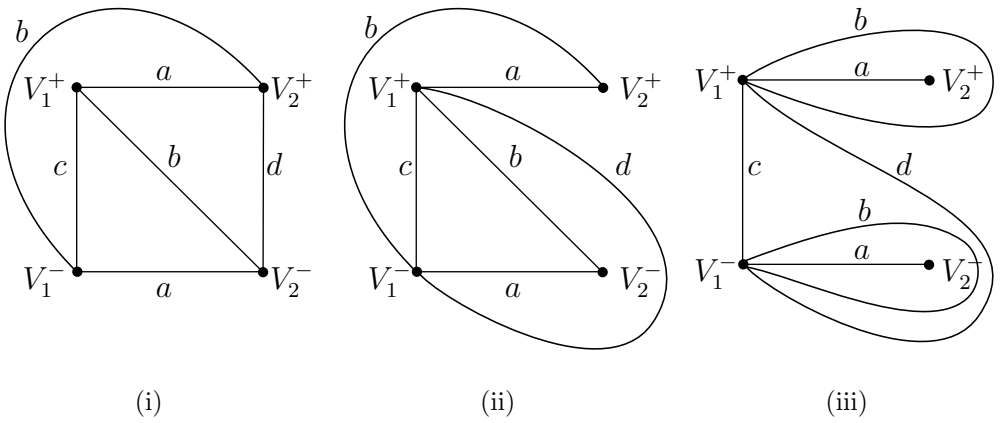

FIGURE 3. The three graphs given in [18].

(2) When Σ is the boundary of a genus two handlebody V with a fixed meridian system $\{v_1, v_2\}$ a standard wave ζ with respect to v_i is called an *s-wave* if $\zeta \cap v_j = \emptyset$.

(3) Assume $\widehat{V}$ and $\widehat{W}$ are oriented. An s-wave $\eta \subset \Sigma$ with respect to a meridian $v_i \subset \widehat{V}$ is called a *shortcut* with respect to v_i if the number of intersections of η with $\widehat{W}$ is strictly less than the number of intersections of $\widehat{W}$ with each of the two sub-arcs of $v_i \setminus \eta$. A shortcut η with respect to v_i satisfying $int(\eta) \cap \widehat{W} = \emptyset$ is called a *wave* with respect to v_i.

Definition 1.3.8. In case there exists an s-wave η with respect to v_i each of the three boundary components of $\mathcal{N}(v_i \cup \eta)$ bounds a disk in V, since $int(\eta) \cap \widehat{V} = \emptyset$. If V is of genus two we necessarily have two of the boundary components homotopic to the meridional curves in $\widehat{V}$, while the third component is the boundary of a new disk. We call the operation of replacing V_i in $\hat{V}$ by the new disk the *shortening* of v_i along η, or a *wave move* with respect to v_i along η. Note that if η is a shortcut then the new disk has less intersection points with $\widehat{W}$.

Remark 1.3.9. Since we are assuming throughout that the handlebodies V and W are of genus two the condition on the number of intersection points assures that exactly one of the boundary components $\mathcal{N}(v_i \cup \eta)$ will be isotopic to v_i. One of the other components will therefore be isotopic to v_j with $j \neq i$, and therefore the shortening, which is the third boundary component, will be a non separating disk as both of v_i and v_j are on the same side that component.

The main theorem of Homma, Ochiai and Takahashi in [14] states:

Theorem 1.3.10 (Homma, Ochiai, Takahashi)**.** *Any genus 2 Heegaard diagram for S^3 is either standard or is reducible, i.e., contains a wave.*

Definition 1.3.11. Define the *Heegaard complexity* of a Heegaard diagram to be the minimal total geometric intersection number of representative curves in the isotopy classes of the curves in the diagram.

Define the complexity of a curve $\eta \subset \Sigma$ to be $min\{|\eta \cap \widehat{V}|\}$. The complexity will be denoted by $c(\eta)$. A curve η is *shorter* than a curve μ if it is of smaller complexity.

Now Theorem 1.3.10 can be rephrased as:

Theorem (Homma, Ochiai, Takahashi). *A non standard diagram always contains a wave, and any wave move will reduce the Heegaard complexity.*

Note that the complexity of a standard Heegaard diagram for a genus two Heegaard splitting of S^3 is two. As an immediate application of Theorem 1.3.10 we get:

Corollary 1.3.12. *If $\hat{V} = \{V_1, V_2\}$ and $\hat{W} = \{W_1, W_2\}$ are complete meridian sets for a genus two Heegaard splitting (V, W) for a 3-manifold M and the Whitehead graph of $\Gamma(\widehat{V})$ has edges connecting the vertices as in one of the following cases:*

(1) v_1^+ to v_1^- and v_2^+ to v_2^-, or

(2) v_1^+ to v_2^+ or v_1^- to v_2^- and one of v_1^+ to v_2^- or v_1^- to v_2^+

Then the Heegaard diagram $(\widehat{V}, \widehat{W})$ contains no waves with respect to $\widehat{V}$.

Proof. Since this is a Heegaard diagram of a 3-manifold, Theorem 1 of [18] applies and the Whitehead graph is as in Figure 3. For case (1) an edge between v_i^+ to v_i^- prevents a wave with respect to v_j, $i \neq j$, $i, j \in \{1, 2\}$.

For case(2) suppose we have the edges v_1^+ to v_2^+ and v_1^+ to v_2^-. Then we cannot have a wave with respect to v_1^- and v_2^+ . Since the Whitehead graph is symmetric with respect to v_i^+ and v_i^- , $i = 1, 2$, we cannot have waves at all.

Note that having edges v_1^+ to v_2^- and v_2^- to v_2^+ is not sufficient as by changing the orientation of one of the curves the pattern becomes as in graph (iii) and the conclusion does not follow. □

Definition 1.3.13. If the Whitehead graph of the Heegaard diagram of a Heegaard splitting $(\widehat{V}, \widehat{W})$ contains edges as either in Case (1) or Case (2) of Lemma 1.3.12 we say the Heegaard splitting has *blocking edges* with respect to V.

As a consequence of the Minimality assumption 1.3.4 we have:

Proposition 1.3.14.

(1) Any shortcut with respect to ε must intersect $\partial_+ P$, and

(2) For any ε so that $\{\delta, \varepsilon\}$ is a complete set of meridians, there can be no shortcut η with respect to δ so that $|\, \eta \cap \partial_+ P \,| \leq 1$. Moreover,

(3) Any arc τ with endpoints on the same side of δ will divide δ into two arcs: δ' and δ'', so that $|\, \delta' \cap \partial_+ P \,| = 1$ and $|\, \delta'' \cap \partial_+ P \,| = 0$. If $|\, \tau \cap \partial_+ P \,| = 1$ then $c(\tau) \geq c(\delta')$ and if $|\, \tau \cap \partial_+ P \,| = 0$ then $c(\tau) > c(\delta'')$.

Proof. The proof is an immediate application of the definitions once we note for (3) that otherwise either $\tau \cup \delta'$ or $\tau \cup \delta''$ is a simple closed curve with a single intersection point with $\partial_+ P$. Thus $\tau \cup \delta'$ and $\tau \cup \delta''$ are non-separating and we can replace δ by one of them to reduce the complexity. □

CHAPTER 2

Planar surfaces in genus two handle bodies

In order to deal with possible Heegaard diagrams we need to have a canonical form for the bounded surface $\Sigma \setminus \partial_+ P$. This is done in this chapter and it is also shown that all planar surfaces in a reducing pair (P_N, D) are admissible, namely they intersect standard meridians $\{\alpha, \beta, \gamma\}$ of the handlebody V in a "nice"way.

2.1. Fixing the decomposition of $\Sigma \setminus \partial_+ P$

Throughout the paper when we write $\Sigma \setminus \partial_+ P$ we mean $\Sigma \setminus \mathcal{N}(\partial_+ P)$.

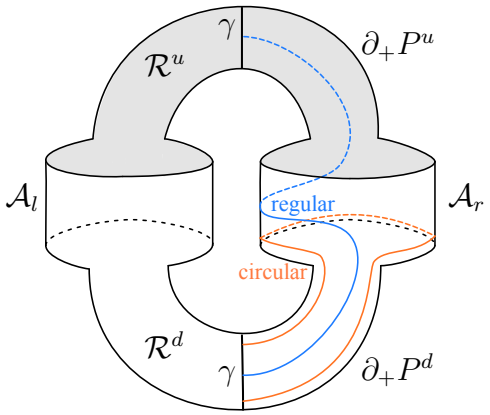

Figure 4. Regular and circular arcs

The boundary components of $\Sigma \setminus \partial_+ P$ are denoted by $\partial_+ P^u$ and $\partial_+ P^d$. A twice punctured torus can always be described as a union of two annuli $\mathcal{A}_r$ and $\mathcal{A}_l$ connected by two rectangles $\mathcal{R}^u$ and $\mathcal{R}^d$, as in Figure 4. The core curves of the annuli are denoted by $\mathfrak{a}_r$ and $\mathfrak{a}_l$ respectively, and the edges of the rectangle $\mathcal{R}^i$, $i \in \{u, d\}$ which are in the intersection with $\mathcal{A}_r$ and $\mathcal{A}_l$ will be denoted by $\mathcal{R}^i_l$ and $\mathcal{R}^i_r$.

Cutting Σ along $\partial_+ P$ and then along the rectangle edges $\mathcal{R}^i_l$ and $\mathcal{R}^i_r$, $i \in \{u, d\}$, will cut δ into a collection of sub-arcs. The image of the point X in $\partial_+ P^d$ ($\partial_+ P^u$) will be denoted by X^d (X^u respectively). Since $\varepsilon \cap \partial_+ P = \emptyset$ the curve ε is contained in the interior of $\Sigma \setminus \partial_+ P$.

Sub-arcs of δ and ε through one of the annuli which have both endpoints on the same edge of some rectangle will be called *circular arcs*. Arcs in δ and ε are called *regular arcs* if they do not contain circular sub-arcs (see Figure 4).

Arcs in the rectangles which are parallel to the boundary edges on which the rectangles are glued to the annuli will be called *co-core arcs in the rectangles*, and an an arc isotopic to an arc connecting $\mathcal{R}^i$ to $\mathcal{R}^j$ through an annulus will be called a co-core of the annulus. The co-cores of the annuli are not uniquely determined by the decomposition, but we would like to fix them as part of our description of $\Sigma \setminus \mathcal{N}(\partial_+ P)$.

One of the goals of this section is to show that for any planar surface $P_N, N \geq 2$ there is such a decomposition so that:

(1) Sub-arcs of γ and α are co-core arcs of the annuli $\mathcal{A}_r$ and $\mathcal{A}_l$ and rectangles $\mathcal{R}^u$ and $\mathcal{R}^d$.

(2) The curves δ and ε contain no circular sub-arcs.

(3) Each of the rectangles has at least one sub-arc of γ.

These γ-arcs are also depicted in Figure 4.

Lemma 2.1.1. *The rectangle-annulus decomposition of $\Sigma \setminus \partial_+ P$ in Figure 4 can be chosen so that all segments of $\alpha \cup \gamma \setminus \partial_+ P$ are co-core arcs. Furthermore, in each of the rectangles there is a γ segment which is a co-core arc for the rectangle.*

Proof. By Corollary 1.2.4 $P \cap C \neq \emptyset$ hence there is an outermost arc of intersection ρ on C. The other boundary arc of the boundary compression disk is an arc κ_1 of $\gamma \setminus \partial_+ P$ that connects the same sides of P, say, $\partial_+ P^d$ to itself. As γ is a closed curve we are guaranteed to have another arc κ_2 of $\gamma \setminus \partial_+ P$ that connects $\partial_+ P^u$ to itself.

Consider a regular neighborhood $\mathcal{N}(\kappa_1)$ of the arc κ_1 in $\Sigma \setminus \partial_+ P$ and expand $\mathcal{N}(\kappa_1)$ along the $\partial_+ P$-arcs to both sides of C as follows:

Extend the sub-arcs of $\mathcal{N}(\kappa_1) \cap \partial_+ P$ separately on both sides till they both meet α or γ. If κ_1 union $\partial_+ P$-arcs union α (or γ) sub-arcs bounds a rectangle on Σ add a neighbourhood of the rectangle to $\mathcal{N}(\kappa_1)$. If this domain is not a rectangle stop. Continue with this process on both sides of κ_1 to obtain a maximal such extension. Perform the same operation on κ_2. We have defined two rectangles with co-core arcs which are parallel segments of γ and perhaps α. The complement of these rectangles in $\Sigma \setminus \partial_+ P$ is a pair of annuli as can be seen by removing two arcs from a twice punctured torus connecting each boundary component to itself. If the annuli intersect α or γ we choose the segments on α and γ to be the co-core curves of the annuli. Note that the co-cores of the annuli connect $\partial_+ P^d$ to $\partial_+ P^u$. This gives the required decomposition. $\square$

Lemma 2.1.2. *Given the set of meridians $\widehat{V} = \{\alpha, \gamma\}$ for V then any wave move for α through a wave ω in the complement of $\partial_+ P$ results in a disk A^1 which intersects the knot K once. There is always a homeomorphism of V taking A^1 to A so that some of vertical annuli are still "straight".*

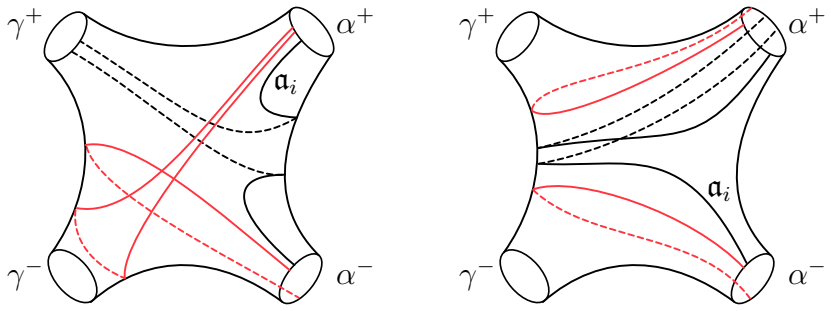

FIGURE 5. The possible α waves in the complement of an external annulus and the band it connects to.

Proof. Since $\omega \cap P = \emptyset$ by assumption then ω does not intersect a standard external annulus in P which exists by Remark 1.3.2. As we have the freedom of twisting around $B^\perp$ there is a unique choice of a disk B up to a half twist in $\beta^\perp$ so that the band of the external annulus does not twist around $\beta^\perp = \partial B^\perp$.

Consider the four punctured sphere $\Sigma^* = \Sigma \setminus (\alpha \cup \gamma)$ and the sub-arc in $\partial_+ P$ consisting of this external annulus with its band. The band can either connect to C as shown in Figure 5(i) or to A as shown in Figure 5(ii).

If the band connects the external annulus directly to, say, γ^+ then we have seams connecting α^+ to γ^+ and α^- to γ^+. (A *seam* is an arc in a surface connecting two different boundary components.) These seams prevent every wave except one for each of α^+ and α^- as can be seen in Figure 5(i). The wave move replaces A by a disk isotopic to B or B with a half twist in $B^\perp$ which intersects K in a single point. A similar argument holds when the band connects to γ^-.

If the band connects a straight external annulus directly to α^+ we get an α^+ to α^- seam which prevents waves from winding around β see Figure 5(ii). Note that in this case there are two waves with respect to α^+ and one with respect to α^-. Hence after the wave move we obtain a disk intersecting K is a single point isotopic to B. Similar arguments hold when the band connects to α^-. Twisting about a half twist of $\beta^\perp$ does effect the "straightness" of the annuli. So the required homeomorphism is the one switching A and B. □

Remark 2.1.3. Note that in the proof of Lemma 2.1.2 we show that it is enough to require only that a wave does not intersect a single external annulus with its band.

Lemma 2.1.4. *Let $\widehat{V} = \{\alpha, \gamma\}$ and $\widehat{W} = \{\delta, \varepsilon\}$ be meridian curves as before. The curves δ and ε do not contain sub-arcs which are waves with respect to α or γ.*

Proof. Assume that there is a sub-arc ω of δ or ε which is a wave with respect to α. The wave ω intersects $\partial_+ P$ at most once. Hence there is an external annulus with its band which ω does not intersect. It now follows from Lemma 2.1.2 that changing α by this wave move results in a meridional disk which intersects K in a single point but has less intersection points with δ and ε this is contradiction to the minimality assumption 1.3.4.

We now prove that δ and ε contain no waves with respect to γ. Assume in contradiction that there is a wave ω with respect to γ meeting γ from the, say, γ^- side so that $\omega \subset \{\delta \cup \varepsilon\}$ as a sub-arc. This implies (by Theorem 1 of [18]) that the Whitehead graph $\Gamma(\alpha, \gamma)$ is a graph of type (iii), as in Figure 3 with $b > 0$. It follows from the symmetry of the graph that there is a second wave ω^*, with respect to γ^+, contained as a sub-arc either in δ or in ε. Let $\mathfrak{a}$ be an external annulus of P. It cannot happen that both ω and ω^* meet $\mathfrak{a}$ or the part of its band up to γ as this would imply that $|\{\delta \cup \varepsilon\} \cap \partial_+ P| \geq 2$ in contradiction.

Hence we can assume that, say, ω does not meet $\mathfrak{a}$ or its band. By Definition 1.3.7 we have $\mathring{\omega} \cap \widehat{V} = \emptyset$. One can check that the only two possibilities for such a wave ω are shown as ω_1 and ω_2 in Figure 6. Note that both can occur only if the band is as shown in the figure. Furthermore note that any wave with respect to γ^+ must intersect either $\mathfrak{a}$ or its attaching band.

Thus the pair $\{\omega, \omega^*\}$, must have an intersection point with each external annulus of P or its corresponding band as can be seen from Figure 6. However P has at least two external annuli, while $\delta \cup \varepsilon$ can have no more than one intersection point with P. It follows that there are no such waves with respect to γ. □

In particular we have proved:

Corollary 2.1.5.

(1) Any wave with respect to α' must intersect $\partial_+ P$ in at least two points.

(2) Any pair of dual waves $\{\omega, \omega^*\}$ with respect to γ must intersects $\partial_+ P$ at least twice. □

We now prove:

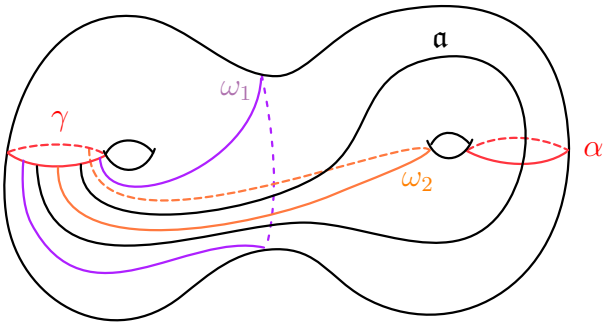

FIGURE 6. Two possible waves, not intersecting an external annulus $\mathfrak{a}$. If the band is attached to $\mathfrak{a}$ in any other way, the waves will have to intersect it.

Proposition 2.1.6. *The curves δ and ε contain only regular sub-arcs.*

Proof. First note that by Lemma 2.1.1 we can assume that we have a decomposition of $\Sigma \setminus \partial_+ P$ as depicted in Figure 4 for a general planar surface P. Hence the term *regular arc* has a concrete meaning. If, say, δ (or ε) contains a circular arc we can elongate it at both endpoints in one of the rectangles so that it meets some sub-arc of γ or α which is contained in each of the rectangles $\mathcal{R}^u$ and $\mathcal{R}^d$ by Lemma 2.1.1. This is true unless the continuation of the sub-arc of δ contains the intersection point X. In this case we isotope δ out of the rectangle without changing the intersection pattern and we eliminate this case.

Thus we have an arc connecting the same side of γ or α to itself, say γ^+ to γ^+. Denote an innermost such arc by τ. If τ does not have other intersection points with γ or α in between, τ is a wave. But, by Lemma 2.1.4 the curves δ and ε contain no waves with respect to γ or α'. Hence τ must intersect α in its interior. These intersections with α have the same orientations (otherwise τ contains a wave so it is not innermost).

The previous paragraph shows that τ must have two sub-arcs, one connecting γ^+ to α^-, and the other connecting γ^+ to α^+. Thus, the Whitehead graph $\Gamma(\alpha, \gamma)$ contains the blocking edges $[\gamma^+, \alpha^+]$ and $[\gamma^+, \alpha^-]$ and hence by Corollary 1.3.12 there can be no wave with respect to α or γ. The same argument works when we assume that δ or ε have circular arcs connecting γ^- to γ^-.

On the other hand, the elongated circular arc in δ also implies that γ has a sub-arc η in one of the rectangles connecting the same side of δ to itself, say δ^+ to δ^+, that does not intersect $\partial_+ P$. We may assume that η is an innermost such arc and hence does not meet δ in its interior. As if it did it would be possible to choose a shorter

sub-arc η connecting δ^+ to δ^+. The arc η must intersect ε, as otherwise there would be a wave not intersecting $\partial_+ P$ with respect to δ, contradicting the minimality of δ. All intersection points of η with ε must have the same sign, as otherwise there will be a wave with respect to ε, parallel to η and not intersecting $\partial_+ P$, contradicting the minimality of ε. Thus, there are sub-arcs of γ (and η) connecting δ^+ both to ε^+ and to ε^-. Hence the Whitehead graph $\Gamma(\delta, \varepsilon)$ contains the blocking edges $[\delta^+, \varepsilon^+]$ and $[\delta^+, \varepsilon^-]$ and it follows from Corollary 1.3.12 that there are no waves with respect to $\{D, E\}$. Since there are no waves with respect to both V and W and by Corollary 1.2.5 the number of intersection points is at least four this is not a Heegaard diagram oft S^3 by Theorem 1.3.10. The same argument shows that there are no circular arcs on ε. □

Lemma 2.1.7. *An innermost band is contained in one of the rectangles $\mathcal{R}^u$ or $\mathcal{R}^d$. Furthermore each of $\mathcal{R}^u$ and $\mathcal{R}^d$ contains at most one innermost band. The curves δ and ε meet both rectangles essentially. In particular, they each intersect the co-core curves of $\mathcal{R}^u$ and $\mathcal{R}^d$ at least twice.*

Proof. The sub-arc of $\gamma = \partial C$ in the boundary of a compression disk of an innermost band is a co-core arc in the decomposition of $\Sigma \setminus \partial_+ P$ into $\mathcal{A}_l \cup \mathcal{R}^d \cup \mathcal{A}_r \cup \mathcal{R}^u$. Since it connects either $\partial_+ P^u$ to itself or $\partial_+ P^d$ to itself it must be contained in one of the rectangles $\mathcal{R}^u$ or $\mathcal{R}^d$, say $\mathcal{R}^d$.

If $\mathcal{R}^d$, contains two innermost bands then the region in $\mathcal{R}^d$ between them can be pushed slightly to a disk Δ in the compression body U with boundary in P so that $\partial\Delta$ is composed of four arcs. Two arcs in ∂P_+ connected by two arcs in P itself. If $\partial\Delta$ bounds a disk in P then the two innermost bands are actually a single band. If $\partial\Delta$ is a non-trivial loop in the planar surface P then the disk Δ is a compression disk for P in contradiction to the minimality of N. Thus $\mathcal{R}^d$ contains a single innermost band. Therefore by Claim 1.2.1 there are at least two δ sub-arcs which meet $\mathcal{R}^d$ essentially.

The only way that X^d can be connected to X^u, so that the intersection of δ with $\mathcal{R}^u$ or in $\mathcal{R}^d$ cannot be simplified is if δ goes through both $\mathcal{R}^d$ and $\mathcal{R}^u$. As δ intersects $\mathcal{R}^d$ twice it must also intersect $\mathcal{R}^u$ twice as well

Since an innermost compression disk on C corresponds to a rectangle, say $\mathcal{R}^d$, and each innermost compression disk is isotopic to a meridional disk Q for H_1 (see beginning of Section 1.3) which meets E at least $p \geq 2$ times then so does $\mathcal{R}^d$. But that implies that so does $\mathcal{R}^u$ as ε is a closed curve and there are no circular arcs. □

2.2. The δ, ε and $\partial_+ P$ curves

Endow $\Sigma \setminus \partial_+ P$ with the structure from Lemma 2.1.1. Therefore, we have a decomposition of $\Sigma \setminus \partial_+ P$ as two annuli and two rectangles $\mathcal{A}_r \cup \mathcal{R}^u \cup \mathcal{A}_l \cup \mathcal{R}^d$.

Remark 2.2.1. This surface, as in Figure 4 has the following symmetries:

(1) A reflection in a vertical plane cutting through the "middle" of the figure. It interchanges the annulus on the right $\mathcal{A}_r$ with the annulus on the left $\mathcal{A}_l$.

(2) Rotation in a horizontal axis. It interchanges $\mathcal{R}^u$ with $\mathcal{R}^d$.

(3) A reflection in a cylinder which meets each of $\mathcal{R}^u$ and $\mathcal{R}^d$ in a core arc and each of $\mathcal{A}_r$ and $\mathcal{A}_l$ in co-core arcs connecting the arcs of the rectangles. This symmetry exchanges the notions of "right" and "left" within each of the annuli and each of the rectangles.

Two sub-arcs in $\Sigma \setminus \partial_+ P$, are said to be *parallel* if they intersect the same α and γ segments in $\Sigma \setminus \partial_+ P$ in identical sequences. Two sub-arcs intersecting in a point are said to be *tight on one side* if they have no parallel initial segments on one side of the intersection point and *tight on two sides* if they have no parallel initial segments on both sides of the intersection point.

Note that the intersection point $X = \delta \cap \partial_+ P$ can be chosen so that δ and $\partial_+ P$ are tight to one side, since δ and $\partial_+ P$ are not parallel. Therefore, given the decomposition $\mathcal{A}_r \cup \mathcal{R}^u \cup \mathcal{A}_l \cup \mathcal{R}^d$ we can assume, using the first two symmetries in Remark 2.2.1, that the intersection point X is located in $\mathcal{A}_r \cap \partial P^u$ and δ and∂P^u are tight in $\mathcal{A}_r$. It will be denoted there by X^u. The location of X on $\partial_+ P^d$ depends on the identification of $\partial_+ P^d$ with $\partial_+ P^u$. That point will be denoted by X^d and we cannot assume it is tight with respect to $\partial_+ P^d$.

Remark 2.2.2. It follows from the fact that there are only regular arcs (Proposition 2.1.6) and the fact that the curves ε and δ do not intersect, that there can be only two isotopy classes of arcs through each annulus. The isotopy classes can differ by at most a single twist around a core curve of an annulus.

Definition 2.2.3. An isotopy class of sub-arcs of δ or ε in $\mathcal{A}_r \cup R^u$ or $\mathcal{A}_l \cup R^d$ will be called a *path*. It follows from Remark 2.2.2 that for any set of curves ε and δ there are at most four paths, two in each annulus.

Thus both δ and ε are composed of a sequence of regular arcs with the exception of the two sub-arcs containing the intersection points with $X^d, X^u \subset \partial_+ P$. Fixing some

orientation on δ a special sub-arc will be called the *tail* (or *head*, respectively) of δ depending on wether δ emerges from or ends at the point. If there is no orientation chosen we will call these arcs δ-tails, similarly for ε.

We will say that a curve, say δ, *takes a path* if δ contains sub-arcs which belong to that path. We can also choose orientations for δ and ε, so that the sub-arcs of ε and δ pass through the rectangles in a counter clockwise orientation.

Thus with the exception of the two δ-tails, the curves δ and ε consist of parallel arcs except in *"splitting regions"* two, in each annulus. In each annulus in one splitting region curves separate into different paths and the other region curves from different paths become parallel, as in Figure 7. In each of the annuli the intersection of the splitting regions with $\partial_+ P$ define *separating segments*, denoted by $J_r^u, J_l^u, J_r^d, J_l^d$, one on the upper and one on the lower boundary components $\partial_+ P^u$ and $\partial_+ P^d$, which are the maximal segments on the boundaries from which any point can be connected to both paths, by an arc not intersecting either α or γ. Since we can assume that the intersection point X is tight on one side, we can assume that $X^u \subset J_r^u$ up to a reflection and or a rotation of the figure. Note that in Figure 7 we depict the paths, and that the figure is exact up to possibly a number of Dehn twists along the core curves $\mathfrak{a}_r$ or $\mathfrak{a}_l$ of the $\mathcal{A}_r$ and $\mathcal{A}_l$ annuli respectively.

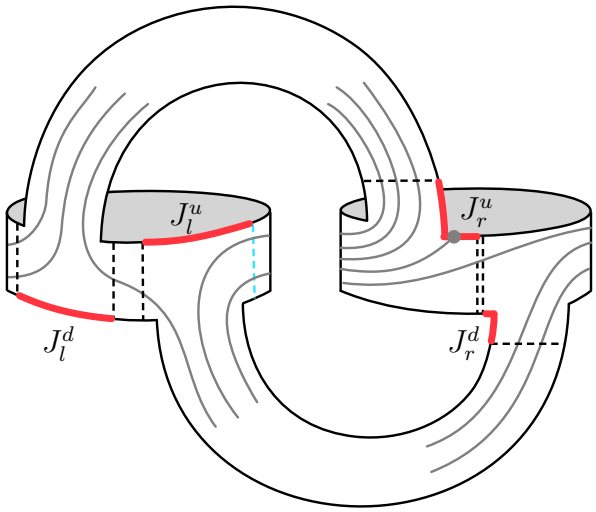

FIGURE 7. The separating segments $J_r^u, J_l^u, J_r^d, J_l^d$ on the boundaries. The dashed curve indicate segments of α and γ.

We now use the structure that we have endowed the surface $\Sigma \setminus \partial_+ P$ with, to analyze the possible planar surfaces P_N.

Definition 2.2.4. A vertical annulus $\mathfrak{a}$ with two bands emanating from it will be called *one sided* if both bands meet $\mathfrak{a}$ from one side and called *two sided* if they meet $\mathfrak{a}$ from both sides.

Definition 2.2.5. A planar surface P_N, $N \geq 2$, in the compression body V will be called *admissible* if:

(1) Every band meets the curve γ exactly once.
(2) Each of the internal vertical annuli has exactly two bands emanating from them and the bands meet γ from different sides.
(3) The planar surface P_N has exactly two external annuli whose bands $\mathfrak{b}_1$ and $\mathfrak{b}_k$ meet the curve γ from different side.
(4) The specific admissible surface P_2 depicted in Figure 8 will be called *standard*.

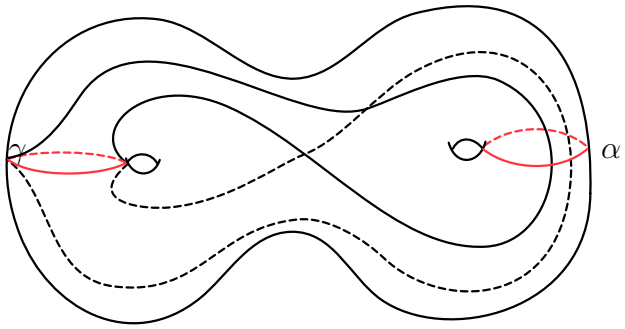

FIGURE 8. A *standard* planar surface.

The boundary $\partial_+ P$ of an admissible planar surface P is depicted in Figure 9 below.

Fix the convention that the $'+'$ side of an oriented curve is on the right. Choose the orientations on α and γ as in Figure 9, so that the $'+'$ side is depicted on the "top side" of the figure as in Figure 1. We now have:

Lemma 2.2.6. *If there are no waves with respect to $\widehat{W}$, both of the curves δ and ε meets α and γ always with the same orientation.*

Proof. Assume in contradiction that either δ or ε meets α or γ with opposite orientations. That would mean that there are sub-arcs of δ or ε connecting, say γ^+ to γ^+. Since δ or ε contain no waves these sub-arcs must intersect α and contain sub-arcs connecting γ^+ to α^+ and γ^+ to α^- So by Corollary 1.3.12 there can be no waves with

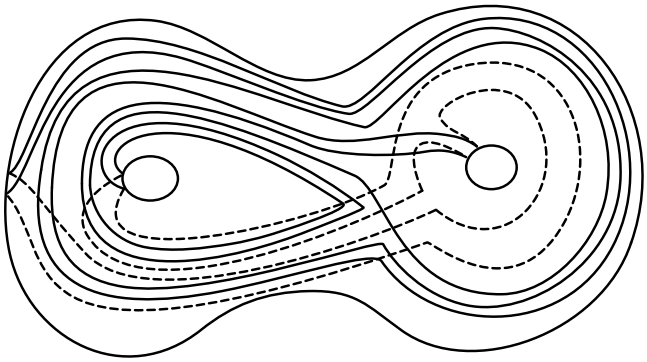

FIGURE 9. An admissible planar surface, with three one sided annuli and one two sided annulus.

respect to α or γ. As there are also no waves with respect to $\widehat{W}$, and since this is a Heegaard splitting of S^3 of complexity at least four (counting intersections between $\delta \in \widehat{W}$ and $\gamma \in \widehat{V}$), we have a contradiction to Theorem 1.3.10. The same argument can be used for ε. Hence, we can conclude that each of δ and ε intersect α and γ with consistent orientation.

We showed in Lemma 2.1.1, that each of the rectangles contains a γ segment. The orientations of δ and ε are fixed so that they traverse the rectangles counter clockwise. Thus the orientations of their intersections with γ agree. If the orientations of their intersections with α disagreed, we would obtain the edges $[\alpha^-, \gamma^-]$ and $[\alpha^+, \gamma^-]$ which are blocking edges in $\Gamma(\alpha, \gamma)$ which is a contradiction as above. □

Lemma 2.2.7. *Each of the four paths in $\Sigma \setminus \partial_+ P = \mathcal{A}_r \cup \mathcal{R}^u \cup \mathcal{A}_l \cup \mathcal{R}^d$ is taken at least once by a sub-arc of δ or ε, i.e., there can be no empty path.*

Proof. The proof is by contradiction. There are two cases depending on whether the empty path is contained in the right or left annulus of the decomposition. The picture is not symmetric in the annuli because the curves δ and ε have a particular orientation and the fact that the location of X^u was fixed on $\partial_+ P^u$.

Case 1: Assume that the empty path is contained in the right annulus $\mathcal{A}_r$ as in Figure 10. Note that we can assume that the empty path is the one on the left when entering $\mathcal{A}_r$ from $\mathcal{R}^d$. This is because symmetry (3) in Remark 2.2.1 interchanges between the path turning left and the path turning right in each annulus.

Consider the arc τ as in Figure 10. The closed curve τ does not meet δ and ε and meets $\partial_+ P$ is a single point so it bounds an essential disk $\Delta \subset W$. It does not meet

$\mathcal{R}^u$ and crosses $\mathcal{R}^d$ once. By Lemma 2.1.7 there is an innermost band which meets Δ less than twice. Thus boundary compressing P_N along the innermost band yields a planar surface with less than N annuli as in Claim 1.2.1. This a contradiction to the minimality of P_N.

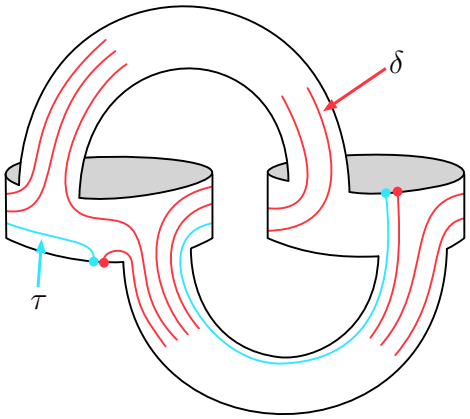

FIGURE 10. The boundary ε' of the new disk.

Case 2: Assume the empty path is in the left annulus $\mathcal{A}_r$. As before because of the symmetries we can assume that the empty path is on the left. The proof in this case is similar to the proof in Case 1, except for the fact that the curve τ is slightly different. The curve τ for this case is depicted in Figure 11.

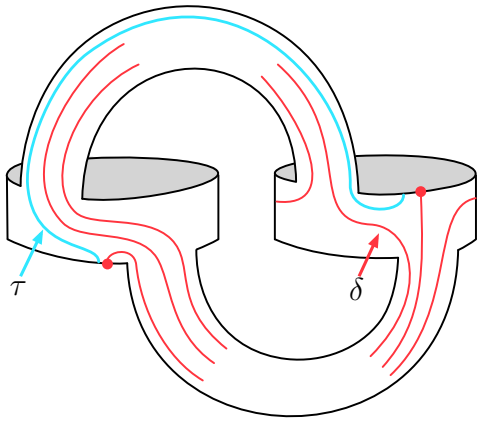

FIGURE 11. The shortcut η.

The figures are determined up to Dehn twists in the core curves of the annuli. However applying Dehn twists to the figures will not affect the argument as the intersection patterns do not change. Thus all possible options lead to contradictions and the proof of Lemma 2.2.7 is complete. □

Lemma 2.2.8. *If there are no waves with respect to W the planar surface P has no external annuli with nested corresponding bands.*

Proof. If P does have external annuli with nested bands, denote the region between them in $\Sigma \setminus \partial_+ P$ by R. If R contains a sub-arc of δ or ε, this sub-arc will meet γ then α, since it goes between the external annuli and then it will meet γ again with the opposite orientation, contradicting Lemma 2.2.6. We conclude that $R \cap \{\delta \cup \varepsilon\} = \emptyset$. Since R contains components of $\gamma \cup \alpha \setminus \partial_+ P$ as co-core curves, there is some co-core curve of the decomposition which does not meet δ or ε, contradicting Lemma 2.2.7. □

Corollary 2.2.9. *Since there are no nested external annuli there can be only two such annuli: Two external annuli can be arranged on the genus two surface so that their bands are not nested (see Figure 9). However the band of a third such annulus must nest or be nested n one of the bands of the previous annuli. In particular every annulus can have at most two bands connected to it.*

Remark 2.2.10. As a consequence we can fix an order on the vertical annuli $\mathfrak{a}_1, \ldots, \mathfrak{a}_N$ and an orientation on the bands $\mathfrak{b}_i$, $i = 1, \ldots . N-1$. So each band $\mathfrak{b}_i$ has a well defined *beginning of* $\mathfrak{b}_i$ on $\mathfrak{a}_i$ and an *end of* $\mathfrak{b}_i$ on $\mathfrak{a}_{i+1}$

Let Σ be a standardly embedded genus two surface in $\mathbb{R}^3$ symmetrically with respect to the (x, y) plane which cuts it into two twice punctured disks. The part of the surface with positive z coordinates will be called the *top* of the surface and those with negative z coordinates will be called the *bottom* of the surface. Bands on Σ can be either on the top or on the bottom and can change sides by either going through one of the two "holes" or passing over the "sides" of Σ, or by banding with the disk C.

Lemma 2.2.11. *If there are no waves with respect to $\widehat{W}$, the bands emanating from the external annuli $\mathfrak{a}_1, \mathfrak{a}_N$ must meet γ from different sides, before meeting α.*

Proof. Assume in contradiction that a band of some external annulus, say $\mathfrak{a}_1$, meets α first. If the intersection point $X = \delta \cap \partial_+ P$ is not on the band then the arc which is parallel to one of the band boundaries and the part of $\mathfrak{a}_1$ connecting it to the same side of α is a wave which does not intersect P. This contradicts Corollary 2.1.5. Thus if both bands of the external annuli connect to α before they connect to γ, one of them will not contain the point $\delta \cap \partial_+ P$ and the claim immediately follows.

Assume therefore that one external annulus, say $\mathfrak{a}_1$, is connected directly by $\mathfrak{b}_1$ to γ, while the second external annulus $\mathfrak{a}_N$ is connected by $\mathfrak{b}_{n-1}$ first to α, say to the

α^- side. Consider first the case where $\mathfrak{a}_N$ is not "straight", i.e., it is a band sum of a straight annulus and C. Note that if the copy of C is on the C^- side the band $\mathfrak{b}_{N-1}$ can be slid around $\mathfrak{a}_N$ so that its intersection with α is removed. Thus the situation is as in Figure 12.

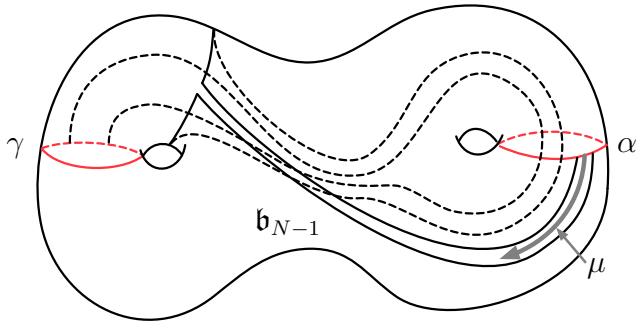

FIGURE 12. The bands $\mathfrak{b}_1$ and $\mathfrak{b}_{N-1}$ with a non-straight annulus $\mathfrak{a}_1$

The arc of intersection of $\mathfrak{b}_{N-1}$ with the disk A determines a boundary compression disk for $\mathfrak{b}_{N-1}$ which meets δ at least twice by Lemma 1.2.1. There exists a sub-arc $\mu \subset \delta$ "in" $\mathfrak{b}_{N-1}$ which does not meet the point X. Follow μ from one of the intersection points on the boundary compression disk in the direction towards $\mathfrak{a}_N$. The arc μ cannot meet α^- as otherwise this sub-arc would determine a wave in δ with respect to α in contradiction to Lemma 2.1.4. There are two cases:

(1) μ meets α^+. It cannot go back into $\mathfrak{b}_{N-1}$ as it would eventually have to meet α^- and thus there would be a δ wave with respect to α in contradiction. So, after passing through α possibly a few times, μ must continue through the hole and meet γ^+.

(2) μ does not meet α^+. In this case, by the same argument as in (1), μ must meet γ^+.

In both cases this results in an arc between α^- and γ^+. Next consider the continuation of μ to the other side. It emanates from α^+ and cannot return to α^+. Thus, after perhaps meeting α^- a few times it must continue through the hole and connect α^+ to γ^+.

It now follows from Corollary 1.3.12 that there are no waves with respect to α and γ. By assumption there are no δ and ε waves. Furthermore, the complexity of the diagram is greater than four, so by Theorem 1.3.10 this is not a Heegaard diagram for S^3 in contradiction.

Next consider the case $\mathfrak{a}_N$ is "straight". The only difference in this case is that the band $\mathfrak{b}_{N-1}$ must flip through the left hole as in Figure 13 and meet α. This implies that the band $\mathfrak{b}_{N-1}$ runs along the bottom of Σ as in Figure 13 and that $\mathfrak{b}_1$ connects to γ^+ . As before, we can choose a sub-arc μ of δ emanating from α^- "in" $\mathfrak{b}_{N-1}$ in the direction towards $\mathfrak{a}_N$, not meeting the point X within $\mathfrak{b}_{N-1}$. Now the same argument, exactly as for the non-straight case above, following μ to both directions yields the blocking edges for $\Gamma(\alpha, \gamma)$. Again as above we obtain a contradiction by Corollary 1.3.12 and Theorem 1.3.10. Thus both $\mathfrak{b}_1$ and $\mathfrak{b}_{N-1}$ meet γ before they meet α.

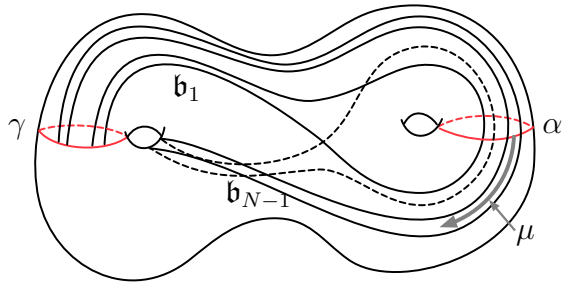

FIGURE 13. The bands $\mathfrak{b}_1$ and $\mathfrak{b}_{N-1}$ with a straight annulus $\mathfrak{a}_1$

To see that the bands $\mathfrak{b}_{N-1}$ and $\mathfrak{b}_1$ connect to γ from different sides consider the sub-arcs of δ or ε in $\mathfrak{b}_1$. These arcs cannot return to γ through $\mathfrak{b}_1$ as this would imply that δ or ε meet γ in opposite orientations contradicting Lemma 2.2.6. Thus the sub-arcs must continue through $\mathfrak{b}_{N-1}$ which, again by Lemma 2.2.6, must be connected to the other side of γ. □

Definition 2.2.12.

(1) We say that a band $\mathfrak{b}_k$, $1 \leq k \leq N-1$ *disk sums with*, or *sums*, for short, with the disk C if there is an ε neighborhood $\mathcal{N}_\varepsilon(C)$ of C in V and two co-core arcs b_1, b_2 of $\mathfrak{b}_j$ in $\mathcal{N}_\varepsilon(C)$ so that a component of $\mathfrak{b}_j \setminus \{b_1 \cup b_2\}$ is isotopic to C in $\mathcal{N}_\varepsilon(C)$. We assume that the disk summing with the disk C occurs before the bands meet the disk C from the γ^+ side.

(2) We say that two bands $\mathfrak{b}_k, \mathfrak{b}_{N-1}$ *connect* to each other if $k = N-1$ or, in other words, if they merge together to form a single band. Similarly a band $\mathfrak{b}_k$ meets an annulus $\mathfrak{a}_j$, if $j = k+1$ and a band $\mathfrak{b}_k$ emerges from an annulus $\mathfrak{a}_j$, if $j = k$.

Definition 2.2.13.

(1) Note that $P \subset U$ is two sided. We say that the intersection $P \cap C$ is *standard* if it is a set of parallel arcs $\zeta_i \subset C$ and there is an arc $\kappa \subset C$ so that $\partial\kappa \subset \partial C \setminus \zeta_i$ and κ meets all $\zeta_i \subset C$ from the same side of P.

(2) Given a standard intersection between P and C and an arc κ as above starting at the "bottom" of Σ and ending at the "top" of Σ . We define the *right side* and *left side* of C to be the part of C to the right and left of κ respectively.

Proposition 2.2.14. *If there are no waves with respect to $\widehat{W}$ then the planar surface P is admissible.*

Proof. By Corollary 2.2.9 we know that that there are exactly two external bands and that each internal annulus has at most two band emanating from it. So according to Definition 2.2.5 we need to show that every band $\mathfrak{b}_k$, $1 \leq k \leq N-1$, meets the curve C exactly once and that two bands emanating from the same annulus meet γ from different sides. We prove by induction on k:

Consider first the band $\mathfrak{b}_1$. Without loss of generality we may assume that the band $\mathfrak{b}_1$ connects $\mathfrak{a}_1$ to the γ^+ side. By Lemma 2.2.11 the beginning of $\mathfrak{b}_1$ and end of $\mathfrak{b}_{N-1}$ are connected to γ from different sides so after $\mathfrak{b}_1$ crosses γ it can either:

(1) Connect directly to $\mathfrak{b}_{N-1}$ or

(2) be nested in $\mathfrak{b}_{N-1}$ or

(3) nest $\mathfrak{b}_{N-1}$ or

(4) $\mathfrak{b}_1$ and $\mathfrak{b}_{N-1}$ have disjoint compression disks abbreviated as $\mathfrak{b}_1$ is *beside* $\mathfrak{b}_{N-1}$.

(1) In this case we can see directly that $\mathfrak{b}_1$ must sum C as otherwise we obtain a closed curve μ_0, depicted in Figure 14, which is separating and so cannot equal $\partial_+ P$. Furthermore after summing C it connects to $\mathfrak{b}_{N-1}$ so we have $N = 2$ and $\partial_+ P$ is standard and in particular admissible.

(2) We first claim that $\mathfrak{b}_1$ must sum with the disk C just before it reaches γ for the first time: Assume in contradiction that $\mathfrak{b}_1$ does not sum with C. Then the curve μ_0 can be isotoped to a curve contained in $\partial_+ P$ except for two small arcs μ' and μ'' on γ connecting the two bands as in Figure 15(i). Note that μ_0 is a separating curve on Σ and that the continuation of $\mathfrak{b}_1$ is on one side, say A, of μ_0 while the continuation of $\mathfrak{b}_{N-1}$ is on the other side B. As $\mathfrak{b}_1$ always arrives at C from the γ^+ side it cannot cross the μ', μ'' arcs because the $'+'$ side of μ', μ'', as induced from the $'+'$ side of γ is on the B side while the continuation of $\mathfrak{b}_1$ is always is on the A side of μ_0. (see Figure 14).

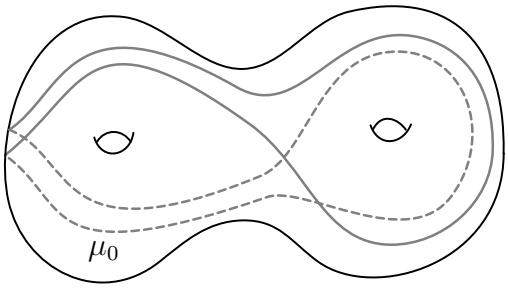

FIGURE 14. The The curve μ_0

Thus $\mathfrak{b}_1$ cannot close up with $\mathfrak{b}_{N-1}$ to form $\partial_+ P$. Thus we conclude that $\mathfrak{b}_1$ must sum with the disk C before it enters $\mathfrak{b}_{N-1}$.

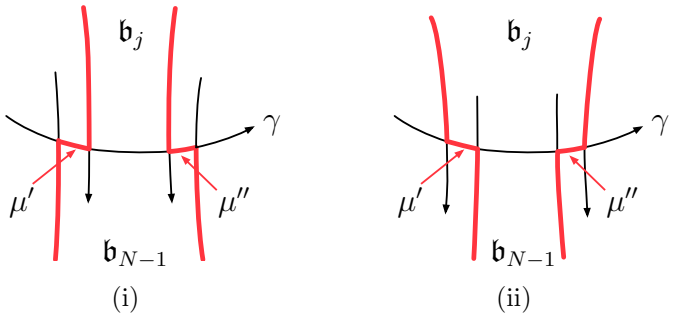

FIGURE 15. The deformation of the curve μ_i, in case $\mathfrak{b}_j$ is nested in $\mathfrak{b}_{N-1}$, and in case it nests $\mathfrak{b}_{N-1}$.

Now we prove that the band $\mathfrak{b}_1$ must intersect C once, and then connect to an internal annulus (before reaching γ again).

Assume in contradiction that the band $\mathfrak{b}_1$ disk sums C and enters $\mathfrak{b}_{N-1}$ and then meets the curve γ before meeting an internal annulus. There are two cases:

(2.a) The curve $\mathfrak{b}_1$ *does not sum with the disk* C (for the second time) before it meets γ again. In this case one of two things can happen after $\mathfrak{b}_1$ crosses γ:

(2.a.*i*) *The band* $\mathfrak{b}_1$ *does not meet an internal annulus* $\mathfrak{a}_2$ *before it enters* $\mathfrak{b}_{N-1}$. In this case $\mathfrak{b}_1$ winds around the surface Σ and, since it dose not self intersect, is forced by the first disk sum with C to arrive from the $'+'$ side of γ and either re-nest in $\mathfrak{b}_1 \subset \mathfrak{b}_{N-1}$ or re-nest in $\mathfrak{b}_{N-1}$ beside $\mathfrak{b}_1$. In the first case it spirals in itself so it can never connect to $\mathfrak{b}_{N-1}$ and close up to a simple closed curve $\partial_+ P$. In the second case as it is beside $\mathfrak{b}_1$ "in" $\mathfrak{b}_1$ the only way it can connect to $\mathfrak{b}_{N-1}$ which is "outside" of $\mathfrak{b}_1$ is by disk summing at some point with C again. If it sums with C for the second time

and then connects to $\mathfrak{b}_{N-1}$ the obtained closed curve μ_1 is homologous to two copies of γ and two copies of $\partial\mathfrak{a}_1$ which separates Σ and thus cannot equal $\partial_+ P$.

If it does not connect to $\mathfrak{b}_{N-1}$ it either nest or becomes nested in $\mathfrak{b}_{N-1}$. The the curve μ_1 can be isotoped to a separating curve contained in $\partial_+ P$ except for two small arcs μ' and μ'' on γ connecting the two bands as in Figure 15 (i) and (ii). In both cases the continuation of $\mathfrak{b}_1$ is on one side of μ_1 while $\mathfrak{b}_{N-1}$ is on the other so $\mathfrak{b}_1$ cannot connect to $\mathfrak{b}_{N-1}$ to form $\partial_+ P$.

(2.a.*ii*) *The band* $\mathfrak{b}_1$ *does meet an internal annulus* $\mathfrak{a}_2$ *before it enters* $\mathfrak{b}_{N-1}$. The second band $\mathfrak{b}_2$ of $\mathfrak{a}_2$ must nest $\mathfrak{b}_1$ and not $\mathfrak{b}_{N-1}$ as otherwise the δ and ε-arcs contained in $\mathfrak{b}_2$ will meet γ and α with conflicting orientations contradicting Lemma 2.2.6. Now the band $\mathfrak{b}_2$ has no choice but to follow $\mathfrak{b}_1$, disk sum with C and get "stuck" in the region S as in Figure 16 between itself and $\mathfrak{b}_1$. In this case $\mathfrak{b}_2$ cannot continue to close up and form $\partial_+ P$.

We conclude that Case (2.a) cannot happen and we have Case (2.b):

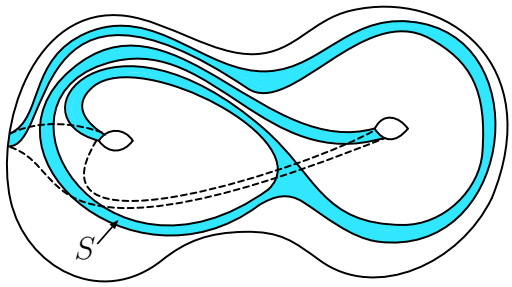

FIGURE 16. The Region S in the argument for case (2.b)

(2.b) The curve $\mathfrak{b}_1$ sums with C the first two times it crosses γ. If after $\mathfrak{b}_1$ crosses γ for the second time it connects to $\mathfrak{b}_{N-1}$, then as in Case (1), the boundary of the involved bands and annuli is a separating curve, denoted by μ_2, since together with $\mathfrak{a}_N$ there is an even number of annuli and an even number of disks C. Thus the curve μ_2 cannot be equal to a $\partial_+ P$ curve and this case cannot happen. Otherwise it can either nest or be nested, (note that $\mathfrak{b}_1$ now nests itself and cannot be besides $\mathfrak{b}_{N-1}$). Now the same argument used before with respect to the curve μ_1 applied to the curve μ_2 proves that the curve cannot close up to form $\partial_+ P$. Thus, $\mathfrak{b}_1$ crosses γ exactly once summing with C there, and then must meet some annulus.

(3) As $\mathfrak{b}_1$ nests $\mathfrak{b}_{N-1}$ the claim that $\mathfrak{b}_1$ connects to an internal annulus before it meets γ again follows immediately, as it must connect to an internal annulus before $\mathfrak{b}_{N-1}$ connects to $\mathfrak{a}_N$.

(4) In this case $\mathfrak{b}_1$ crosses γ and is besides $\mathfrak{b}_{N-1}$. Suppose in contradiction that it reaches γ again (perhaps several times) without meeting an internal annulus. It cannot cross γ from the $'-'$ side as this would result in conflicting orientations on δ and ε contradicting Lemma 2.2.6. Thus, finally, it can either:

(4.a) Connect directly to $\mathfrak{b}_{N-1}$ This results in a curve μ_3. It is separating as it is homologous two $\mathfrak{a}_1 \cup \mathfrak{a}_N$. Thus μ_2 cannot be equal to $\partial_+ P$ as seen above.

(4.b) Nest or be nested in $\mathfrak{b}_{N-1}$, but in this case the same argument that was used for μ_0, μ_1 and μ_2 applied to μ_3 results in a contradiction.

(4.c) Meet γ several times (≥ 2) besides $\mathfrak{b}_{N-1}$ and then meet an annulus $\mathfrak{a}_2$.

In case (4.c), the annulus $\mathfrak{a}_2$ will have a second band $\mathfrak{b}_2$ nesting $\mathfrak{b}_1$. This process can repeat itself several times but in each case the last band, say $\mathfrak{b}_k$ will have the a portion of $\mathfrak{b}_1$ both nested and beside it. Therefore it will always nest $\mathfrak{b}_1$ and as a result cannot connect to $\mathfrak{b}_{N-1}$ which does not nest $\mathfrak{b}_1$. Hence the bands can never close up to form $\partial_+ P$.

Thus, for all cases (1) - (4), $\mathfrak{b}_1$ meets an internal annulus before it returns to γ for the second time as claimed.

Note that in Case (2) $\mathfrak{b}_1$ does sum with C. The annulus $\mathfrak{a}_2$ is internal and it must be two sided as $\mathfrak{b}_1$ is nested in $\mathfrak{b}_{N-1}$. In Case (4) $\mathfrak{b}_1$ does not sum with C. As $\mathfrak{b}_1$ is beside $\mathfrak{b}_{N-1}$ the annulus is one sided and it's second band $\mathfrak{b}_2$ nests $\mathfrak{b}_1$.

The induction hypothesis: Assume that for all $j < k \leq N-1$ any band $\mathfrak{b}_j$ intersects γ once from the same side and then meets the next annulus.

Note the following remarks:

($*$) If for all $j < k$, $\mathfrak{b}_j$ does not sum with C then since $\mathfrak{b}_j$ nests $\mathfrak{b}_{j-1}$ and the annulus $\mathfrak{a}_{j+1}$ must be one sided and has a second band nesting $\mathfrak{b}_j$.
($**$) If $\mathfrak{b}_j$ sums with C then $\mathfrak{b}_j$ either connects to $\mathfrak{b}_{N-1}$ to obtain a closed curve, or is nested in or nests $\mathfrak{b}_{N-1}$. If it is nested in $\mathfrak{b}_{N-1}$ it must connect to a two sided annulus $\mathfrak{a}_{j+1}$ that has a second band nested in $\mathfrak{b}_1$. If it nests $\mathfrak{b}_{N-1}$, the continuation of $\mathfrak{b}_j$ together with the annulus $\mathfrak{a}_{j+1}$ can be isotoped to the top side of the surface Σ at the expense of introducing a summing with C in the $\mathfrak{b}_{j+1}$. Therefore we may assume that $\mathfrak{b}_j$ is nested in $\mathfrak{b}_{N-1}$.
($***$) The intersections of all bands $\mathfrak{b}_j$, $j < k$ with the disk C is a collection of parallel arcs on C. However the corresponding bands are separated into two sets. A set $\mathfrak{A}$ of nested bands which do not sum with C and a set $\mathfrak{B}$ of nested bands which do. Note

that a band which connects to $\mathfrak{b}_{N-1}$ must nest every arc on C which is in $\mathfrak{A}$, as all bands in $\mathfrak{B}$ become nested in $\mathfrak{b}_{N-1}$ after the summing with C.

We next prove that the next band $\mathfrak{b}_k$ also intersects γ exactly once before it meets an internal (or external if $k = N-1$) annulus:

Consider the first time $\mathfrak{b}_k$ intersects γ. As all previous bands arrive on the γ^+ side and are nested in each other, we can conclude that $\mathfrak{b}_k$ is connected to an internal annulus unless:

(i) It is nested in all the bands in the set $\mathfrak{B}$ or

(ii) It is nested in all the bands in the set $\mathfrak{A}$.

In case (i), if $\mathfrak{b}_k$ returns to C without meeting an internal annulus it must be an innermost band which is nested in $\mathfrak{b}_1$ beside other bands nested in it, if they exist. In this case $\mathfrak{b}_k$ will be forced to return to C repeatedly without meeting an internal annulus until eventually it reaches γ^+ and intersects C in an arc which is beside the outermost band in $\mathfrak{A}$ (between $\mathfrak{A}$ and $\mathfrak{B}$). However, $\mathfrak{b}_k$ can now only continue if it is nested in itself and thus spirals and cannot close up with $\mathfrak{b}_{N-1}$.

Thus the band $\mathfrak{b}_k$ must meet an internal annulus at some point. It can connect to an internal annulus $\mathfrak{a}_{k+1}$ only if when it becomes nested in $\mathfrak{b}_1$ it is innermost in the set $\mathfrak{A}$. This means that it is the only band in $\mathfrak{B}$ and that all previous bands where in $\mathfrak{A}$. Thus, $\mathfrak{a}_{k+1}$ is next to and parallel to $\mathfrak{a}_1$. Now $\mathfrak{b}_{k+1}$ continues nesting $\mathfrak{b}_1$ and connects to an annulus $\mathfrak{a}_{k+2}$ which is next to and parallel to $\mathfrak{a}_2$. This process continues until $\mathfrak{b}_{2k-1}$ arrives at γ^+ nesting all the bands in set $\mathfrak{A}$ and thus replicates all annuli $\mathfrak{a}_1, \ldots, \mathfrak{a}_{k-1}$. (Recall that the index is $2k-1$ as the outermost band in set $\mathfrak{A}$ is $\mathfrak{b}_{k-1}$.)

If $\mathfrak{b}_{2k-1}$ now sums with C and connects to $\mathfrak{b}_{N-1}$ then as before we obtain a curve μ_4 which is separating as together with $\mathfrak{a}_N$ it is homologous to an even number $(2k-1+1)$ of annuli and two C disks. Thus μ_4 cannot be a $\partial_+ P$ curve. Furthermore the same argument as for μ_0 shows that the curve obtained so far can never close up to a $\partial_+ P$ if $\mathfrak{b}_{2k-1}$ nests or becomes nested in $\mathfrak{b}_{N-1}$, or continues on the top of the surface without summing with C.

In case (ii), if $\mathfrak{b}_k$ returns to C without meeting an internal annulus it must be an innermost band which is beside $\mathfrak{b}_1$. In this case $\mathfrak{b}_k$ will be forced to return to C repeatedly without meeting an internal annulus until eventually it reaches γ^+ and intersects C in an arc which is beside the outermost band in $\mathfrak{A}$ (between $\mathfrak{A}$ and $\mathfrak{B}$) cutting off a boundary compression disk $\Delta \subset C$. At this point it can either:
($ii.a$) Enter $\mathfrak{b}_{N-1}$ and becomes nested in itself and spiral forever, or

(*ii.b*) Continue on the outside of $\mathfrak{b}_{N-1}$ and become nested in the innermost band in $\mathfrak{B}$. When $\mathfrak{b}_k$ emerges from the innermost band in $\mathfrak{B}$ it can either connect to an internal annulus or continue nested in $\mathfrak{b}_1$ between the other bands nested in $\mathfrak{b}_1$. At this stage it must follow the bands till it meets C between $\mathfrak{A}$ and $\mathfrak{B}$ again and then must continue besides itself as an additional innermost band in $\mathfrak{B}$. This procedure can repeat itself several times. Note that in order to connect to $\mathfrak{b}_{N-1}$ it must meet an internal annuls at some point. This annulus will be parallel to $\mathfrak{a}_1$ and $\mathfrak{b}_{k+1}$ will be adjacent to and nested in $\mathfrak{b}_1$. This continue so that $\mathfrak{b}_{k+j}$ will emerge from $\mathfrak{a}_{k+j}$ which is parallel to $\mathfrak{a}_j$ and be adjacent to and nested in $\mathfrak{b}_j$. Finally $\mathfrak{b}_{2k-1}$ is adjacent to and nested in $\mathfrak{b}_{k-1}$ which is the outermost band in $\mathfrak{B}$ (since we know that $\mathfrak{b}_k$ started as the innermost in $\mathfrak{A}$). At this point $\mathfrak{b}_{2k-1}$ can disk sum with C (parallel to $\mathfrak{b}_{k-1}$) and connect to $\mathfrak{b}_{N-1}$ to obtain a closed curve μ_5.

All annuli $\mathfrak{a}_1, \dots, \mathfrak{a}_{k-1}$ have been duplicated, in the process of creating μ_5, and we must also count $\mathfrak{a}_k$ and $\mathfrak{a}_N$ so we have an even number of annuli banded together in μ_5. All the disks sums in $\mathfrak{b}_1, \dots, \mathfrak{b}_{k-1}$ have also been duplicated so μ_5 is separating, as it is homologous to a separating collection of curves, and cannot be equal to a $\partial_+ P$. As before this also rules out the possibility that $\mathfrak{b}_{k-1}$ either nests or is nested in $\mathfrak{b}_{N-1}$.

Thus we have shown that $\mathfrak{b}_k$ intersects γ only once from the same side before it meets the next annulus. This completes the proof of the proposition. □

Corollary 2.2.15. *If P is admissible the intersection $P \cap C$ is standard.*

Proof. If follows directly from the proof of Proposition 2.2.14 and remarks $(*)$, $(**)$ and $(***)$ above, that the arcs of intersection of $P \cap C$ split into two families $\mathfrak{A}$ and $\mathfrak{B}$ of nested arcs which must be parallel to each other. □

Before we state the next lemma recall that given two simple closed curves θ and τ which intersect at a point p, a *positive Dehn twist* of θ along τ is the curve obtained from θ by removing a small regular neighbourhood of p from θ making a right hand turn at p then traversing τ once and reconnecting to $\theta \setminus \mathcal{N}(p)$.

Lemma 2.2.16. *If P is admissible then by changing α by wave moves we can choose α so that for all $1 \leq k \leq N-1$ the band $\mathfrak{b}_k$ does not intersect α while the conclusions of Lemma 2.1.4 are still satisfied.*

Proof. Each band belongs to one of the families $\mathfrak{A}$ or $\mathfrak{B}$ as in 2.2.14. If a band in $\mathfrak{A}$ (or $\mathfrak{B}$ respectively) intersect α then since they are nested in each other all the bands in $\mathfrak{A}$ (or $\mathfrak{B}$ respectively) intersects α the same number of times except for $\mathfrak{b}_{N-1}$. Thus

any admissible P is a collection of vertical annuli connected by bands meeting only γ (not α) up to Dehn twists in the curves c_1 and c_2 as in Figure 19.

Assume that the innermost band in $\mathfrak{A}$ meets α k times . i.e., the Dehn twist in c_1 is iterated k times. By Lemma 2.1.4 the Dehn twists have to be positive as otherwise we will have a sub-arc of δ which has conflicting orientations with respect to α. In this case we have an s-wave η_1 with respect to α as in Figure 17. In case the innermost band in $\mathfrak{B}$ intersects α we have an s-wave η_2 depicted in Figure 18. The s-waves η_1 and η_2 do not intersect the external annulus on the bottom of Σ thus by Remark 2.1.3 (2) performing the wave move on the s-wave results in a meridian disk intersecting the knot once. This move on the s-wave does not increase the intersections of δ and ε with α as it can be seen in the figures that any path which intersects the s-wave η_i (thus intersecting the "new" α) also meets the part of α removed by the wave move. Thus the minimality of α is preserved.

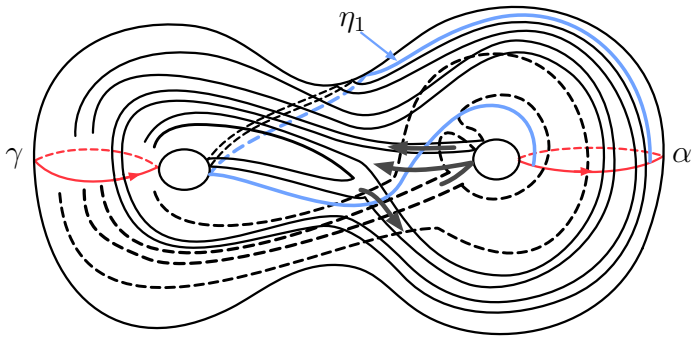

FIGURE 17. The s-wave η_1 with respect to α. The thick arrows represent the paths intersecting η_1, the number of which depends on the number of bands in $\mathfrak{A}$. Tracing these paths forward, one can see that each of these paths intersect α along the part which is removed by the move on the s-wave (the half of α on the top of Σ).

Performing the wave move on A using η_1 as in Figure 17 we obtain a new disk A^1 which equals B. Lemma 2.2.11 states that the two external annuli are connected one to C^+ and the other to C^-. Hence there are sub-arcs of $\partial_+ P$ corresponding to the external annuli and their bands which give rise to all four seams connecting $\gamma^\pm$ to $\beta^\pm$. It follows that any wave with respect to β must intersect $\partial_+ P$. Therefore the curves δ and ε cannot have sub-arcs which are waves with respect to $\alpha^1 = \beta$ as $\delta \cup \varepsilon$ intersect $\partial_+ P$ exactly once and there are at least two such waves. Hence the curve $\alpha^1 = \partial A^1$ satisfies the conclusions of Lemma 2.1.4.

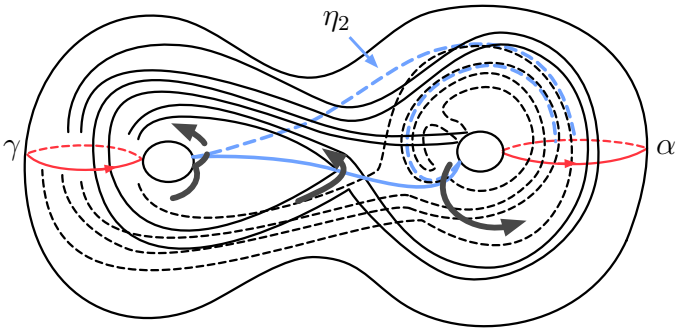

FIGURE 18. The s-wave η_2 with respect to α. The thick arrows represent the paths intersecting η_1, the number of which depends on the number of bands in $\mathfrak{A}$. Tracing the right and left paths forward, and the middle path, and any additional path parallel to it backwards, one can see that each of these paths intersect α along the part which is removed by the wave move (all α except the short interval between the endpoints of η_2).

Furthermore, the number of intersection points of $\alpha^1 = \beta$ with the innermost band of $\mathfrak{A}$ is one less than that of α. This is because the part of α removed in the wave move contains exactly one such intersection point and the wave dose not intersect the innermost band. Thus each wave move reduces the number of Dehn twists by one.

After iterating the wave moves we can assume that there are no Dehn twists in c_1. Similarly if we replace η_1 by η_2, as in Figure 18, we may assume that there are no Dehn twists in c_2 as well. □

Remark 2.2.17. Note, that after changing α by a wave move we no longer know that there are no waves with respect to δ and ε. However, P remains admissible with respect to the new system as the Definition 2.2.5, of admissible P, depends only on the intersections with γ which are not changed.

Remark 2.2.18. If P_N is standard (*i.e.*, $N = 2$) Dehn twisting along c_1 and c_2 do not change $\partial_+ P_2$ as $(c_1 \cup c_2) \cap \partial_+ P_2 = \emptyset$. However the Dehn twists do change the paths as depicted in Figure 19. If $N > 2$ the intersection with $\partial_+ P_N$ is not empty so Dehn twisting in c_1 and c_2 will change $\partial_+ P_N$.

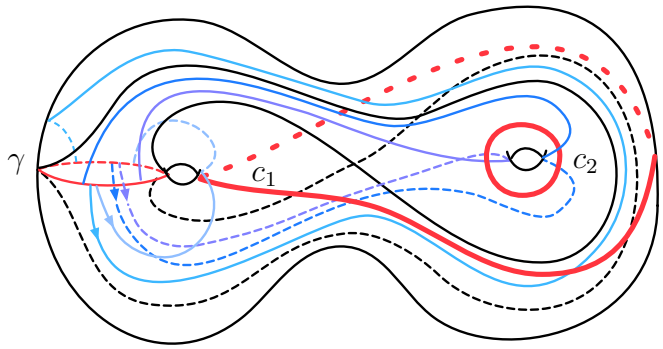

FIGURE 19. The curves c_1 and c_2 in Σ. The paths on $\Sigma \setminus \partial_+ P$, emanating from γ^-, as they appear on Σ for the standard P. The paths are the ones depicted up to some Dehn twists along the annuli cores $\mathfrak{a}_1$ and $\mathfrak{a}_2$ (coinciding with the curves c_1 and c_2 on Σ in this case).

2.3. The related dynamical system

The surface $\Sigma \setminus \partial_+ P = \mathcal{A}_l \cup \mathcal{R}^d \cup \mathcal{A}_r \cup \mathcal{R}^u$ can be endowed with a flow oriented in a counter clockwise direction through the rectangles. This flow exits the boundary at some point in J_r^u and in J_l^d and enters through part of the boundary $\partial_+ P^d$ and part of $J_l^u \setminus \partial_+ P^u$. The flow can be chosen so that δ and ε are orbits of the flow.

The direction of the flow will be the *preferred direction* and relative to it we have the notions of *right* and *left*. Thus sub-arcs have a $+$ side which is the right side with respect to the flow while traversing the arc, and a $-$ side which is the left side. We also have notions of *top, bottom, above* and *below* of a figure defined in the obvious way.

Definition 2.3.1. In the annulus $\mathcal{A}_l$ (as in Figure 20) there is an interval I_1 transversal to the flow with endpoints on δ. The interval is located inside the splitting region, from which the ε-arcs can proceed in two different directions. There is also another interval, I_0, again with endpoints on δ, in which two ε sub-arcs coming from different directions can become parallel. The intervals are shown in Figure 20 for the case δ takes two different paths in $\mathcal{A}_l$.

Claim 2.3.2. *There is a unique choice, up to isotopy, of intervals I_0 and I_1.*

Proof. If δ takes *two paths* as shown in Figure 20, regardless of the specific paths taken, ε can *split* only between the leftmost δ-arc in the right path and the rightmost δ-arc in the left path. Similarly two ε-arcs can become parallel only if they are to the left of

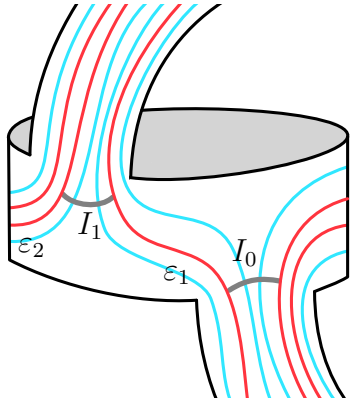

FIGURE 20. One possible configuration for the intervals I_0 and I_1. The $\varepsilon_i, i = 1, 2$ arcs are possible choices for sub-arcs of ε

the leftmost δ-path and rightmost to the right path. Thus there is a unique choice for I_0 and I_1.

Suppose that δ takes only one path in $\mathcal{A}_l$. Then the intervals I_0 and I_1 are as in Figure 21. There are two points where sub-arcs of ε can split into two directions on I_0 and two points where sub-arcs of ε can become parallel on I_1. Which of the points occurs depends on the relative configurations of the curvesδ and ε.

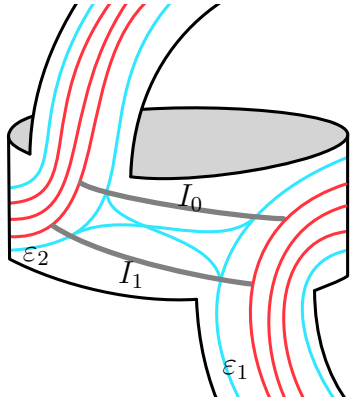

FIGURE 21. The intervals I_0 I_1 when δ takes a single path in $\mathcal{A}_l$. The $\varepsilon_i, i = 1, 2$ arcs are possible choices for sub-arcs of ε

This remains true also when δ takes a path that winds more times around $\mathcal{A}_l$ than the path given in Figure 21 as shown in Figure 22. □

Remark 2.3.3. The annulus $\mathcal{A}_r$ contains the δ-*head* sub-arc of δ which ends at X^u. Divergence of adjacent ε sub-arcs in $\mathcal{A}_r$ would result in forbidden intersection between δ and ε. Hence adjacent sub-arcs of ε can diverge into different directions *only* at $I_1 \subset \mathcal{A}_l$. Similarly sub-arcs of ε and become parallel *only* at $I_0 \subset \mathcal{A}_l$. This is because

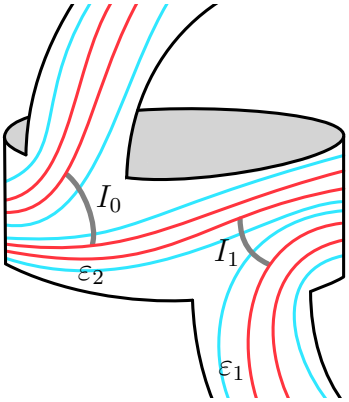

FIGURE 22. The intervals I_0 and I_1 when the single path taken by δ winds around $\mathcal{A}_l$.

the continuation of the δ-tail which emerged from X^d is either the rightmost in the right path in $\mathcal{A}_r$ or leftmost arc in the left path $\mathcal{A}_r$ and hence separates sub-arcs of ε trying to converge in $\mathcal{A}_r$.

Consider an arc along the flow lines starting at I_1 and veering to the left at the splitting point. Denote it by ε_1. It has a δ-arc on its left. The arc ε_1 cannot continue to flow parallel to the δ-arc on its left until it returns to I_1, as that implies δ is a closed curve not meeting $\partial_+ P$. Since δ is a finite arc and since ε_1 cannot always be parallel to δ it must split at some point from the δ arc on its left. This can happen only when the δ arc becomes the δ head and connects to X^u.

The continuation of ε_1 which is adjacent to the δ-head on its right must continue on the bottom of $\mathcal{R}^u$ and meet I_0, arriving from the right. At this point it becomes adjacent to a new δ arc on its left. It continues until it returns to I_1: It must split from this arc as well. This splitting can happen either at the δ head again or by veering right after I_1. In the first case it must pass through I_1 first in order to return to the δ-head. The first time ε_1 will meet I_1 again will be its endpoint. Let Ψ denote the part of ε_1 between I_0 and I_1 as above.

Similarly, denote an arc along the flow lines veering to the right after I_1 until it returns to I_1 by ε_2. The arc ε_2 therefore passes on the left side of the δ-head, and arrives at I_0 from the left. Since any flow line is adjacent to a δ-arc either on its right or on its left, or is part of ε_1 or ε_1 in Figure 21 there is a sub-arc of $\varepsilon_1 \cup \varepsilon_2$ between any two δ-arcs and between δ and the boundary. Note that Ψ is a sub-arc of both ε_1 and ε_2.

The discussion above gives, for a fixed curve δ, a train track structure on $\Sigma \setminus \{\partial_+ P \cup \delta\}$ with two switch points on $\mathcal{A}_l$. One switch point is below I_1 where ε arcs can take two paths and one above I_0 where ε arcs can become parallel.

The train track carries the curve ε in the complement of δ and ε can be described as the union of m arcs of type ε_1 and n arcs of type ε_2. Namely:

$$\varepsilon = m \cdot \varepsilon_1 + n \cdot \varepsilon_2, \text{ where } m, n \in \mathbb{N} \cup \{0\}$$

Proposition 2.3.4. *In the description $\varepsilon = m \cdot \varepsilon_1 + n \cdot \varepsilon_2$ where $m, n \in \mathbb{N} \cup \{0\}$, If one of the coefficients n or m equals zero, then P is admissible.*

Proof. Using symmetry (3) from Remark 2.2.1 which exchanges the right and left in $\mathcal{A}_l$ and thus exchanges m and n it is enough to prove that $m \neq 0$. Therefore, assume in contradiction that $m = 0$ (i.e., ε does not contain sub-arcs of type ε_1).

The lowest sub-arc in $\mathcal{R}^d$ is a sub-arc of δ. The ε arcs (represented by ε_2 in Figures 20 - 22) are the topmost of all arcs in $\mathcal{R}^d$ (except perhaps the δ-tail).

Since both δ and ε traverse $\mathcal{R}^d$ with identical orientations there is a sub-arc of γ in $\mathcal{R}^d$ connecting ε^+ to the δ^-. Hence we have the $[\delta^-, \varepsilon^+]$ edge in the Whitehead graph $\Gamma(\delta, \varepsilon)$.

The δ-tail might pass between the topmost ε-arc and $\partial_+ P$ in $\mathcal{R}^d$ intersecting some segments of $\alpha \cup \gamma$. If the δ-tail intersects some segment of $\alpha \cup \gamma$ with the opposite orientation we have the $[\delta^-, \varepsilon^-]$ edge in the Whitehead graph $\Gamma(\delta, \varepsilon)$. So we have no waves with respect to δ and ε. If the δ-tail intersects some segment of $\alpha \cup \gamma$ with the correct orientation it cannot intersect all the segments of α and γ between the topmost ε-arc and $\partial_+ P$ all the way from J_l^d to J_r^d. As then it would have to start at or pass above J_l^d and then there will be a δ wave between two sub-arcs of δ just above J_l^d (as $m = 0$), contradicting the minimality of δ. Thus one case cannot happen or there are no waves with respect to $\{\delta, \varepsilon\}$.

Thus, we can assume we can connect ε^- to $\partial_+ P^d$ by an arc denoted by ρ_1. We also have an arc ρ_2 connecting δ^+ to $\partial_+ P^d$ (as we are in Case (2)). Any sub-arc of γ or α starting at $\partial_+ P^u$ connects it either to δ^- or to ε^+. If the continuation of ρ_1 (ρ_2 resp.) on the other side of $\partial_+ P$ meets δ^- (or ε^+ resp.) we have the edge $[\delta^-, \varepsilon^-]$ (or $[\delta^+ \varepsilon^+]$). Since we also have the $[\delta^-, \varepsilon^+]$ we conclude the are no $\{\delta, \varepsilon\}$ waves by Corollary 1.3.12. If neither of these happen then the continuation of ρ_1 reaches ε^+ and the continuation of ρ_2 reaches δ^-. Thus we have the $[\varepsilon^+, \varepsilon^-]$ and $[\delta^+, \delta^-]$ edges. We conclude that there cannot be waves with respect to $\{\delta, \varepsilon\}$. As there are no waves with respect to $\{\delta, \varepsilon\}$ in all cases we can apply Proposition 2.2.14 and conclude that P_N is admissible. $\square$

Definition 2.3.5. Given a meridian system $\widehat{V}$ for the handlebody V we will call a path *long with respect to* $\widehat{V}$ if it intersects one of the segments of $\widehat{V} \setminus \partial_+ P$ more than once. Otherwise it will be called a *short* path.

Corollary 2.3.6. *Let $\widehat{V}$ be a meridional system so that any short path intersects $\widehat{V}$. Assume further that δ and ε take only short paths in one of the annuli. If one of the coefficients n or m equals zero, then there are blocking edges in $\Gamma(\widehat{W})$ and therefore there are no waves with respect to δ and ε.*

Proof. Assume $m = 0$. We use the same proof as for Proposition 2.3.4 above: By Lemma 2.2.7 there are no empty paths hence in the annulus where only short paths are taken both short path are taken by $\delta \cup \varepsilon$.

In all the cases in Figures 20 - 22, the topmost arc in $\mathcal{R}^d$ is an ε-arc. This implies that ε must take either the left short path in $\mathcal{A}_r$ or the right short path in $\mathcal{A}_l$. The intersection of $\widehat{V}$ with these paths yields the arc ρ_1 connecting ε^- to $\partial_+ P^d$. The bottommost arc in $\mathcal{R}^d$ is a δ-arc.

The same argument implies that δ must take the right short path in $\mathcal{A}_r$ or the left short path in $\mathcal{A}_l$. The intersection of these paths with $\widehat{V}$ yields the ρ_2 arc connecting δ^+ to $\partial_+ P$ as well and the rest of the proof holds. □

Lemma 2.3.7. *If n and m are both non-zero, the curve ε takes all paths on $\Sigma \setminus \partial_+ P$.*

Proof. As ε contains both ε_1 and ε_2 arcs, the two paths through the left annulus are taken by ε. Furthermore, the δ sub-arc which is connected to the intersection point X^u in the right annulus emerges from $\mathcal{R}^d$ between the initial sub-arcs of ε_1 and ε_2. Hence ε takes both paths through the right annulus as well. □

2.4. P is admissible

In this section we show that P is admissible without the assumption that there are no waves with respect to δ and ε.

Lemma 2.4.1. *If ε takes all paths the intersection with the disk C is standard.*

Proof. Recall the discussion (at the beginning of Section 1.3) where the (U, W) Heegaard splitting of $S^3 \setminus \mathcal{N}(K)$ induces a genus one Heegaard splitting (H_1, H_2) of $L = L(p, q)$ with the disk E as a meridian disk for H_2 and the components of $C \setminus \mathcal{N}(P') = C \setminus \mathcal{N}(P)$ are all isotopic to a meridian disk Q of H_1. We concluded then that each component intersects E algebraically the same number of times, p.

The solid torus H_1 is obtained from the handlebody W by attaching the 2-handle $\mathcal{N}(P')$ to ∂W. Thus the disks $P' \times \{0\}$ and $P' \times \{1\}$ become disks on ∂H_1. A priori there can be a difference between the algebraic and geometric intersection between $\varepsilon = \partial E$ and a meridian of H_1.

Choose an orientation on E and on the boundary compression disk Δ of an innermost band of P. The curve $\partial\Delta$ intersects P' or P in a single arc τ and all intersections of Δ with $\varepsilon = \partial E$ have the same orientation: This is because by Lemma 2.1.7, $\partial\Delta \setminus \tau$ is located in one of the rectangles $\mathcal{R}^u$ or $\mathcal{R}^d$ where all ε sub-arcs have the same direction by Proposition 2.1.6.

However Δ is also a meridian disk for H_1 which intersects exactly one of $P' \times \{0\}$ and $P' \times \{1\}$, say $P' \times \{1\}$, in a single interval. Note that because Δ intersects $P' \times \{1\}$, in a single interval any other meridional disk for H_1 which does not intersect $\delta \cup (P' \times \{0\}) \cup (P' \times \{1\})$ is isotopic to Δ rel. $P' \times \{0\}$. (This would not be true if Δ did not intersect $P' \times \{1\}$.) Hence there is no difference between the algebraic and geometric intersection between ∂E and a meridian of H_1

We can label the arcs of $\gamma \setminus \mathcal{N}(\partial_+ P)$ by $(1,1)$, $(0,0)$, $(1,0) = (0.1)$, depending on the whether the endpoints are on $P' \times \{1\}$ or $P' \times \{0\}$. Note that the 1 side of $\mathcal{N}(P)$ corresponds to either $\partial_+ P^u$ or $\partial_+ P^d$, say $\partial_+ P^u$. Hence any $(1,1)$-arc in γ is contained in $\mathcal{R}^u$. Similarly for a $(0,0)$-arc and $\mathcal{R}^d$. The curve ε passes through both rectangles the same number of times so any arc $(1,1)$ or $(0,0)$ meets ε exactly p times.

Because ε takes all paths, by assumption any arc of $\gamma \setminus \partial_+ P$ meets ε at least once. So any disk component of $C \setminus \mathcal{N}(P)'$ which has a $(1,1)$-arc (or $(0,0)$-arc) on its boundary cannot have any other γ sub-arcs on its boundary. Hence there is at most one $(1,1)$ and one $(0,0)$ sub-arcs. This finishes the proof. □

Lemma 2.4.2. *The planar surface P contains two sub-arcs one connecting γ^+ to itself and one connecting γ^- to itself, each intersecting α exactly once (see figure 23).*

Proof. Similarly to the proof of Lemma 2.2.11, assume that a band emanating from an external annulus of P, say $\mathfrak{a}_1$, meets α before it meets γ. Then the band must loop "through the left hole" as in Figure 13 and meet α. If the intersection point $X = \delta \cap \partial_+ P$ is not on the band then $\partial_+ P$ contains a wave. Namely, the arc which is parallel to one of the band boundaries and the part of $\mathfrak{a}_1$ connecting it to the same side of α is a wave. This contradicts Lemma 2.1.4. Thus the intersection point must be on this band and there can be only one such external annulus. As P has at least two external annuli, there is at least one external annulus for whose band connects directly to γ.

This annulus together with its band, up to γ, yields a sub-arc ν_1 connecting the same side of γ, say γ^+, to itself and intersecting α once. Next, as $\partial_+ P$ is a closed curve, it also has a sub-arc ν_2 connecting γ^- to itself, possibly intersecting α a few times. But the existence of ν_1 forces ν_2 to intersect α exactly once. □

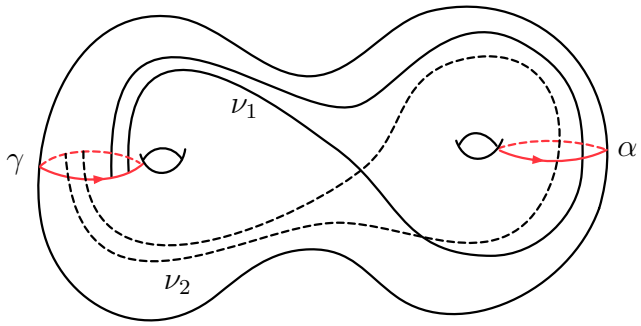

FIGURE 23. The sub-arcs ν_1 and ν_2 of $\partial_+ P$.

Theorem 2.4.3. *The Planar surface P is admissible.*

Proof. If in the description $\varepsilon = m\varepsilon_1 + n\varepsilon_2$ one of m or n are equal to 0 p is admissible by Proposition 2.3.4. If both of $m, n \neq 0$ then by Lemma 2.3.7 the curve ε takes all paths. So by Lemma 2.4.1 the intersection $P \cap C$ is standard.

Assume in contradiction that there is a band $\mathfrak{b}$ in P intersecting C at least twice. The arcs of intersection $\mathfrak{b} \cap C$ define compression disks for $\mathfrak{b}$ contained in C. If the compression disks $\mathfrak{b}$ are not contained in each other then the induced orientation on the arcs of intersection are not consistent which is a contradiction to Lemma 2.4.1. If the compression disks are contained in each other with consistent orientation the band $\mathfrak{b}$ nests itself and cannot continue to eventually form a closed curve. So $\mathfrak{b}$ has a single intersection with C, which is Property (1) of Definition 2.2.5.

Next, assume in contradiction that there are two bands emanating from a vertical annulus and meeting C from the same side. This annulus must be an internal annulus $\mathfrak{a}$. Suppose the bands meeting C from the same side emanate from the same side of $\mathfrak{a}$. Because of Lemma 2.4.2 the bands cannot meet C with compression disks nested in each other as then they must intersect the sub-arcs $\nu_1, \nu_2 \subset \partial_+ P$ as in the proof of Lemma 2.4.2 above. If the compression disks are not nested in each other they induce the wrong orientation on the arcs contradicting Lemma 2.4.1. Suppose the bands meeting C from the same side emanate from the different sides of $\mathfrak{a}$. Because if the

existence of the arcs ν_1 and ν_2 this can happen only if the band emanating from side a of $\mathfrak{a}$ is nested in a band emanating from side b of $\mathfrak{a}$. In this case the induced orientations on the intersection arcs are inconsistent which is a contradiction to Lemma 2.4.1.

Hence there are exactly two bands connected to each internal annulus and these bands connect to different sides of C which is property (2) of Definition 2.2.5. In particular there are two external annuli.

Each of the arcs ν_1 and ν_2 cannot be contained in a band as no bands meets C twice. The arcs ν_1 and ν_2 cannot pass through an internal annuls as this would imply that the annulus has two bands meeting C from the same side. Thus of ν_1 and ν_2 pass through (different) external annuli which implies that the two bands emanating from the external annuli meet C from different sides. This is property (3) of Definition 2.2.5. □

Corollary 2.4.4. *With the above definitions, a planar surface P in a genus two compression body V, so that $\partial_- V$ is a torus, is admissible for some choice of α if and only if it's intersection with the unique non-separating disk in V is standard.*

□

Up to the symmetries in Remark 2.2.1 when the curves δ, ε traverse the rectangles $\mathcal{R}^u$ and $\mathcal{R}^d$ as in Figure 24 in a counter clockwise direction the sequences of intersections with the meridians α, β and γ determine words in α, β and γ.

Lemma 2.4.5. *There is a choice of oriented meridians α, β and γ of V so that the rectangles $\mathcal{R}^u$ and $\mathcal{R}^d$ intersect only γ once as depicted in Figure 24.*

The intersections of α, β and γ with the annuli $\mathcal{A}_r$ and $\mathcal{A}_l$ are measured by the intersections with the rectangles W_{rr}, W_{rl} and W_{lr}, W_{ll} (as in Figure 24) respectively. The corresponding intersections are words denoted by w_{rr}, w_{rl}, w_{lr} and w_{ll} satisfying:

(1) $w_{rr} = \alpha(\gamma\alpha)^t$ and $w_{ll} = \alpha(\gamma\alpha)^s$ for some integers $t, s \geq 0$.

(2) $w_{rl} = \beta(\gamma\beta)^t$ and $w_{lr} = \beta(\gamma\beta)^s$

Proof. The surface P is admissible so by Lemma 2.2.16 we can choose α and by Lemma 2.1.2 we can choose β so that no innermost band meets α or β. Again as P is admissible the rectangular region of Σ confined by an innermost is a rectangle $\mathcal{R}^d$ or $\mathcal{R}^u$. Thus each of $\mathcal{R}^d$ and $\mathcal{R}^u$ intersect γ once. Without loss of generality we can assume that the innermost band in the set $\mathfrak{A}$ is in $\mathcal{R}^d$.

There are two paths emerging from this innermost band into $\mathcal{A}_r$. They enter an annulus on Σ between two vertical annuli. One path turns to the right and the other

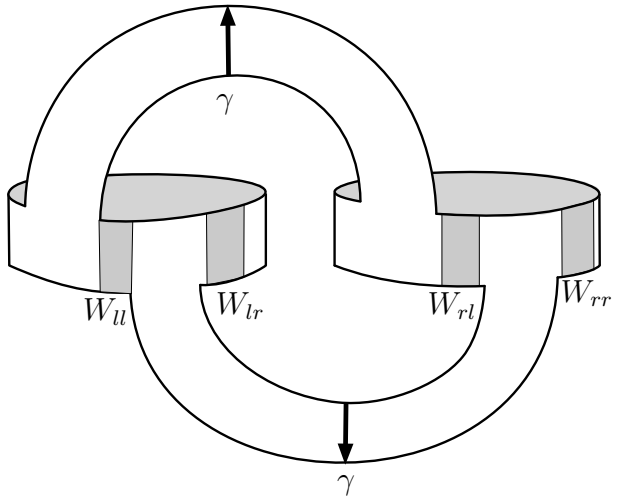

FIGURE 24. The intersections of the four paths with the curves $\{\alpha, \beta, \gamma\}$ as measured in the decomposition $\mathcal{A}_r \cup \mathcal{R}^u \cup \mathcal{A}_l \cup \mathcal{R}^d$.

to the left and they both exit this annulus into the same band, say $\mathfrak{b}_k$, on both sides of the nested bands in $\mathfrak{b}_k$, if there are such nested bands. Let the word w_{rr} describe the intersections of the right path in $\mathcal{A}_r$ as in Figure 25. As the path turns right it must intersect the curve α first and only then intersect γ.

Recall from Remark 2.2.13 and Proposition 2.2.14 in Section 2.2 , that we have a right and left side of C with respect to the innermost bands. Note that a sub-arc of δ or ε can change sides from the right side to the left side of C or vice versa only if it passes through an innermost band. Since these are contained in the rectangles $\mathcal{R}^u$ and $\mathcal{R}^d$ a sub-arc can change sides on C only if it passes through either $\mathcal{R}^u$ and $\mathcal{R}^d$. Hence if a path crosses C on its right (resp. left) side it will still meet its right (resp. left) side the next time it meets C unless it goes through $\mathcal{R}^u$ or $\mathcal{R}^d$.

Thus, as can be seen from Figure 24 the path associated to w_{rr} crosses $\gamma = \partial C$ on its left side. This path must then proceed to cross α and then proceed to meet γ again. This situation might repeat several times, until the path enters the other innermost band at which point we end the symbol w_{rr} as the path then enters the rectangle $\mathcal{R}^u$. Thus either $w_{rr} = \alpha$, or $w_{rr} = \alpha\gamma\alpha \cdots \gamma\alpha$.

Now consider the path emanating from the innermost band and turning left, to which we associate the symbol w_{rl}. Again, as can be seen from Figure 24 the path crosses β and then γ on the right side of C. Consequentially when it continues it intersects β again and so on until it enters the other innermost band. Thus, $w_{rl} = \beta$ or $w_{rl} = \beta\gamma\beta \cdots \gamma\beta$. Since the paths traverse the same bands the symbols w_{rl} and w_{rr} have the same number of letters in them, i.e., they have the same length. A similar argument holds for $\mathcal{A}_l$, w_{ll} and w_{lr}. Thus the intersections are as claimed. □

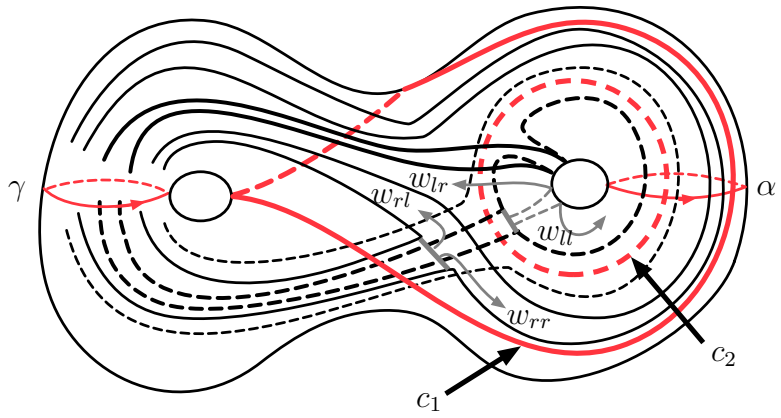

FIGURE 25. The four paths in the complement of an admissible planar surface.

Lemma 2.4.6. *Let P_N be an admissible surface. The core curves $\mathfrak{a}_l$ and $\mathfrak{a}_r$ in the decomposition of $\Sigma \setminus \partial_+ P_N$ bound planar surfaces S^l and S^r so that $\partial_+ S^l = \mathfrak{a}_l$ and $\partial_+ S^r = \mathfrak{a}_r$. Furthermore the components of $\partial_- S^l$ and $\partial_- S^r$ are parallel to $\partial_- P_N$ and we have $|\partial_- S^l \cup \partial_- S^r| = N$*

Proof. Let c_1 and c_2 be the curves as in Figure 25. Note that both c_1 and c_2 bound vertical annuli with ∂_- parallel to $\partial_- P_N$. In what follows and throughout the proof the claims we make rely heavily on the fact that P_N is admissible. If c_1 does not meet a band then P_N cannot have one sided annuli and then c_1 is a core. If c_2 does not meet a band then P_N cannot have two sided annuli and then c_2 is a core. Thus assume that one of the vertical annuli bounded by c_i, $i = 1, 2$, say c_1, meets a band in an arc which defines boundary compression for the band. This arc divides P_N into two planar surfaces. One of these surfaces P' continues along the band in the direction of γ. Define a small push out of P' in the direction, on the vertical annulus, opposite from the boundary compression disk.

If P' does not meet the compression disk of an innermost band, arc sum it with the vertical annulus bounded by c_1. (This operation removes the push out of the boundary compression disk from the vertical annulus.) If P' meets a compression disk of an innermost band, boundary compress P' along that disk. Now arc sum the component of P' after the compression, that meets the vertical annulus, with the vertical annulus. The result is a planar surface S^1 which does not meet a compressing disk of an innermost band. Since $\partial_+ S^1$ does not meet an innermost band it does not meet either $\mathcal{R}^u$ nor $\mathcal{R}^d$ and thus $\partial_+ S^1$ is a core. So it is either $\mathfrak{a}_l$ or $\mathfrak{a}_r$. Perform the

same operation on c_2 to obtain S^2. The only way to connect $\mathfrak{a}_l$ to $\mathfrak{a}_r$ in the complement of $\partial_+ P_N$ is via an innermost band. Therefore the surfaces S^1 and S^2 are disjoint.

No innermost band of P_N meets α. In this case the segments of $\alpha \setminus \partial_+ P_N$ are co-core arcs in the annuli $\mathcal{A}_l$ and $\mathcal{A}_r$ and thus intersect $\partial_+ S^1$ or $\partial_+ S^2$. The bands of the band structure of S^1 and S^2 induced by P_N are parallel to those of P_N. Every such α segment determines a vertical annulus of either P^1 or P^2. Since there are exactly N segments of $\alpha \setminus \partial_+ P_N$ it follows immediately that $|\, \partial_- S^l \cup \partial_- S^r \,| = N$. In particular both $|\, \partial_- S^l \,|$ and $|\, \partial_- S^r \,|$ are less than N. □

Corollary 2.4.7. *Any meridional curve of W intersects both $\mathfrak{a}_r$ and $\mathfrak{a}_l$ multiple times.*

Proof. If there is a meridian of W which intersects one of $\mathfrak{a}_r$ or $\mathfrak{a}_l$ only once chose the corresponding S^i as a new planar surface and which intersect an essential disk of W once. Since P_N was chosen to minimise N this contradicts the minimality of P_N. If W has a meridional disk which does not intersect one of $\mathfrak{a}_r$ or $\mathfrak{a}_l$, the boundary of this meridional disk is contained in a solid torus in S^3 so since S^3 does not contain a nontrivial lens space, K must be a trivial knot in contradiction. □

2.5. Choosing meridians for V

We assume from now on that P_N is an admissible planar surface with $N \geq 2$. We start by choosing new meridional curves for V. We first need a definition:

Definition 2.5.1. Let $\widehat{V} = \{v_1, v_2\}$ be a meridional system for the handlebody V in the (V, W) Heegaard splitting for S^3. We say $\widehat{V}$ satisfies the *intersection property* if every path of $\{\delta, \varepsilon\}$ intersects $\widehat{V}$. Note that if γ is one of the meridians in $\widehat{V}$ then the property is automatically satisfied.

Definition 2.5.2. A concatenation of two paths, π_i and π_j is called a *an extended path* if the π_i is a left (right) path through one of the annuli, and it is followed by π_j which is the right (left) path through the other annulus.

Lemma 2.5.3. *There is a meridional system $\widehat{V} = \{v_1, v_2\}$ for V which satisfies:*

(0) The sub-arcs of $\widehat{V} \setminus \partial_+ P$ are co-core arcs for the rectangles and annuli in the representation of $\Sigma \setminus \partial_+ P$ as $\mathcal{A}_r \cup \mathcal{R}^u \cup \mathcal{A}_l \cup \mathcal{R}^d$.

(1) The intersection property.

(2) If $\widehat{W}$ takes all paths and extended paths, there are no waves with respect to $\widehat{V}$.

Proof. The proof is done by exhibiting an appropriate system of meridians for V for a given admissible planar surface P, and any choice of paths. Recall that by Lemma 2.1.2 there is a fixed choice of a disk $B \subset V$, and denote $\beta = \partial B$. First we have:

Claim: If the paths have conflicting orientations with respect to any curve $v_1 \in \{\alpha, \beta\, \gamma\}$ then we we can choose another curve i$v_2 \in \{\alpha, \beta\, \gamma\}$ so that Properties $(0) - (2)$ are satisfied.

Proof of Claim. Considering the general configuration of the intersection of an admissible P with α, β, γ, as in Figure 24. Properties (0) and (1) are clearly satisfied. Property (2) is also satisfied as it is seen in Figure 24 that *no* path can contain sub-arcs connecting the same side of one of the curves α, β or γ to itself. If there are conflicting orientations and all paths are taken then as in the proof of Lemma 2.2.6 The curve of $\widehat{W}$ must contain the blocking edges $[v_1^+, v_2^+]$ and $[v_1^-, v_2^+]$. Hence by Corollary 1.3.12 there are no waves with respect to $\widehat{V}$. □

Case (I) Assume $P = P_N$ with $N \geq 3$: As noted before, the rectangles always contain γ sub-arcs. Also, as can be seen in Figure 25, at least one of the annuli $\mathcal{A}_l$ or $\mathcal{A}_r$, say $\mathcal{A}_r$, meets a non innermost band $\mathfrak{b}_k$ for some k. As the non-innermost bands meet C the annulus must meet $\partial C = \gamma$. If a path meets both rectangles W_{rr} and W_{rl} then this path meets γ with conflicting orientations, see Figure 25. So by the claim we have the required choice of $\widehat{V}$.

We may thus assume that the two paths through any annulus which meets γ each intersect only one of W_{rr} and W_{rl} (or only one of W_{lr} and W_{ll}).

Assume that there is an annulus, say $\mathcal{A}_l$, that does not meet γ. However the other annulus does meet γ and the rectangles W_{rr} and W_{rl} contain both α and β segments with a certain orientation. So this choice of orientations determines the intersections with $\mathcal{A}_l$. If there are conflicting orientations we are in the case of the claim above. If there are no conflicting intersections each path meets one of the rectangles W_{lr} or W_{ll} once.

Choose $\widehat{V} = \{\alpha, \beta\}$ as a meridian set. As $N \geq 3$ one of the annuli $\mathcal{A}_l$ or $\mathcal{A}_r$ meets an non innermost band and thus meets γ. Hence at least one of the words ω_{ll} and ω_{rr} have multiple appearances of α so after omitting γ from the symbols we obtain the $[\alpha^-, \alpha^+]$ edge. Similarly at least one of the words ω_{lr} and ω_{rl} have multiple appearances of β so we obtain the $[\beta^-, \beta^+]$ edge. So Property (2) is satisfied. Each path intersect either α or β and Property (1) is satisfied. Property (0) is satisfied trivially and we are done.

Case (II) Assume $P = P_2$ (P is standard). Recall that paths are only determined up to Dehn twists in the annuli. Set the base configuration of paths as the four short paths

with respect to $\{\alpha, \beta\}$, i.e. the paths each intersecting either only α or only β once. Every configuration of paths is indexed by μ the number of *positive* Dehn twists twists in $c_1 = \mathfrak{a}_r$ and by ν which counts the number of *negative* twists in $c_2 = \mathfrak{a}_l$.

Assume $\mu \geq 0$ and $\nu < 0$. Note that in the base configuration the intersections of the paths with α in both $\mathcal{A}_l$ and $\mathcal{A}_r$ have consistent orientations, This corresponds to the case $\mu = \nu = 0$. If $\nu \geq 0$ we add Dehn twists with respect to $\mathcal{A}_l$ and this flips the orientations in $\mathcal{A}_l$ while keeping the orientations in $\mathcal{A}_r$. So we have conflicting orientations and we are done by the Claim above. Similarly for the case or $\mu < 0$ and $\nu \geq 0$ and $\mathcal{A}_r$.

Thus, we may assume that $\mu < 0$ if and only if $\nu < 0$. As the third symmetry in Remark 2.2.1 interchanges the left and right in each annulus, and hence interchanges α and β we need to prove the lemma in the cases that either $\mu = \nu = 0$ or $\mu, \nu > 0$.

(a) In case $\nu = \mu = 0$. Choose the meridian set $\{\alpha, \beta\}$. Properties (0) and (1) are satisfied as before. By Lemma 2.4.5 we have up to symmetries $\omega_{rr} = \omega_{ll} = \alpha$, and $\omega_{rl} = \omega_{lr} = \beta$. As P is standard each of the rectangles $\mathcal{R}^u$ and $\mathcal{R}^d$ does not meet α or β. The extended path through ω_{rr} and ω_{ll} gives us the $[\alpha^-, \alpha^+]$ edge. Similarly extended path through ω_{rl} and ω_{lr} give us the $[\beta^-, \beta^+]$ edge. Hence we have Property (2) as well.

(b) Assume $\nu, \mu > 0$. In this case there is a wave η with respect to α intersecting $\partial_+ P$ once as in Figure 26 contradicting Corollary 2.1.5 □

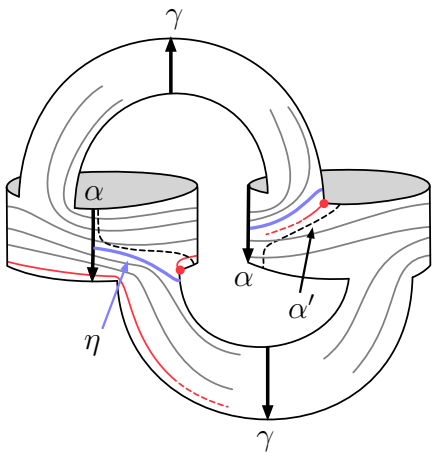

FIGURE 26. The wave η with respect to α for Case (b) where $\mu, \nu > 0$.

Remark 2.5.4. It follows from the proof of Lemma 2.5.3 that we can always choose $\widehat{V}$ to be $\{\alpha, \beta\}$.

CHAPTER 3

Obtaining the contradiction

In this chapter we prove that we can always choose a meridional system $\widehat{W}$ so that together with a system of $\widehat{V}$, chosen in Section 2.5, the Heegaard diagram $\{\widehat{V}, \widehat{W}\}$ has high complexity and no waves.

First it is shown in Section 3.1 that when the curve δ takes a long path or δ takes all paths then (V, W) is not a Heegaard splitting of S^3. Then in Sections 3.2 and 3.3 it is shown that when δ takes three paths then (V, W) is not a Heegaard splitting of S^3. In Section 3.4 it is shown that when δ takes only two paths then (V, W) is not a Heegaard splitting of S^3 and in Section 3.5 these results are combined to give the proof of Theorem 0.0.4.

3.1. Choosing meridians for W

In this section we prove that δ does not take a long path with respect to $\widehat{V}$ and that we can modify the meridional system for W so that when δ takes all paths the Heegaard diagram $\{\widehat{V}, \widehat{W}\}$ has high complexity and no waves.

Lemma 3.1.1. *We may assume that the curve δ takes only short paths with respect to $\{\alpha, \gamma\}$ or to $\{\alpha, \beta\}$.*

Proof. By the proof of Lemma 2.5.3 if δ takes a long path, say in $\mathcal{A}_r$, there is at least one path in $\mathcal{A}_l$ with conflicting orientations.

Assume therefore, that δ takes a path in $\mathcal{A}_l$ intersecting α with conflicting orientations. In this case α contains an innermost arc ρ connecting δ^- to δ^- and meeting $\partial_+ P$ once. This can be seen as follows: By Lemma 2.4.5 if δ intersects α in both annuli, it intersects W_{rr} and W_{ll} so it intersects all segments $\alpha \setminus \partial_+ P$. Hence there must be a segment in $\mathcal{A}_r$ which connects through $\partial_+ P$ to a segment in $\mathcal{A}_r$. If ρ meets ε then if an innermost segment of $\rho \setminus \varepsilon$ connects intersection points of ε with conflicting orientations we have a wave with respect to ε. Performing a wave move will eliminate these intersection points. If ρ does not meet ε or if all intersection points with ε are eliminated, as above, then we have a wave with respect to δ which intersects $\partial_+ P$ at

most once. The new meridian obtained by the wave moves contradicts the minimality of δ, see Proposition 1.3.14.

Thus we may assume that there are intersection points of $\varepsilon \cap \rho$ which have the same orientations and since the adjacent intersections with δ have conflicting orientations we obtain the blocking edges $[\delta^-, \varepsilon^+]$ and $[\delta^-, \varepsilon^-]$ for $\widehat{W}$. Finally, as δ meets α with conflicting orientations we also have blocking edges $[\alpha^+, \beta^+]$ and $[\alpha^+, \beta^-]$ with respect to $\widehat{V}$ by the Claim in the proof of Lemma 2.5.3.

The only option left is that there is only one path in $\mathcal{A}_l$ whose intersections with the segments of $\{\alpha, \beta\}$ are conflicting with the orientations of the long path that δ takes in $\mathcal{A}_r$. Furthermore, only ε takes that path. In this case δ does not intersect α in $\mathcal{A}_l$.

Assume P_N is not standard ($N \geq 3$) and the number i of α segments in $\mathcal{A}_r$ is larger than the number of α segments in $\mathcal{A}_l$. The point Y^u between the two rectangles W_{rr} and W_{rl} in $\mathcal{A}_r$ is identified with the point Y^d between the two rectangles W_{lr} and W_{ll} in $\mathcal{A}_l$ (see Figure 25). The top endpoint of the γ segment in $\mathcal{R}^u$ is the i-th γ intersection to the left of Y^u, and is thus glued to the i-th γ intersection to the left of Y^d, which is the bottom endpoint of a γ segment in $\mathcal{A}_r$. The curve γ contains an innermost arc ρ connecting δ^+ to δ^+ which also meets $\partial_+ P$ once. Hence we reach a contradiction as in the previous paragraphs.

Assume that the number of α segments in $\mathcal{A}_l$ is larger than the the number i of α segments in $\mathcal{A}_r$. Then the point X^u, lies i α segments to the left of Y^u. It is identified with a point X^d which lies i α segments to the left of Y^d which by assumption is in W_{lr}. This implies that the δ tail does intersect α with orientations conflicting with the orientations of the intersections of the long path in $\mathcal{A}_r$ with α. This is again a contradiction by the same argument as above as α contains an innermost arc ρ connecting δ^- to δ^- and meeting $\partial_+ P$ once.

Thus the number i of α segments in $\mathcal{A}_l$ equals the number of α segments in $\mathcal{A}_r$ and the position of the point X^d is as in Figure 27. Consider the top endpoint of the γ segment in $\mathcal{R}^u$. It is the first γ intersection of $\partial_+ P^u$ to the left of X^u and thus is identified to the first γ intersection of $\partial_+ P^d$ to the left of X^d, which is the top endpoint of the γ segment in $\mathcal{R}^d$. The bottom endpoint of the γ segment in $\mathcal{R}^u$ is the i-th γ intersection to the right of Y^u, and is thus identified to the i-th γ intersection to the right of Y^d, which is the bottom endpoint of the γ segment in $\mathcal{R}^d$. We conclude that γ consists entirely of the two segments in the rectangles $\mathcal{R}^u$ and $\mathcal{R}^d$, and does not intersect the annuli $\mathcal{A}_l$ and $\mathcal{A}_r$, therefore P is standard and $i = 1$.

There are now two cases:

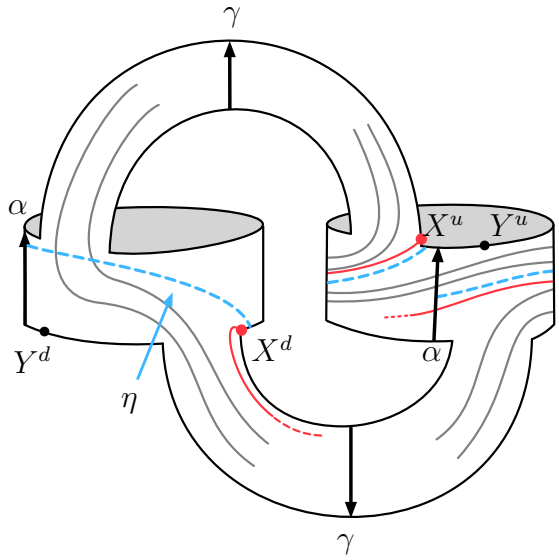

FIGURE 27. The wave η with respect to α for Case (b) where $\mu, \nu > 0$.

Case (1): The δ head intersects α in $\mathcal{A}_r$. The arc η depicted in Figure 27 is an s-wave with respect to α. All the δ-arcs which intersect η in $\mathcal{A}_l$ intersect the top part of α in $\mathcal{A}_r$. So the corresponding intersection points in $\mathcal{A}_r$ are eliminated by the wave move plus an additional intersection point with the δ-head which is also removed by the wave move. Note that η intersects $\partial_+ P$ in a single point. Thus the new meridian intersects K once and this is a contradiction to the minimality of α.
Case (2): The δ-head does not intersect α in $\mathcal{A}_r$. Note that in this case no path intersects α twice and hence the path that appears long within $\mathcal{A}_r$ in Figure 28 is not long according to Definition 2.3.5. The closed curve β' depicted in Figure 28 can be isotoped to two vertical co-core arcs for the annuli $\mathcal{A}_l$ and $\mathcal{A}_r$ without changing α or γ. In this configuration the paths that δ takes in both annuli are short paths. This finishes the proof with respect to $\{\alpha, \gamma\}$.

Furthermore note that the curve β' does not intersect α or γ, and hence is a new meridian. The meridian β' intersects W_{ll}, W_{lr}, W_{rl} and W_{rr} as does β in Lemma 2.4.5. As it is obtained by a wave move on γ intersecting $\partial_+ P$ once the wave move has to be ω_2 as in Figure 6. Thus the meridian β' is equal to the meridian β and intersects the knot K once. This finishes the proof with respect to $\{\alpha, \beta\}$.

Now assume that δ takes a long path in $\mathcal{A}_l$. If this long path meets a single segment of α twice then we have an s-wave η'' with respect to α, depicted in Figure 29. The curve δ meets the new meridian α', obtained after the η'' wave move in conflicting orientations. Thus, after perhaps a finite number of wave moves with respect to ε, either we have a wave with respect to δ meeting $\partial_+ P$ once which contradicts the minimality assumption

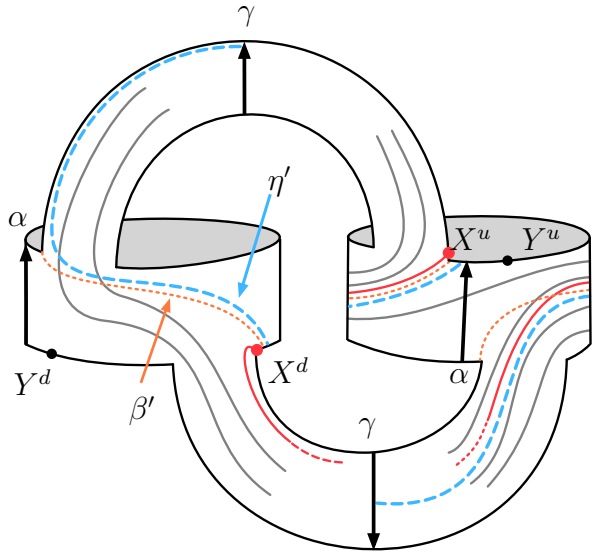

FIGURE 28. The wave η' with respect to γ and the new meridian β' for Case (2) where $\mu, \nu > 0$.

1.3.4, or we have blocking edges with respect to both V and W, but the complexity is still at least four contradicting Theorem 1.3.10.

If the path meets all α segments only once then the curve η'' depicted in Figure 29 can be slightly elongated at its endpoints parallel to δ to become a wave with respect to γ. The resulting meridian β'' can be "straightened" as above to obtain a meridional system $\{\alpha, \beta''\}$ with respect to which δ takes only short paths. This completes the proof with respect to $\{\alpha, \gamma\}$. Furthermore, as η'' intersects $\partial_+ P$ once, the meridian bounded by β'' intersects K once and β'' intersects W_{ll}, W_{lr}, W_{rl} and W_{rr} as does β in Lemma 2.4.5. We therefore rename it as β. This finishes the proof with respect to $\{\alpha, \beta\}$. □

Lemma 3.1.2. *In the description $\varepsilon = m\varepsilon_1 + n\varepsilon_2$, $m, n \in \mathbb{N} \cup \{\emptyset\}$ (before Proposition 2.3.4) both m, n are greater than zero.*

Proof. Fix $\widehat{V}$. If δ takes more than two paths then by Lemma 3.1.1 there is one annulus $\mathcal{A}_l$ or $\mathcal{A}_r$ in which all paths are short as there are only two paths in each annulus. If one of $m, n = 0$ then by Corollary 2.3.6there are no wave with respect to $\{\delta, \varepsilon\}$. There are no waves with respect to $\widehat{V}$ as $\{\delta, \varepsilon\}$ together take all paths since there cannot be any empty paths.

Assume therefore that δ takes exactly two paths. If takes a left path in one annulus and a right path in the other then δ does not meet either α or β, see Figure 30, which is a contradiction by Lemma 1.3.3.

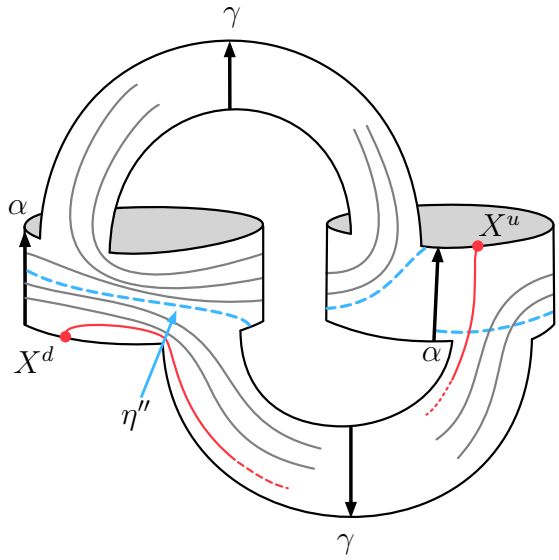

FIGURE 29. The s-wave η'' with respect to α for Case (2).

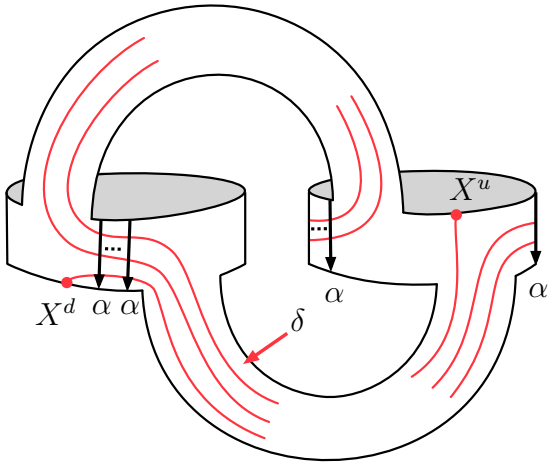

FIGURE 30. δ takes a right path in one annulus and a left path in the other.

So we can assume up to symmetries that δ takes the right path in both $\mathcal{A}_l$ and $\mathcal{A}_r$. Let $\varepsilon = m\varepsilon_1 + n\varepsilon_2$, then $m \neq 0$ as there cannot be an empty path. If $n = 0$ then ε does not split and hence $m = 1$ as otherwise ε will consist of at least two parallel curves. Thus ε intersects the cores $\mathfrak{a}_r$ and $\mathfrak{a}_l$ exactly once contradicting Corollary 2.4.7, see Figure 31. □

Remark 3.1.3. In particular, as ε is a single curve $g.c.d.(m, n) = 1$.

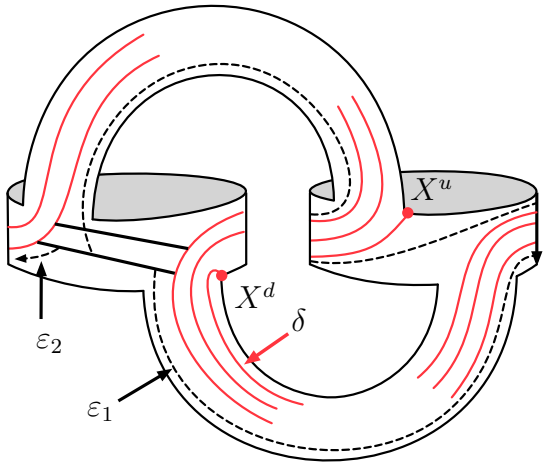

FIGURE 31. δ takes a right path in both annuli. Note that regardless of the number of δ-arcs in $\mathcal{R}^u$ the curve ε_1 is fixed.

Recall the arc Ψ defined in Section 2.3. It is a representative of the class of arcs from I_0 to I_1. Obtain a simple closed curve Ψ' from Ψ by adding an arc π between its endpoints to close it up to a simple closed curve. Choose π as follows:

The δ-tail emerges from the point X^d and turns either right or left. Connect the endpoint of Ψ that lies on I_1 to a point on $\partial_+ P^d$ to the right of X^d if the δ-tail turns left and to the left of X^d if the δ-tail turns right (see Figure 32). The arc π emerges from $\partial_+ P^u$ at a point either to the right or left of X^u. It continues away from X^u running parallel to $\partial_+ P^u$ until it reaches J_l^u and then connects to the other endpoint of ψ on I_0. An example of this is shown in Figure 32.

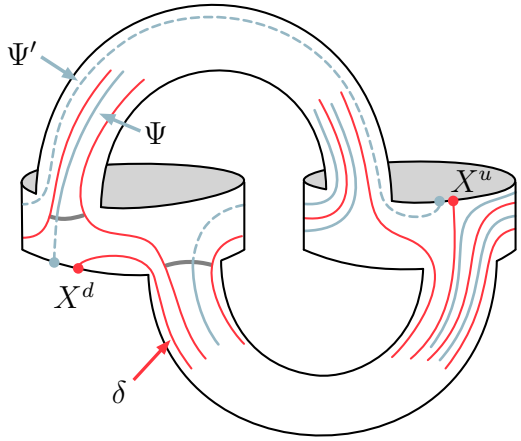

FIGURE 32. An example of the curve Ψ'

Lemma 3.1.4. *Given a curve $\varepsilon = m\varepsilon_1 + n\varepsilon_2$, there is a sequence of curves $\varepsilon = \varepsilon^1, \dots, \varepsilon^{k+1}$, each bounding a disk in V and a sequence of waves ω^i with respect to ε^i, $i = 1, \dots, k$, so that ε^{i+1} is obtained by performing a wave move along ω^i on ε^i. The waves ω^i can be chosen so that after preforming these wave moves successively, ε is replaced by $\varepsilon' = \varepsilon^{k+1}$ where ε' is one of $|m-n|\varepsilon_i + (\min\{m,n\})\Psi'$, where $i = 1$ or 2. In particular ε' will contain sub-arcs of only one type, either ε_1 or ε_2.*

Proof. By Lemma 3.1.2 the curve ε contains both ε_1 and ε_2-arcs. Hence there is a wave with respect to ε, shown in Figure 33 and denoted by ω^1, which is obtained as follows:

First note that since the point X^u is contained in J^u_r it is possible to connect $\partial_+ P^u$ to ε^- by an arc starting at a point just to the right of X^u. We can also connect $\partial_+ P^u$ to ε^+ by an arc starting at a point just to the to the left of X^u. These short arcs do not intersect α and γ.

If the δ-tail turns right (left) we choose the above short arc to the left (right) of X^u. This chosen arc can then be continued from a point to the left (right) of X^d on $\partial_+ P^d$ to meet ε^+ (or ε^-). The concatenation of these arcs is the required wave ω^1.

If ω^1 emerges to the right of X^d then it will connect $\partial_+ P^d$ to the leftmost arc of ε parallel to ε_2. Hence, in this case the wave move removes the leftmost arc parallel to ε_2 and the leftmost arc parallel to ε_1 from ε, and adds Ψ' to it.

If ω^1 emerges to the left of X^d then ω^1 connects $\partial_+ P^d$ to the rightmost arc of ε parallel to ε_1. Hence, in this case the wave move removes the rightmost arc parallel to ε_1 and the rightmost arc parallel to ε_2 from ε, and adds Ψ' to it. Therefore, in both cases, the new curve ε^2 is given by $\varepsilon^2 = (m-1)\varepsilon_1 + (n-1)\varepsilon_2 + \Psi'$.

If ε^2 still contains arcs of both types ε_1 and ε_2 there is a second wave with respect to it denoted by ω^2 which is parallel to ω^1 and which can be continued at its endpoints till it meets ε^2. Since $\varepsilon = m\varepsilon_1 + n\varepsilon_2$ and at each step we obtain a curve with the coefficient of both of ε_1 and ε_2 reduced by one this procedure can continue $k = \min\{m,n\}$ times and results in a curve ε^{k+1} with the desired form. □

Lemma 3.1.5. *If δ takes all paths then (V, W) cannot be a Heegaard splitting of S^3.*

Proof. Choose $\widehat{V}$ as in Lemma 2.5.3 and let $\widehat{W} = \{\delta, \varepsilon'\}$. As δ takes all paths, by assumption, it also takes all extended paths. By Property (2) of Lemma 2.5.3 there are edges in the $\Gamma(\widehat{V})$ graph which prevent waves with respect to $\widehat{V}$.

We now show that there are always two adjacent ε' sub-arcs along one of the paths. As δ takes all paths Ψ must go through $\mathcal{R}^d$. Recall that Ψ is a sub-arc of both Ψ' and ε_i for $i = 1, 2$. Hence the only way we can fail to have two adjacent ε' sub-arcs in

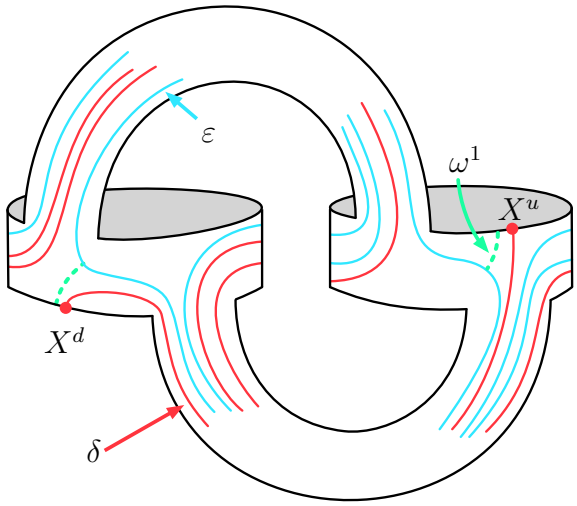

FIGURE 33. The wave ω^1 with respect to ε, in this case it is on the left of X^u and X^d as the δ tail turns right.

$\mathcal{R}^d$ is if the coefficient of Ψ' is 1 and the coefficient of ε_i is 0, namely if $\varepsilon' = \Psi'$ and $m = n = 1$ in the original ε.

We show that this cannot happen: In this case the top and bottom sub-arcs in $\mathcal{R}^d$ are δ sub-arcs, and these arcs take different paths in $\mathcal{A}_r$ by the assumption that δ takes all paths. Hence we can connect J_r^d to both sides δ^+ and δ^- by arcs ρ_1 and ρ_2 which do not meet Ψ'. The segment J_r^d is glued to J_l^u and the arc Ψ' is either to the left or right of J_l^u. Thus ρ_1 and ρ_2 can be continued to connect to either δ^+ or δ^-. So one of them connects the same side of δ to itself. Hence it is a wave with respect to δ intersecting $\partial_+ P$ once, contradicting the minimality of δ.

We conclude that both coefficients of ε' are non zero and hence here are two adjacent ε'-arcs in $\mathcal{R}^d$. Furthermore, as the δ-head connecting to X^u separates between the two paths in $\mathcal{A}_r$, the two adjacent ε'-arcs continue through the same path in $\mathcal{A}_r$ and into $\mathcal{R}^u$, thus they are adjacent along an entire path.

We next turn to prove there are two adjacent δ-arcs in a path. As δ takes both paths in $\mathcal{A}_r$, either the ε-arcs on the left of δ-head or the ε-arcs on the right of the δ-head vanish, as either ε_1 or ε_2-arcs do not appear in ε'. Thus the δ-head connecting to X^u is adjacent to another δ-arc in $\mathcal{R}^d$. Furthermore, since Ψ passes between the two paths in $\mathcal{A}_l$ these two δ-arcs must belong to the same path in $\mathcal{A}_l$.

As there are two adjacent ε'-arcs and two adjacent δ-arcs along entire paths, these adjacent sub-arcs will intersect a meridian in $\widehat{V}$ at least once, as $\widehat{V}$ was chosen to satisfy Property (1) in Lemma 2.5.3 i.e., Each path intersects $\widehat{V}$. Thus we have the $[\delta^-, \delta^+]$

and $[\varepsilon'^-, \varepsilon'^+]$ blocking edges in the Whitehead graph $\Gamma(\widehat{W})$ and there are no waves with respect to $\widehat{W}$.

The complexity of the systems $\{\delta, \varepsilon'\}$ and $\{v_1, v_2\} \subset \{\alpha, \beta, \gamma\}$ is at least 4 and there are no waves with respect to both $\widehat{V}$ and $\widehat{W}$. Hence by Corollary 1.3.12 and Theorem 1.3.10 (V, W) is not a Heegaard splitting of S^3. □

3.2. One path in $\mathcal{A}_l$ and two paths in $\mathcal{A}_r$

In this section we assume that δ takes one path in $\mathcal{A}_l$ and two paths in $\mathcal{A}_r$ and we prove the following:

Lemma 3.2.1. *The Heegaard splitting (V, W) cannot be a Heegaard splitting of S^3 when the curve δ takes a single path in $\mathcal{A}_l$ and two paths in $\mathcal{A}_r$.*

Proof. Fix $\widehat{V} = \{\alpha, \beta\}$ and using the symmetries as in Remark 2.2.1 assume that δ takes the right path in $\mathcal{A}_l$ is as in Figure 34.

Recall that the intervals I_0 and I_1 were chosen so as to indicate the areas in the annulus $\mathcal{A}_l$ where sub-arcs of ε meet and diverge. In the case in question it is more convenient to locate the intervals I_0 and I_1 as in Figure 34 which is slightly different than the location in Section 2.3.

There are two possibilities for the ε curves and the intervals I_0 and I_1 which are depicted as Case (i) and (ii) in Figure 34, i.e., Either ε takes two short paths in $\mathcal{A}_r$ (Case (i)) or one short and one long path (Case (ii)). Both cases must be considered:

Case (i): We claim that in this case the sub-arc Ψ_0 of Ψ adjacent to the bottom edge of $\mathcal{R}^u$ contains at least two sub-arcs of ε': Since the coefficients of ε_1 and ε_2 are both non-zero the arc Ψ_0 contains at least two sub-arcs of ε. Let ω^1 be the first wave move on ε guaranteed by Lemma 3.1.4. In this case the wave ω^1 connects a point to the right of $X^d \subset \partial_+ P^d$ to ε_2 and the continuation of ω^1 emerges to the right of X^u and connects it to Ψ. An arc of type ε_2 passes through Ψ_0 exactly once and the ω^1 wave move on ε replaces a sub-arc of type $\varepsilon_2 \setminus \Psi_0$ by ω^1. Neither ω^1 nor the replaced sub-arc arc meets Ψ_0. Hence the number of ε_2-arcs through Ψ_0 is the same as the number of ε-arcs through Ψ which is at least two.

The following waves $\omega^2, \ldots, \omega^n$ (where n is the coefficient of ε_2 in ε) are all parallel to ω^1 except for minute continuations at their ends, so the same argument applied to these waves shows that after all the wave moves the number of ε'-arcs in Ψ_0 is the same

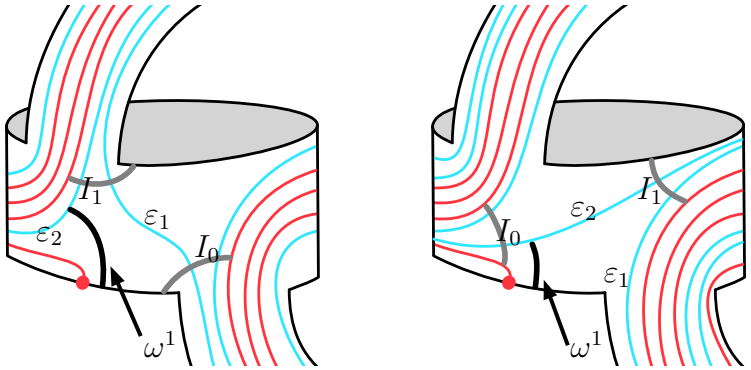

FIGURE 34. The two choices for ε_1 and ε_2, and accordingly I_0, I_1 and Ψ, given a single short path taken by δ in $\mathcal{A}_l$. Note that the path taken by δ in (i) is the right path, but it becomes the left path for the second choice of ε paths as in (ii).

as the number of ε-arcs in Ψ. Hence ε' contains adjacent arcs in Ψ_0 which intersect either α or β in $\mathcal{A}_r$ these give the $[\varepsilon'^-, \varepsilon'^+]$ edge in $\Gamma(\widehat{W})$.

As the ω^i waves connect ε_2 to Ψ, after the wave move, there are no ε_2 sub-arcs in ε'. Hence the δ-tail will be adjacent to the first δ sub-arc above it $\mathcal{A}_l$. These two adjacent δ-arcs give the $[\delta^-, \delta^+]$ edge in $\Gamma(\widehat{W})$. Together we have the blocking edges for $\widehat{W}$.

Now consider $\widehat{V}$. The curve ε' contains ε_1-arcs, which are not affected by the wave moves, so it takes the path through $\mathcal{A}_l$ that δ does not take. There is an ε' sub-arc continuing from the right path in $\mathcal{A}_r$ to the left path in $\mathcal{A}_l$ and a δ sub-arc continuing from the right path in $\mathcal{A}_l$ to the left path in $\mathcal{A}_r$. Thus, by Lemma 2.5.3, we have the required blocking edges to prevent waves with respect to $\widehat{V}$.

The complexity of the systems $\{\delta, \varepsilon'\}$ and $\{\alpha, \beta\}$ is at least 4 and there are no waves with respect to both $\widehat{V}$ and $\widehat{W}$. Hence by Theorem 1.3.10 (V, W) is not a Heegaard splitting of S^3.

Case (ii): In this case we need to deal with three different sub-cases.

Sub-case (a) $m = n = 1$:

Note that the top and bottommost arcs in $\mathcal{R}^d$ are both δ-arcs which become adjacent in $\mathcal{R}^u$ and thus in $\mathcal{A}_l$. Furthermore the bottom arc is the δ-tail. Hence δ passes through the right path of $\mathcal{A}_l$ at least once more than ε'. The intersection point of ε' with $\partial_+ P$ can be slid to the right, which occurs simultaneously in both $\mathcal{A}_l$ and $\mathcal{A}_r$ (see Figure 35). This slide eliminates at least one of the intersections of ε' with $\widehat{V}$ in $\mathcal{A}_l$.

By Lemma 2.4.5, both paths in $\mathcal{A}_l$ have the same number of intersection points with $\widehat{V}$ thus ε' is strictly shorter than δ. It intersects $\partial_+ P$ in one point, contradicting the minimality of δ. This finishes Sub-case (a).

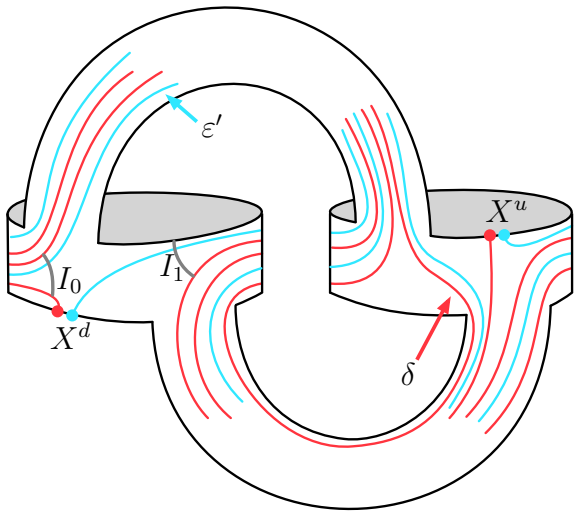

FIGURE 35. The curve ε', which is a contradiction to the minimality of δ in the case $m = n = 1$.

For all other cases, note that since the waves ω^i connect ε_1-arcs near X^u to Ψ arcs near X^d, once all the wave moves are performed, there will be no more ε_1-arcs arriving through R^d between the δ-head and the δ-arc to its right (which must exist as δ takes both paths in $\mathcal{A}_r$ by assumption). Since g.c.d.$(m, n) = 1$ by 3.1.3, $m \neq n$. Note that if $m > n$ the curve ε' (obtained by Lemma 3.1.4) will be obtained after n wave moves. However we must perform $m-n$ additional wave moves to remove all m arcs of type ε_1. The meridian obtained after $m - n$ additional wave moves will be denoted by ε''. Let ε^* denote either ε' or ε''. (The distinction between ε' and ε'' will be stated explicitly when needed.)

The curve ε^*, created by the wave moves is not tight and we describe the result of a tightening isotopy on it. The m wave moves create m intersection points of ε^* immediately to the right of X (both X^u and X^d). We tighten one intersection point at a time, starting with the rightmost intersection point as follows:

Tightening procedure

(1) If $n > m$ the m intersection points $\varepsilon^* \cap \partial_+ P^d \subset \mathcal{A}_l$ (corresponding to m waves) can be slid to the right until they are contained in a small arc κ in $\partial_+ P^d$, adjacent to $\mathcal{A}_l \cap R^d$. The arc κ is chosen so as to not meet $\widehat{V}$. The m

intersection points to the right of X^u are also slid simultaneously to the right. Note that the resulting curve is tight and the procedure is finished.

(2) If $n < m$ use the same procedure as above to tighten the rightmost n intersection points. If at the end of the slide these points are in $\mathcal{A}_r$ or in R^u the curve ε^* is tight and the procedure is finished.

(3) If $n < m$ and at the end of the slide these intersection points are in $\mathcal{A}_l$ the curve ε^* is still not tight and we must keep tightening it. There are now some segments of ε^* contained in $\mathcal{A}_l$, which start at $\partial_+ P^u$ and after crossing some $\widehat{V}$ segments from right to left, end on $J_l^d \subset \partial_+ P^d$. Slide the intersection points on $\partial_+ P^d$ to the right of J_l^d till these segments become vertical.

(4) The slides above will correspond to sliding intersection points in $\partial_+ P^u$ which might create additional diagonal segments if $m > 2n$. Continue to perform the previous slide until there are no more diagonal ε^* segments in $\mathcal{A}_l$. Now ε^* consists of exactly two types of arcs. One type has one endpoint in $\mathcal{A}_r \cap \partial_+ P^u$, or in $\mathcal{A}_l \cap \partial_+ P^u$, or in $R^u \cap \partial_+ P^u$, and then continues into the right path in $\mathcal{A}_l$ above the δ-tail and ends on $\kappa \subset \partial_+ P^d$. The other type consists of vertical segments contained in $\mathcal{A}_l$. (Some of these may start in R^u and end immediately to the right of X^d so that they are also vertical.) Note that the exact configuration depends on the number of intersections with $\widehat{V}$ in $\mathcal{A}_r$ and $\mathcal{A}_l$. The obtained curve ε^* is now tight.

Sub-case(b) $n > 1$:

When $m < n$ the curve ε^* contains ε_2-arcs. When there are ε_2-arcs or ε^*-tails starting in $\mathcal{A}_l$ (and continuing into the right path in $\mathcal{A}_l$) then these arcs/tails intersect one of α or β with conflicting orientations compared to other intersections of α or β. They will connect α^+ to β^+ in $\mathcal{A}_l$ giving the $[\alpha^+, \beta^+]$ edge. The topmost δ-arc in $\mathcal{A}_l$ connects $\beta^\mp$ to $\alpha^\pm$ thus we have the $[\alpha^\pm, \beta^\mp]$ edge and hence blocking edges with respect to $\{\alpha, \beta\}$.

The meridian in $\widehat{V}$ which ε^* intersects with conflicting orientations in $\mathcal{A}_l$ contains a sub-arc yielding the $[\delta^+, \varepsilon^+]$ edge. The other meridian in $\widehat{V}$, which both δ and ε^* intersect with consistent orientations gives rise to the $[\delta^+, \varepsilon^-]$ edge. Thus we have blocking edges with respect to $\{\delta, \varepsilon^*\}$.

Summing up, when either $m < n$ or if there are ε^*-tails starting in $\mathcal{A}_l$ we have blocking edges for both $\widehat{V}$ and $\widehat{W}$. Note also that δ takes two paths in $\mathcal{A}_r$ which intersect $\widehat{V}$ so the complexity is greater than two. So by Theorem 1.3.10 the Heegaard splitting (V, W) is not a Heegaard splitting for S^3.

Since $n > 1$ there are two adjacent ε_2-arcs in ε^* which intersect α or β and define an $[\varepsilon^{*-}, \varepsilon^{*+}]$ edge. Since there are no more ε_1-arcs then the δ-head is adjacent to another δ-arc and together they intersect a β segment in $\mathcal{A}_l$ giving a $[\delta^-, \delta^+]$ edge. Note that the tightening procedure did not remove these $[\varepsilon^{*-}, \varepsilon^{*+}]$ and $[\delta^-, \delta^+]$ edges. If there are two α intersections in $\mathcal{A}_r$ we have the $[\alpha^-, \alpha^+]$ edge from any arc taking the right path in $\mathcal{A}_r$ and the $[\beta^-, \beta^+]$ edge from any arc taking the left path or vice versa. Thus we have the required edges for both $\widehat{V}$ and $\widehat{W}$ in this case.

The remaining case: $m > n > 1$, there is a single α segment in $\mathcal{A}_r$, and no ε^*-tails starting in $\mathcal{A}_l$.

Remark 3.2.2. Note that δ intersects a single meridian α or β in $\mathcal{A}_l$. As δ takes two paths in $\mathcal{A}_r$ and both merge into the same path in $\mathcal{A}_l$, this meridian is met by δ in $\mathcal{A}_l$ more times than the other meridian is met in $\mathcal{A}_r$. Therefore the meridian δ intersects in $\mathcal{A}_l$ must be β since the minimality assumption (Assumption 1.3.4) applies to α and not to β. Furthermore the segment in the right path in $\mathcal{A}_r$ is an α segment and the segment in the left path in $\mathcal{A}_r$ is a β segment.

With these assumptions there is no $[\alpha^-, \alpha^+]$ edge and we show that by performing wave moves on β we obtain a new system of disks $\{\alpha, \beta'\}$ for V for which we do have the $[\alpha^-, \alpha^+]$ and $[\beta'^-, \beta'^+]$ edges:

Denote the last intersection point of the δ-head (δ_h) with some segment $\xi \subset \beta \in \widehat{V}$ in $\mathcal{A}_l$ before meeting X^u in $\mathcal{A}_r$ by p_h. The bottommost arc through R^d must be a δ-arc as there are no more ε-arcs of type ε_1 (since they were removed by the m wave moves). Denote this bottommost δ arc by δ_b. After passing through $\mathcal{A}_r$ it continues through R^u into $\mathcal{A}_l$ and intersects all the β segments met by the right path in $\mathcal{A}_l$ including ξ. Denote the intersection point of δ_b with ξ by p_b.

The dashed arc starting and ending on β^+ in $\mathcal{A}_l$ in Figure 36 is a wave denoted by η. The wave move on η removes the part of β between the endpoints of η which is contained in $\mathcal{A}_l$, and adds η instead. There is a wave parallel to η and extended at its endpoints for each β segment in $\mathcal{A}_l$. Perform all such wave moves on β. Each wave move removes some part of β contained in $\mathcal{A}_l$.

If δ_b meets β again after passing through $\mathcal{R}^d$, one can extend the endpoints of η further into and through $\mathcal{R}^d$ parallel to the δ and ε^* arcs. (Note that δ_b meets β again if and only if p_b is below p_h.) As both arcs extending η are above the δ-head in R^d they will both take the left path in $\mathcal{A}_r$ and meet the unique β segment in $\mathcal{A}_r$. This defines a wave η' and we perform the wave move along η'. We now can extend the endpoints of η' through R^u into $\mathcal{A}_l$ till they meet the first β segment. This defines a

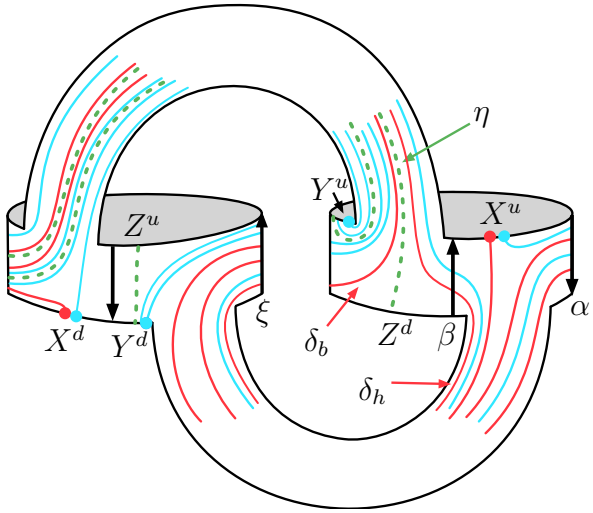

FIGURE 36. The wave η with respect to β, when there is a single α intersection in $\mathcal{A}_r$.

wave η'' and again we perform the wave move along η''. The endpoints of η'' can be extended in $\mathcal{A}_l$ till they meet ξ. Now the top endpoint of the extension of η'' on ξ lies just above an intersection point of δ and ξ which is the next intersection of δ_b and ξ and which we denote by p_b^1. Note that p_b^1 is above p_b as it is determined by an arc in $\mathcal{R}^u$ which is above the arc determining p_b. Iterate this procedure to obtain a collection of points $\{p_b^i\}$, $0 \leq i \leq i_0$, where p_b^{i+1} is above p_b^i. The process can continue as long as p_b^i is below p_h, thus $p_b^{i_0}$ is either above p_h or equal to p_h.

Suppose $p_b^{i_0}$ is above p_h on ξ: As the δ sub-arc between p_b and $p_b^{i_0}$ does not have any intersections with the β' curve obtained after the wave moves, its continuations in both directions meet α segments and this gives the $[\alpha^-, \alpha^+]$ edge. The $[\beta'^-, \beta'^+]$ edge is obtained from the δ-tail which starts at X^d intersects a β' segment in $\mathcal{A}_l$ continues through $\mathcal{R}^d$ and intersects a β' segment on $\mathcal{A}_r$ connecting β'^- to β'^+.

Since β' replaced β in the argument, we need to show the existence of the $[\delta^-, \delta^+]$ and $[\varepsilon^{*-}, \varepsilon^{*+}]$ edges: We have the $[\delta^-, \delta^+]$ edge, as when p_b^i is above p_h the δ_b-arc continues all the way to α together with the adjacent δ arc on its right and hence there are two adjacent δ-arcs which intersect α. Note that the top part of $\xi \subset \{\beta \cap \mathcal{A}_l\}$ is not affected by the wave moves since the segment removed by the waves always has its top endpoint below an intersection point with δ. Hence this top part is equal for β and β'. Since $n \geq 2$ the top part of ξ will intersect two adjacent ε^*-arcs giving the $[\varepsilon^{*-}, \varepsilon^{*+}]$ edge.

Furthermore, since $\widehat{V} = \{\delta, \varepsilon^*\}$ and $\widehat{W} = \{\alpha, \beta\}$ or $\{\alpha, \beta'\}$ and by assumption, δ takes two paths in $\mathcal{A}_r$ and one path in $\mathcal{A}_r$ the complexity of the meridional systems

$\{\delta, \varepsilon^*\}$ and $\{\alpha, \beta\}$ or $\{\alpha, \beta'\}$ is greater than 4. So in this case ($n > 1$) the Heegaard splitting (V, W) is not a Heegaard splitting for S^3 by Corollary 1.3.12 and Theorem 1.3.10.

To finish the case $n > 1$ we must still consider the following case:

Suppose $p_b^{i_0} = p_h$: Let Δ denote the number of ε^* tails staring immediately to the right of X^u (see Figure 36). If $\Delta > n$ then at least one of these tails, after passing through $\mathcal{R}^u$, will connect to $\partial_+ P$ to the right of X^d and emerge as another tail to the right of X^u. The sub-arc of ε^* passing through both of these tails will connect α^- to α^+ giving the $[\alpha^-, \alpha^+]$ edge. In this case the blocking edges $[\beta'^-, \beta'^+]$, $[\delta^-, \delta^+]$ and $[\varepsilon^{*-}, \varepsilon^{*+}]$ from the above case where $p_b^{i_0}$ is above p_h are not affected so we have all blocking edges with respects to V and W and we are done as above.

Note that Δ is computed after performing m wave moves and then sliding groups of n tails to straighten the diagonal arcs in $\mathcal{A}_l$. So Δ is equal to m minus some integer multiple of n and since $\gcd(n, m) = 1$ so is $\gcd(n, \Delta) = 1$. Thus $\Delta < n$.

There is an s-wave ρ, depicted in Figure 37, which starts at a point on ε^* below Y^u on the topmost arc of the Δ ε^*-tails. It then meets $\partial_+ P^u$ and continues from Y^d in $\mathcal{A}_r$ upwards to meet Z^u and then it emerges at Z^d and continues to the right of the δ_b arc into $\mathcal{R}^u$. The s-wave ρ continues parallel and to the right of δ_b until δ_b meets $\partial_+ P^u$ to the right of X^u. It emerges at X^d and meets ε^- on the leftmost of the n ε_2 arcs. Perform a shortening of ε^* along ρ and parallel s-waves (if they exist) on the obtained meridians. There are Δ such ρ wave moves.

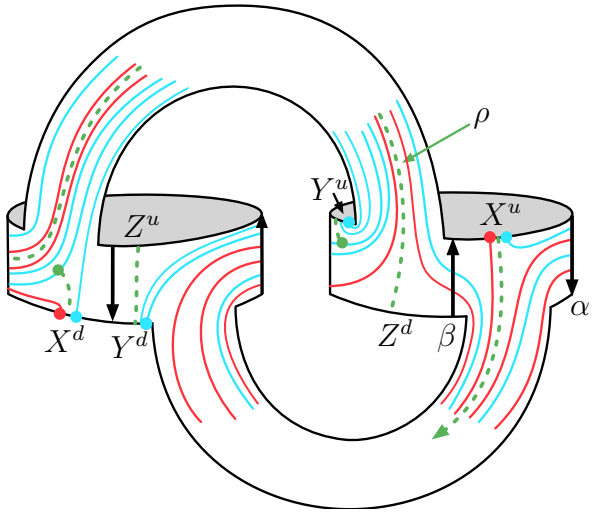

FIGURE 37. The s-wave ρ with respect to ε^*.

After the ρ wave moves we obtain a new meridian which we denote by θ. Note that as we have performed Δ wave moves (and $\Delta < n$) all the θ tails starting at X^u now continue into $\mathcal{R}^d$. Thus the topmost and bottommost intersections along the α segment in $\mathcal{A}_r$ are δ intersections.

Next we perform a sequence of wave moves on β, along the wave η depicted in Figure 38 and waves parallel to it and elongated at their endpoints. The endpoints of this η wave are on the rightmost β segment in $\mathcal{A}_l$. The exact configuration of η depends on the quantities Δ and n as follows:

If $n > 2\Delta$. The bottom endpoint of η must lies between the δ-tail and the δ-arc above it. There are $n-\Delta$ sub-arcs of θ there so this endpoint has Δ intersection points of $\theta \cap \beta$ above it and there is at least one θ sub-arc immediately below it.

Tracing η from its bottom endpoint on β it meets Y^u with Δ sub-arcs of θ to its left. These Δ sub-arcs continue upwards from Y^d to Z^u in $\mathcal{A}_l$. So η can continue, after emanating to the right of Z^d to the right of all θ sub-arcs adjacent to δ_b and connect to β^+ below the δ intersection above δ_b. After the wave move there is at least one θ intersection with the modified β above the δ tail.

If $n < 2\Delta$ the bottom endpoint of η lies below all the $n-\Delta$ sub-arcs of θ above the δ-tail. It continues through Y and Z and connects to β^+ with at least one θ intersection point immediately above its top endpoint. In this intersection point θ crosses β from left to right and has conflicting orientations relative to the intersections of δ and β.

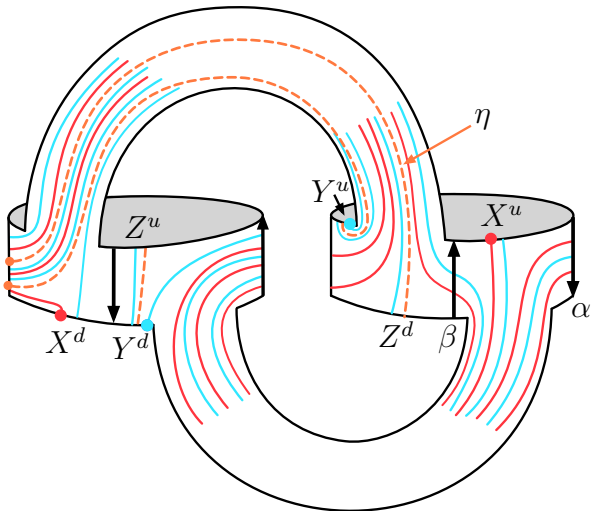

FIGURE 38. The wave η with respect to β.

In the case where $n - \Delta = \Delta$ all intersection points of β with θ between the δ-tail and the δ intersection above p_b are eliminated by the wave moves. Continue to perform

η wave moves to remove sub-segments of β and replace them with η waves, until the part of ξ containing $p_b^i = p_h$ is removed.

In all three cases we obtain a new meridian β'. The arc η', depicted in Figure 39, connects to β' at the top endpoint of the last η wave which is located $min\{\Delta, n-\Delta\}$ θ intersection points above p_h. The η' wave meets $\partial_+ P^u$ at a point which is $min\{\Delta, n-\Delta\}$ θ intersection points to the right of X^u. It then emerges to the right of X^d through $\mathcal{R}^u$ and connects to Y^u. After emerging to the right of Y^d it turns right and connects to β'^-. Again the exact point at which η' emerges near Y^d depends on the quantities Δ and n. It can emerge between the ε_2 arcs of θ, and then the modified meridian β'' will have intersections with θ above the top endpoint of η'. It can emerge between the vertical arcs of θ passing from Z^u to Y^u, in which case it will not be a wave but only a shortcut as it will intersect some of these segments to reach β^-, or it can emerge between these two types of η arcs and connect to the top point of the β' in $\mathcal{A}_l$

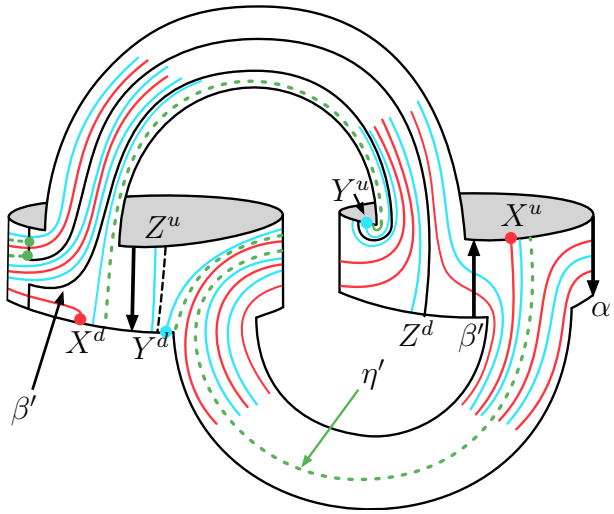

FIGURE 39. The wave η' with respect to β'.

At this point perform all possible additional wave moves with respect to β', along waves parallel to η' depicted in Figure 39, to obtain a meridian β''.

If $n > 2\Delta$, then there $n - \Delta \geq 2$ adjacent ε_2 sub-arcs of θ which must intersect α in $\mathcal{A}_r$ (as θ must meet α and this is the only place where it does). Since there are two θ adjacent such arcs we get the $[\theta^-, \theta^+]$ edge. There is also a sub-arc of α yielding the $[\delta^-, \delta^+]$ edge, as the topmost and bottommost intersections along α are δ intersections. Thus there are blocking edges with respect to W.

In this case η connects to β above all the Δ intersections with θ above p_b^i. Thus η' connects above all these intersection points and meet $\partial_+ P$ to the right of all the θ intersections near X^u and similarly near Y^d. Thus, the top θ intersection along each β

segment was not removed by the η' wave move. The sub-arc of θ going through these intersection points gives rise to the $[\beta''^-, \beta''^+]$ edge. For the $[\alpha^-, \alpha^+]$ edge, note that there are at least two δ sub-arcs through the right path in $\mathcal{A}_r$, as otherwise θ does not intersect α. The δ sub-arc to the left of δ_b starting at α^- continues without meeting β'' as it intersects ξ below p_b and above the δ-tail. It meets the part of the β segments that were removed by the η wave moves. It splits from δ_b when δ_b connects to X^u, however it then meets β *(not β'')* at a part that was removed by the η' wave move. Finally it emerges from $\mathcal{A}_l$ as the topmost sub-arc and continues to meet α^-. So in the case of $n > 2\Delta$ we have blocking edges for V and W.

If $n < 2\Delta$ and $p_b = p_h$ (i.e. $i_0 = 0$), then all the η waves affect the β segments only in $\mathcal{A}_l$. Perform all possible wave moves on η'-arcs which are *waves*. There is an additional arc η'_0 parallel to η' and elongated at its endpoints which are on β'. The arc η'_0 is not a wave as it intersects θ but it is an s-wave. Perform a wave move with respect to η'_0. This wave move will introduce new intersection points of β'' and θ. The orientation induced on β'' by β is such that θ crosses it from the $'+'$ side to the $'-'$ side. The topmost intersection point in $\mathcal{A}_r$ of β'' and θ was not affected by the η'_0 wave move so θ crosses β'' from the $'+'$ side to the $'-'$ side there. Thus we have the $[\theta^-, \theta^+]$ edge.

There is also a sub-arc of α yielding the $[\delta^-, \delta^+]$ edge, as the topmost and bottommost intersections along α are δ intersections. Thus there are blocking edges with respect to W.

The argument for the other edges is exactly as above: The top θ intersection along each β segment which was not removed by the wave move gives rise to the $[\beta''^-, \beta''^+]$ edge. For the $[\alpha^-, \alpha^+]$ edge, note that there are at least two δ sub-arcs through the right path in $\mathcal{A}_r$, as otherwise θ does not intersect α. The δ sub-arc to the left of δ_b starting at α^- continues without meeting β'' as it intersects ξ below p_b and above the δ-tail. It meets the part of the segments β that were removed by the η wave moves. It splits from δ_b when δ_b connects to X^u, however it then meets β *(not β'')* at a part that was removed by the η' wave move. Finally it emerges from $\mathcal{A}_l$ as the topmost sub-arc and continues to meet α^-. So in the case of $n < 2\Delta$ and $i_0 = 0$ we have blocking edges for V and W.

In the case that $n < 2\Delta$ and $i_0 > 0$, recall that the bottom endpoint of η lies below all the $n - \Delta$ sub-arcs of θ above the δ-tail, and there is at least one θ intersection point immediately above p_b which is not removed by the wave move. In this intersection point θ crosses β from left to right and has conflicting orientations relative to the intersections of δ and β. As $i_0 > 0$ we have performed at least one more η wave move on the same segment of β, removing a second part of the segment, above the first

part removed. Between the two segments that were changed by the η moves there is a intersection point of β and δ. This part of the β segment survives all the wave moves so is contained in β'' and gives the $[\delta^+, \theta^+]$ edge. The α segment in $\mathcal{A}_l$ which has not been changed gives the $[\delta^+, \theta^-]$ edge.

The intersections of the δ tail with β have not been removed, and this yields the $[\beta^+, \beta^-]$ edge. There is also a sub-arc of δ, as in the previous case, connecting α^- to α^+. Thus we have blocking edges with respect to V and W and the complexity is at least four.

Remark 3.2.3. In the last case it might happen (when $\Delta/2 < n - \Delta < \Delta$) that θ intersects β'' in conflicting orientations. Thus, one should be concerned whether the intersections are tight, or whether θ contains a wave with respect to β''. However, as between any intersections of β with θ of opposite orientations, β'' intersects a δ-arc, the curves are tight. Furthermore, as we obtain the $[\alpha^+, \alpha^-]$ edge from a sub-arc of δ there are no waves with respect to β, and in particular no such wave can be a sub-arc of θ.

One may also check directly that in this case, that θ intersects α between any two intersections of conflicting orientations with β. Hence θ is tight and has no wave with respect to β.

The remaining possibility is when $n = 2\Delta$. Since $\gcd(n, \Delta) = 1$ this implies that $\Delta = 1$ and $n = 2$.

(†) Consider the δ-tail emanating from X^d and turning left. It will determine the topmost arc in $\mathcal{R}^d$ which must take the left path in $\mathcal{A}_r$. After the splitting point this δ-tail becomes parallel to the δ-arc δ_b which determines p_b. These two sub-arcs of δ must run parallel to each other and the only place they can separate is when δ_b (continuing from p_b) meets X^u. At this point the right arc (of the pair) becomes parallel to an ε^*-arc and remains parallel to it until it meets X^u.

This implies that the δ curve is separated into two parts δ_1 and δ_2. The δ_1 part includes the δ-tail and the part of δ that has a δ-arc on its left and the δ_2 part has an ε^*-arc on its left. If the δ_1-arc meets α in $\mathcal{A}_r$ then so will the δ_b-arc on its left. In order to meet α in $\mathcal{A}_r$ the δ_b must be to the right of the δ-head in $\mathcal{R}^d$ and so meets ξ above p_h. This implies that p_b^i is above p_h for some i, in contradiction.

Thus the δ_1 arc does not meet α in $\mathcal{A}_r$ and only δ_2 meets α.

Note that the δ_2 sub-arc of δ starts below X^u in $\mathcal{A}_r$ and has a number of parallel ε^* sub-arcs to its left. Some more ε^* sub-arcs emanating next to Y^u might become parallel to it before entering $\mathcal{R}^u$ and some ε^* sub-arcs might split from it when entering

$\mathcal{A}_l$. However once it takes the right path in $\mathcal{A}_l$ there are exactly n ε^* sub-arcs which stay parallel to it until it meets X^u.

We compute the values of the previous $\{\delta, \varepsilon^*\}$ curves in the Homology of $H_1(V)$:

(1) Let r denote the number of δ-arcs taking the right path in $\mathcal{A}_r$ and let l denote the number of δ-arcs taking the left path. Then δ has $r \geq 2$ intersections with α and l intersections with β in $\mathcal{A}_r$.

(2) Let k denote the number of β segments in $\mathcal{A}_l$.

(3) The intersection points of δ with each β segment in $\mathcal{A}_l$ consists of l points from arcs taking the left path $\mathcal{A}_r$ plus r points from arcs taking the right path $\mathcal{A}_r$ and the intersections with the δ-tail starting at X^d. Thus there are $(l+r+1)k$ intersection points in $\mathcal{A}_l$.

(4) In $H_1(V)$ we have $[\delta] = r \cdot \mathbf{x} + (l + (l+r+1)k) \cdot \mathbf{y}$, where $\mathbf{x}, \mathbf{y}$ are the generators of $H_1(V)$ determined by the disks A and B respectively.

(5) There are n ε^*-arcs above any arc of δ taking the right path in $\mathcal{A}_r$ (by assumption) except for the topmost δ-arc. Above it there are Δ ε^*-arcs which come from ε^*-tails emanating next to X^u. Thus $|\, \varepsilon^* \cap \alpha \,| = (r-1)n + \Delta$.

(6) i_0 is the number of times the δ-arc starting at p_b crosses the β segment in $\mathcal{A}_r$ before it connects to p_h. This is exactly the number of times that δ takes the left path in $\mathcal{A}_r$ and there is no ε^*-arc to its right. There is one more time that δ passes through $\mathcal{A}_l$ only with no ε^*-arc to its right, corresponding to the intersection point p_b itself.

(7) There are exactly n ε^*-arcs meeting $\partial_+ P^d$ next to Y^d and with no δ-arcs separating them. Thus any time the δ-arc has an ε^*-arc to its right there are in fact n such ε^*-arcs.

(8) Thus in homology $[\varepsilon^*] = (rn + \Delta) \cdot \mathbf{x} + [n(l + (l+r+1)k) - ni_0(k+1) - nk] \cdot \mathbf{y}$.

(9) All the δ-arcs which took the right path in $\mathcal{A}_r$ are to the left of δ_b. Hence when ever δ_b makes a left turn so do they. This occurs i_0 times. The arc δ_b then connects to X^u and then the $r-1$ other δ-arcs make a left turn one last time. Thus $l = ri_0 + r - 1$

Let A be the matrix which describes $\{\varepsilon^*, \delta\}$ with respect to $\{\alpha, \beta\}$ in homology. We compute $\det A$ to get:

$$\det(A) = r - ri_0 - ri_0 k - 1.$$

When $i_0 > 0$, $\det A < -2$. This contradicts the fact that $\{\varepsilon^*, \delta\}$ is a basis for the homology of W.

Finally, when $i_0 = 0$ the situation is exactly as in Figures 37, 38 and 39. The last η' wave connects to β' in $\mathcal{A}_r$ below all the θ and δ curves. Its top endpoint is below the topmost intersection with θ. Hence the sub-arc of β'' starting at the intersection point of the leftmost β segment in $\mathcal{A}_l$ with θ, continues through $\partial_+ P$ into $\mathcal{A}_r$ and connects immediately to θ, giving the $[\theta^-, \theta^+]$ edge. The $[\delta^-, \delta^+]$ edge is in the α segment in $\mathcal{A}_r$ as before. The topmost θ-arc in $\mathcal{R}^u$ connects β''^+ to β''^- giving the $[\beta''^-, \beta''^+]$ edge. There is a δ-arc which gives the $[\alpha''^-, \alpha''^+]$ edge exactly as before. Thus we have the blocking edges for V and W in the case as well and as the complexity is bigger than four (which can be seen form the multiple intersection of the system (V, W)) is not a Heegaard splitting for S^3. This finishes the case $n > 1$

Remark 3.2.4. When $n > 1$ there were a pair of ε^* segments which run parallel through β in $\mathcal{A}_l$ so we obtain the $[\varepsilon^{*-}, \varepsilon^{*+}]$ edge. When $n = 1$ we no longer have this above edge and on the other hand we do have a wave ρ with respect to δ, see Figure 40. Thus a wave move with respect to ρ must be performed obtaining a δ' meridian curve and we need to look for the edges with respect to it. Thus this case must be treated separately.

Sub-case(c): $n = 1$:

Since $m > n$ we have removes all ε_2-arcs by the wave moves and we can assume that there are no ε^*-tails starting in $\mathcal{A}_l$, as in this case we have the blocking edges with respect to both V and W, as before.

If there are two or more ε''-tails emanating to the right of X^u which intersect α in $\mathcal{A}_r$ we get a $[\varepsilon''^-, \varepsilon''^+]$ edge. As we have removed all ε_1-arcs using the wave moves, the δ-head becomes adjacent to a δ-arc to its right and both are in the same path in $\mathcal{A}_l$. Thus we obtain a $[\delta^-, \delta^+]$ edge. It is clear that we have the $[\alpha^-, \alpha^+]$ edge if there is more than one α segment in $\mathcal{A}_r$. Note that we also get the $[\alpha^-, \alpha^+]$ edge if there is a single such segment: There is a sub-arc of ε'' connecting the intersection points with the single α segment in $\mathcal{A}_r$ on two adjacent ε''-tails. The $[\beta^-, \beta^+]$ edge is obtained by the δ-tail which intersects β both in $\mathcal{A}_l$ and $\mathcal{A}_r$. Thus we have blocking edges for both $\widehat{V}$ and $\widehat{W}$.

The only case left is where there is a single ε''-tail starting to the right of X^u after tightening. In this case there is a wave denoted by ρ, shown in Figure 40, with respect to δ. The wave move results in a meridian δ', depicted in Figure 41. We do not know whether after the wave move the bottommost arc in $\mathcal{R}^d$ is an ε''-arc or a δ'-arc.

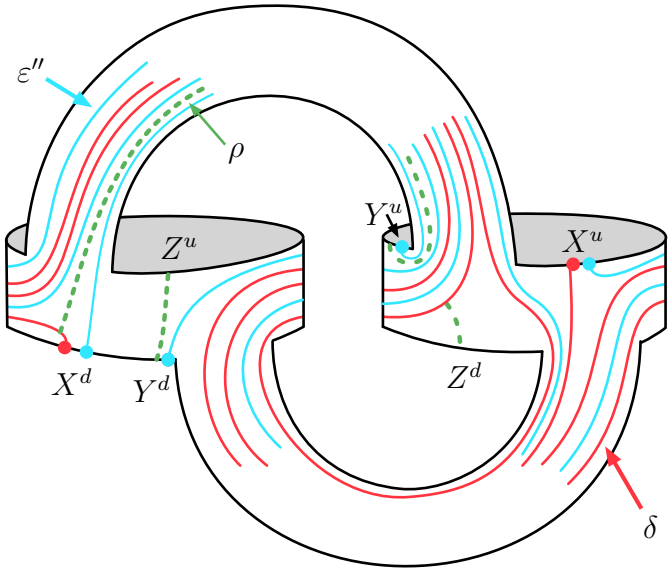

FIGURE 40. The wave ρ with respect to δ in the case of one intersection in $\mathcal{A}_l$ and $m = 2,\ n = 1$. If there are more intersections, m is larger and both ε'' and ρ will have a few vertical segments in $\mathcal{A}_l$ one between any two α segments.

If it is a δ'-arc, we perform a shortening of δ' along the shortcut τ depicted in Figure 41. We obtain a new curve δ''. It is a meridional curve as one boundary component of $\mathcal{N}(\theta)$ is isotopic to ε'' and the other to δ', where $\theta = \delta' \cup \tau$. Continue to perform shortenings on the obtained meridians along arcs parallel to τ if they exist. This procedure must stop at a meridian curve denoted by δ'' which does not pass below the lowest ε''-arc in $\mathcal{R}^d$. We now have some number of δ''-tails starting to the right of Z^d in $\mathcal{A}_r$ "turning right" and continuing through $\mathcal{R}^d$ into $\mathcal{A}_l$. They are contained in the right path in $\mathcal{A}_l$ and intersect the β segments in the opposite orientation relative to the other δ'' and ε''-arcs.

We have a shortcut η depicted in Figure 42 and we shorten ε'' along η. A shortcut similar to η will exist as long as the bottommost arc in $\mathcal{R}^d$ is a ε'': As a single ε''-arc connects to Y^d the number of ε''-arcs which are topmost in the left path in $\mathcal{A}_r$ is greater by one than the number of ε''-arcs which are bottom most in the left path in $\mathcal{A}_r$.

Continue to perform the shortening until we obtain a meridian ε''' for which the bottommost arc in $\mathcal{R}^d$ is again a δ''-arc. Such a δ''-arc exists as δ'' must intersect α by Lemma 1.3.3 and hence it must take the right path in $\mathcal{A}_r$ at least once.

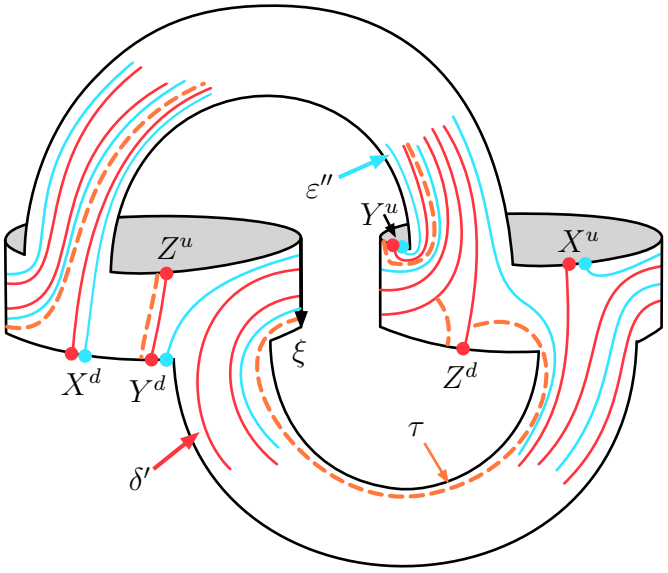

FIGURE 41. The meridian δ' and shortcut τ which exists as long as the bottommost arc in $\mathcal{R}^d$ is a δ'-arc. Note the shortcut is depicted in the case where there is a single α segment in $\mathcal{A}_l$, and in other cases will have vertical segments in $\mathcal{A}_l$.

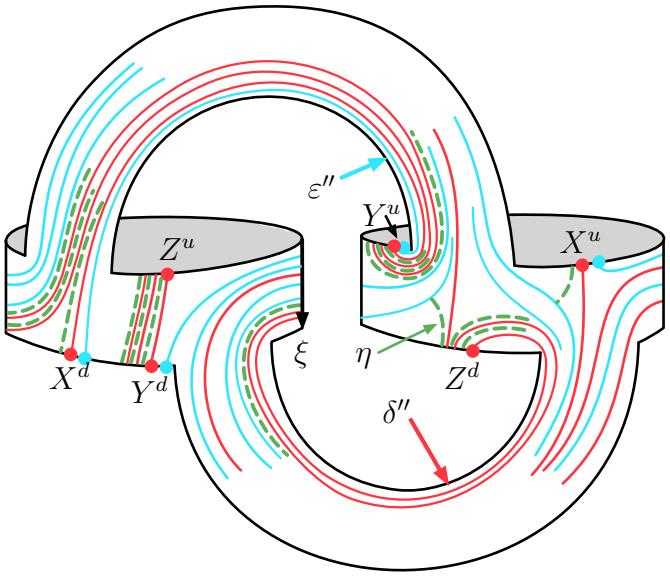

FIGURE 42. The shortcut η with respect to ε'', which again exists as long as the bottommost arc in $\mathcal{R}^d$ is an ε''-arc. η passes once above each δ''-tail emanating from Z^d.

At this point, we have a $[\delta''^-, \delta''^+]$ edge given by a sub-arc of β in $\mathcal{A}_r$ as the δ''-arc emanating upwards from Z^d becomes adjacent to the bottommost sub-arc of δ'' in the right path in $\mathcal{A}_r$ and both intersect the β segment in $\mathcal{A}_l$.

The two topmost ε''' sub-arcs in $\mathcal{R}^u$ are adjacent and their continuation in $\mathcal{A}_l$ meet a β segment and give the $[\varepsilon'''^-, \varepsilon'''^+]$ edge there. If there is more than one segment of α in $\mathcal{A}_r$ we obtain the $[\alpha^-, \alpha^+]$ edge. By Lemma 2.4.5 there are at least two β segments in the left path and these give the $[\beta^-, \beta^+]$ edge. We have all blocking edges for $\widehat{V}$ and $\widehat{W}$. Note that as we have adjacent arcs the complexity of the system is greater than four and (V, W) is not a Heegaard splitting for S^3 by Theorem 1.3.10.

So assume that there is a single α segment in $\mathcal{A}_r$.

We proceed as in the $n > 1$ case by performing wave moves along β. Consider the sub-arc δ''_t of δ'' emanating upwards to the left of Z^d in $\mathcal{A}_r$. This arc continues through $\mathcal{R}^u$ into the right path in $\mathcal{A}_l$ and intersects the rightmost segment $\xi \subset (\beta \cap \mathcal{A}_l)$ at a point p''_t. The arc δ''_b which is the δ''-arc immediately to the left of δ''_t goes through $\mathcal{R}^u$ into the right path in $\mathcal{A}_l$ and intersects ξ at a point p''_b which is just below p''_t.

Consider the arc σ , depicted in Figure 43. It is a wave with respect to β. The precise location of σ depends on how many δ''-tails emanated around Z^d and turn right into $\mathcal{R}^d$. If there are such tails, the first wave σ starts just above p''_t and is parallel to δ''_t all the way to the intersection point of δ to the left of Z^d. This arc continues down from Z^u with single δ''-arc to its left to the left of Y^d. It continues from Y^u into $\mathcal{R}^u$ (with a single δ''-tail to its right) until it enters $\mathcal{A}_l$ and intersects β there.

If there are no such δ''-tails let σ be an arc starting just below p_t and parallel to δ''_t all the way to its intersection point at Z^d. Continues down vertically from Z^u in $\mathcal{A}_l$ between the single δ'' and the ε'''-arcs. It continues to the left of Y^u in $\mathcal{A}_r$ into $\mathcal{R}^u$ and intersects $\partial_+ P^d$ to the left of X^d. It emerges in to the left of X^u in $\mathcal{A}_r$ between the δ''-head and ε'''-tails (to its left) and turns parallel to these tails till it intersects β.

A wave move along σ removes the part of β segment between its endpoints which is within $\mathcal{A}_l$ if there are δ''-tails, and includes the top part of the β segment in $\mathcal{A}_r$ if there are no tails.

If there are, say k, β segments in $\mathcal{A}_l$ we can perform k wave moves along waves parallel to σ and elongated at the endpoints obtaining a meridian $\beta' = \beta^{k+1}$, by removing a parallel segment from each β segment in $\mathcal{A}_l$.

Define p_h, as in the case $n > 1$, to be the last intersection point of the δ''-head with ξ before it connects to X^u. Note that both δ and δ'' define the same point p_h.

Claim 3.2.5. *The point p''_b defined by δ'' is not equal to p_h.*

Proof. Assume in contradiction that $p''_b = p_h$ and further assume that there is at least one δ''-tail emanating near Z^d and turning right. Consider the $\delta''_b \subset \delta''$ sub-arc emanating from α^- in $\mathcal{A}_r$. It turns into $\mathcal{R}^u$ passes through $\mathcal{A}_l$ without intersecting β'

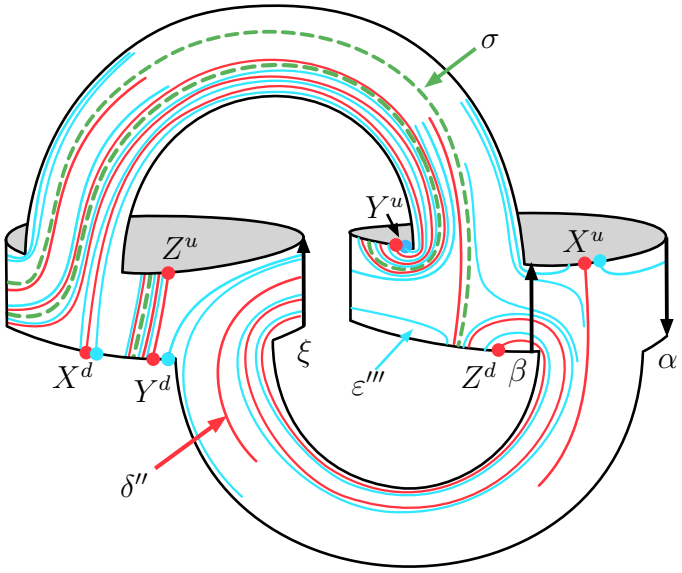

FIGURE 43. The wave σ with respect to β.

and then continues into $\mathcal{R}^d$ and then connects exactly to X^u since $p_b'' = p_h$. It then continues up from X^d into $\mathcal{R}^u$ turns right and connects to $\partial_+ P^u$ to the left of Y^u. It emerges to the left of Y^d and connects to Z^u. It then emerges at Z^d turns right and meets β'^-. Thus we have the $[\alpha^-, \beta'^-]$ edge. We have the $[\alpha^+, \beta'^-]$ edge from any arc, which is not a tail, taking the right path in $\mathcal{A}_r$.

As for the blocking edges with respect to δ'' and ε''': There is at least one δ''-tail emanating right from Z^d and a ε'''-tail adjacent to it (see Figure 42). These arcs meet the β' segment in $\mathcal{A}_r$ with opposite orientations thus we have the $[\delta''^-, \varepsilon'''^-]$ edge. The arc δ_b'' meets α in $\mathcal{A}_r$ above the ε'''-heads so a sub-arc of α gives the $[\delta''^+, \varepsilon'''^-]$ as well. Thus we have blocking edges with respect to $\widehat{V}$ and $\widehat{W}$ the complexity is greater than four as above so (V, W) is not a Heegaard splitting for S^3 by Theorem 1.3.10.

If there are no δ''-tails:

We now perform a wave move on ε''' along the shortcut τ described in Figure 44. The resulting curve will be denoted by ε^*. Note that $\varepsilon^* \cap \mathcal{A}_r$ contains only ε^*-tails and no arcs which take the left or right paths in $\mathcal{A}_r$. Let l and r denote the number of times that δ'' takes the *left* and *right* paths in $\mathcal{A}_r$ respectively. Now perform a wave move on δ'' along a shortcut η described in Figure 45. The resulting curve will be denoted by δ^1. We do this wave move l times. Each wave move replaces a δ'' sub-arc taking the left path in $\mathcal{A}_r$ and one δ'' sub-arc taking the right path in $\mathcal{A}_r$, thus eliminating one intersection point of with α.

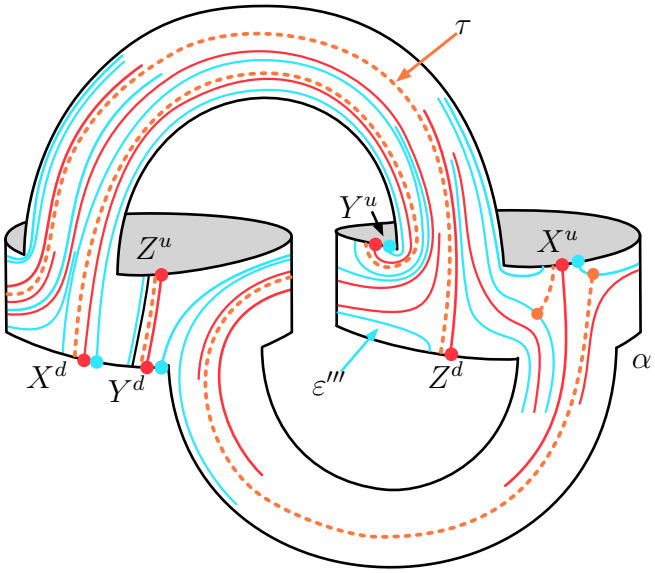

FIGURE 44. The shortcut τ with respect to ε''' in case there are no δ'' tails starting near Z^d and turning right. τ starts to the left to X^u, travels parallel and to the right of δ_1 and connects to ε''' again to the right of X^u.

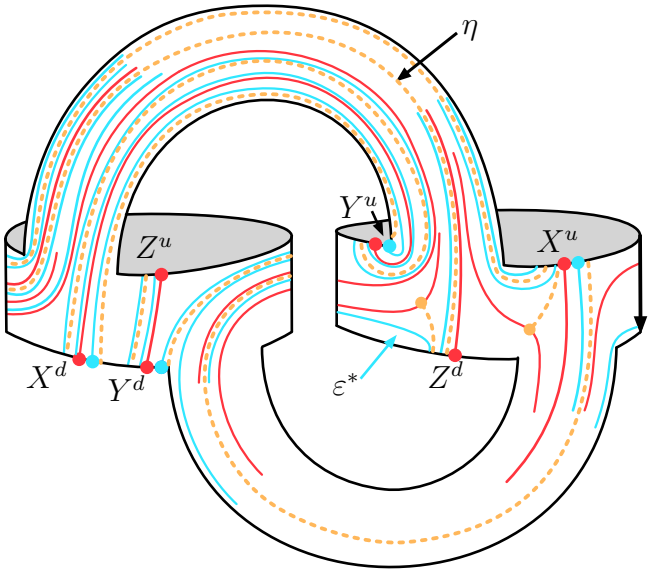

FIGURE 45. The curve ε^* and the wave η with respect to δ''. The wave starts to the left of X^u, and ends to the left of Z^d.

The next shortcut parallel to η and on it's left near X^u will connect to another sub-arc taking the left path through X^u, and to a sub-arc taking the right path near Z^d. Notice that each time an arc passes through $\mathcal{A}_l$ it's continuation in $\mathcal{A}_r$ changes sides

relative to the δ''-head. Thus each arc taking the right path in $\mathcal{A}_r$ contributes one to the number of arcs taking the left path except for the bottommost one δ''_b, which does not contribute to l. Thus $r = l + 1$. Hence, the curve δ^*, which is the curve obtained after all the l wave moves, intersects α exactly once. Next, there is another shortcut η' to the left of all the η shortcuts near X^u connecting to the δ tail emanating from Z^d there, and connecting to the last sub-arc of δ'' taking the right path near Z^d. The resulting curve δ^* does not intersect α, in contradiction to Lemma 1.3.3. □

Assume p''_b is above p_h. Since p_t is above p''_b then, regardless of the number of δ''-tails, p_t is above p_h. So the arcs δ''_t and δ''_b both continue after intersecting the β segments in $\mathcal{A}_l$ to meet the α segment i n $\mathcal{A}_r$. As the wave moves remove the intersections of δ''_b with β the arc δ''_b connects α^- to α^+ giving the $[\alpha^-, \alpha^+]$ edge. As the two δ''-arcs meet α at adjacent intersection points the α segment between them gives the $[\delta''^-, \delta''^+]$ edge.

We obtain the $[\beta'^-, \beta'^+]$ edge from the ε'''-arc next to the δ''-head which intersects β' in $\mathcal{A}_r$ and continues through $\mathcal{R}^u$ to the top part of ξ, which was not removed by the wave moves.

Finally we have the $[\varepsilon'''^-, \varepsilon'''^+]$ edge from the top part of the leftmost β segment in $\mathcal{A}_l$: Note that there are two adjacent ε''' intersecting β segments in $\mathcal{A}_l$ since one ε'''-arc will connect to Y^d and there is at least one more ε'''-arc next to it, continuing into a ε'''-tail (see Figure 43) and the top part of the leftmost β is not removed by the wave move. Thus, we have all blocking edges when p_b is above p_h on ξ. Since there are at least two intersections of δ'' and α and at least two intersections of ε''' and β' the complexity is at least four and we done by Theorem 1.3.10.

Assume p''_b is below p_h. As in the case $n > 1$, there is an additional wave parallel to σ in Figure 43 and elongated at its endpoints by arcs through $\mathcal{R}^d$. In the case there is a δ''-tail starting at Z^d and turning to the right, this wave has both its endpoints on the single β' segment in $\mathcal{A}_r$. The bottom endpoint is below the top such δ''-tail and the top endpoint is above the continuation of δ''_t. In this case the wave move removes the part of β' in $\mathcal{A}_r$ between the two endpoints. In the case there are no such δ''-tails, the bottom endpoint of the wave is on the top part of the leftmost β segment in $\mathcal{A}_l$, and the wave move removes the part of the leftmost segment upwards from the endpoint and the part of the segment in $\mathcal{A}_r$ below the other endpoint. Perform this wave move to obtain a meridian β''.

$(*)$ When there are no δ''-tails which start around Z^d and turn to the right, we have the blocking edges with respect to both sides: The bottommost and uppermost arcs intersecting α in $\mathcal{A}_r$ are both ε'''-arcs. Thus we obtain the $[\varepsilon'''^-, \varepsilon'''^+]$ edge from the

sub-arc of α which starts at this top intersection point and proceeds upwards, passing through all α segments in $\mathcal{A}_l$, which have no intersections with δ'' or ε''', and arrives at the bottom intersection point.

For the rest of the blocking edges note that if p_b'' is below p_h, so is p_t'': First recall that p_b'' and p_t'' are adjacent on β so cannot be separated by p_h. If p_t'' equals p_h the curve δ'' which bounds a meridian in W does not intersect α in contradiction to Lemma 1.3.3. So δ_t'' and δ_b'' continue parallel through the left path in $\mathcal{A}_r$ and intersect ξ at two adjacent points which lie above the part of ξ which was removed by the first wave move. Thus the sub-arc of ξ between these two intersection points yields the $[\delta''^-, \delta''^+]$ edge. The $[\beta''^-, \beta''^+]$ edge is obtained as before from the sub-arc of ε''' arriving from $\mathcal{R}^d$ to the left of the δ-head and then intersecting β'' in $\mathcal{A}_r$ and again in $\mathcal{A}_l$. The sub-arc of ε''' intersects β at points that lie below the sections removed by the wave moves and thus intersects β''.

Finally, there is a sub-arc of ε''' yielding the $[\alpha^-, \alpha^+]$ edge obtained as follows: Start with the bottommost intersection point along the α segment in $\mathcal{A}_r$ (it is an intersection with a ε'''-head) and continue to the right along ε'''. The ε''' sub-arc reaches $\partial_+ P^d$ and continues through a vertical segment in $\mathcal{A}_l$. It emerges in $\mathcal{A}_r$ as the leftmost tail to left of Y^u. It then connects again to $\partial_+ P^d$ to the left of X^d. This sub-arc continues as the topmost arc in $\mathcal{R}^u$. Note that all intersection points of this sub-arc with β in $\mathcal{A}_r$ and $\mathcal{A}_l$ have been removed by the wave moves. Thus it continues without intersecting β'' and connects to Y^d. At this point it continues from Y^u to the intersection point to the right of X^d and finally continues from the right of X^u to the right and meets α again. Hence when there are no δ''-tails we have all blocking edges with respect to $\widehat{V}$ and $\widehat{W}$.

$(**)$ Suppose there is one δ''-tail. We show that we have blocking edges for the systems $\{\alpha, \beta''\}$ and $\{\delta'', \varepsilon'''\}$. The bottommost ε'''-tail connecting to $\partial_+ P^d$ to the left of Z^d continues through a vertical segment in $\mathcal{A}_l$, then emanates from Y^u and continues along the lower part of $\mathcal{R}^u$, and then as the topmost ε'''-head to the left of X^u. It then continues through $\mathcal{A}_r$, $\mathcal{R}^u$ and $\mathcal{A}_l$, without intersecting β'' (as these intersections have been removed by the wave moves). It finally connects to $\partial_+ P^d$ at Y^d, continues as the lowermost tail at the bottom of $\mathcal{R}^u$, meets $\partial_+ P^d$ to the right of X^d and emanates to the right of X^u and turns to meet the α segment again giving rise to the $[\alpha^-, \alpha^+]$ edge.

We assume p_b'' is below p_h and therefore δ_t'' is also below p_h and continues through the left path in $\mathcal{A}_r$ and meets β'' in $\mathcal{A}_l$. By the same reason the δ''-head is above p_t'' and intersects β'' in $\mathcal{A}_l$ (as the part of β above p_t was not removed by the wave move). We know that the δ''-tail connects to the δ''- head so connecting these sub-arcs gives the $[\beta''^-, \beta''^]+$ edge in this case as well.

The δ''_t runs parallel and adjacent to δ''_b and both continue to intersect β'' in $\mathcal{A}_l$. This yields the $[\delta''^-, \delta''^+]$ edge. For the $[\varepsilon'''^-, \varepsilon'''^+]$ edge note that the bottommost intersection along the α segment in $\mathcal{A}_r$ is an intersection with ε''', as is the topmost. Thus the $[\varepsilon'''^-, \varepsilon'''^+]$ edge is given by the α-arc between these intersection points, passing through all the α segments in $\mathcal{A}_l$.

$(***)$ Assume there are at least two δ''-tails. The δ''-arc continuing from p''_t will go through $\mathcal{R}^d$, $\mathcal{A}_r$ and $\mathcal{R}^u$ and meet ξ again at a point p^1_t which is above p''_b. This arc can continue producing a finite sequence of ascending intersection points p^i_t with ξ. At some point either there is an i_0 so that $p^{i_0}_t$ is above p_h or $p^{i_0}_t = p_h$. We next show that there is a sequence of waves parallel to σ except for elongations at the endpoints so that the "top point" of the last wave connects to ξ above $p^{i_0}_t$. Performing these wave moves on β yields a meridional system that has all blocking edges:
(#) In order to perform the next wave move it is convenient to slide the k adjacent intersection points of β'' with $\partial_+ P^d$ to the right stoping immediately before last δ''-tail. This slide produces new "trivial" intersections with the δ'' and ε''' which will cancel with intersections of the bottom part of each of the k β segments in $\mathcal{A}_l$: This slide will simultaneously induce a corresponding slide in $\mathcal{A}_l$ of the k vertical segments of β''. The slide can be done keeping these segments vertical. Sliding the "bottom" points of these segments will induce a slide to the right of the intersection of β'' with $\partial_+ P^u$ to the left of Y^u introducing new intersection points there. These last intersection point can be slid along the δ'' and ε''' till they cancel out on β.

Remark 3.2.6. Note that if there is only a single δ'' tail then this "sliding" operation cancels the intersection points of the ε'''-tails to the left of X^u with the top part of the β segments in $\mathcal{A}_l$ and $\mathcal{A}_r$ (which are also the top part of β'' segments).

As the number of tails of δ'' starting to the right of Z^d is at least two then after the slide (which stops before the rightmost δ''-tail) there is a wave starting at the intersection with β'' (between the δ''-tails, see Figure 46) and parallel to the previous waves so that its other endpoint is just above p^1_t. In fact there are $k+1$ "parallel" such waves so that their other endpoints are on the k β segments in $\mathcal{A}_l$ and one in $\mathcal{A}_r$. Now perform the "slide" as in paragraph (#). If p^1_t is below p_h then after the slide there is a new wave ρ with its top endpoint just above p^2_t. This process will end when some $p^{i_0}_t$ is above p_h ($p^{i_0}_t$ cannot equal p_h since it has a δ''-arc to its left while the δ''-head has a ε'''-arc to its left). Denote the resulting meridian by β'''.

When $p^{i_0}_t$ is above p_h the last intersection of the δ''-head arc before X^u is with α^-. After meeting X^u the arc continues through Y^u and Z^u and turns right from

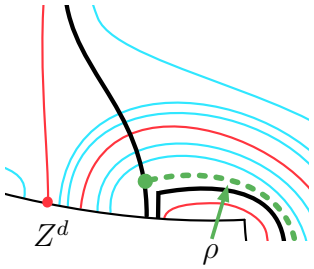

FIGURE 46. The endpoint of the wave ρ between the δ tails.

Z^d to intersect β'''^- giving the $[\alpha^-, \beta'''^-]$ edge. The bottommost arc in $\mathcal{R}^d$ is an ε'''-arc connecting β'''^- in $\mathcal{A}_l$ to α^+ in $\mathcal{A}_r$ thus giving the $[\alpha^+, \beta'''^-]$ edge. The curve β''' intersects at least one δ''-tail and one ε'''-tail at the bottom of $\mathcal{A}_r$ resulting in the $[\delta''^+, \varepsilon'''^+]$ edge. The $[\delta''^+, \varepsilon'''^-]$ edge can be seen in the α segment in $\mathcal{A}_r$ between any two points between δ''^+ and ε'''^-. Thus we have all blocking edges in this case.

Note that in all the above cases $(*)$, $(**)$ and $(***)$ The curve δ'' intersects α at lest once and ε''' intersects α at least twice so the complexity of the diagram is at least three so again we are done by Theorem 1.3.10. □

3.3. One path in $\mathcal{A}_r$ and two paths in $\mathcal{A}_l$

Lemma 3.3.1. *If K is not a Berge knot then the Heegaard splitting $\{V, W\}$ cannot be a Heegaard splitting of S^3 when the curve δ takes a single path in $\mathcal{A}_r$ and two paths in $\mathcal{A}_l$ and when ε takes only short paths.*

Proof. We may assume by Lemma 3.1.1 that the path that δ takes in $\mathcal{A}_r$ is short and up to symmetries we can assume it is the right path. In this case the meridian intersecting the left path in $\mathcal{A}_l$ has less intersections with δ than the one intersecting the right path. So by the minimality assumption 1.3.4 it must be α. As before (see Lemma 3.1.4) $\varepsilon = m\varepsilon_1 + n\varepsilon_2$.

Case (a): $m = n = 1$.

In this case we have an arc η connecting the same side of δ to itself and intersecting $\partial_+ P$ once as in Figure 47. By Lemma 2.4.5 η is a shortcut which is a contradiction to the minimality of δ.

Case (b): $n > m$.
In this case, after the wave moves, there are no ε_1 sub-arcs of the obtained curve ε'. Then the δ-tail connecting to X^d is adjacent to another δ-arc in $\mathcal{A}_l$. Thus we obtain

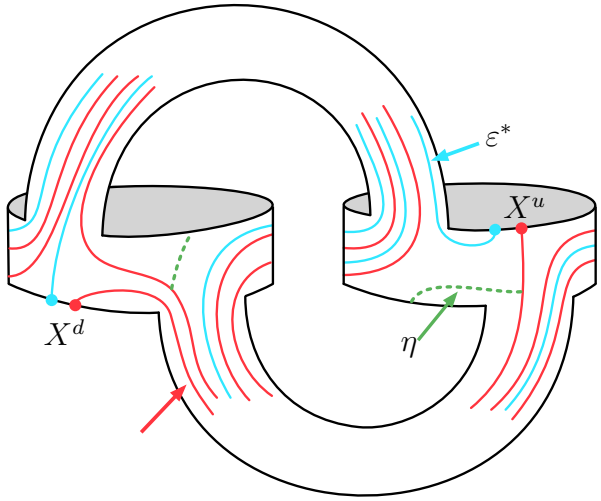

FIGURE 47. The arc η in Case (a).

the $[\delta^-, \delta^+]$ edge there. Since $n > 1$ there are at least two adjacent ε'-arcs in $\mathcal{A}_r$ which intersect a meridian (β in this case) and give rise to the $[\varepsilon'^-, \varepsilon'^+]$ edge. Hence we have the blocking edges with respect to $\widehat{W}$.

The curve ε' still contains ε_2 sub-arcs which take the left path in $\mathcal{A}_r$. Hence in this case, $(n > m)$, the curves $\{\delta, \varepsilon'\}$ take all paths so by Lemma 2.5.3 we have the blocking edges with respect to $\widehat{V}$ as well.

As before since δ take three paths the complexity is greater than four so (V, W) is not a Heegaard splitting of S^3 by Theorem 1.3.10.

Case (c): $m > n$.

In this case there is a wave ω with respect to ε' depicted in Figure 48 which intersects $\partial_+ P$ in a point Z. Perform the wave move to obtain a curve ε'^2. Now slide the points Z^u and Z^d to the right along $\partial_+ P$ till the segment of $\varepsilon'^2 \subset \mathcal{A}_r$ becomes vertical. We continue to perform wave moves followed by the slides on ε'^i as long as we have waves ω^i parallel to ω. This results in a curve ε''. Note that each such wave move shortens one tail (in the sense that it has less intersection points with $\widehat{V}$), removes one $(\varepsilon_1 \setminus \Psi)$-arc and adds a vertical segment within $\mathcal{A}_r$ to ε'. There are three options for the resulting curve ε'':

(i) The curve ε'' contains no ε_1-arcs and there is at least one ε''-tail starting in $\mathcal{A}_r$ with at least one intersection with $\widehat{V}$ in $\mathcal{A}_r$.

(ii) The curve ε'' contains no tail which starts at $\mathcal{A}_r$, and there is at least one ε_1-arc.

(iii) The curve ε'' contains neither ε_1-arcs nor a tail starting in $\mathcal{A}_r$ with intersections with α in $\mathcal{A}_r$.

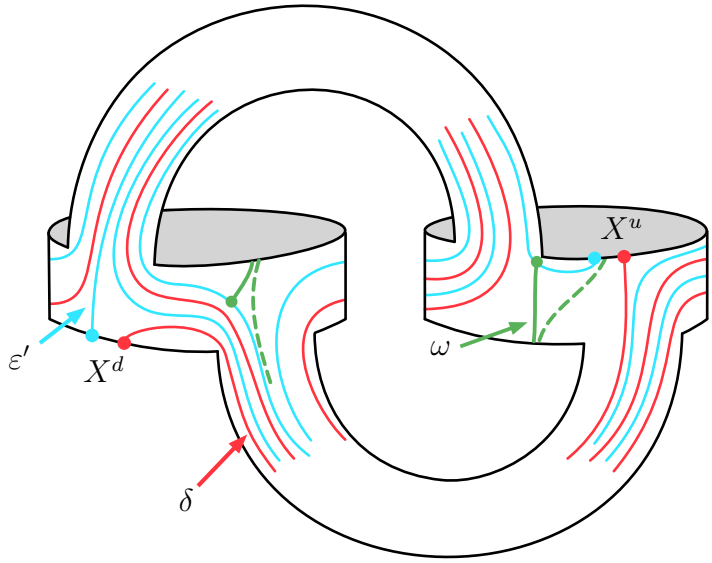

FIGURE 48. The wave ω with respect to ε in Case (2). The dashed curve marks the side of ω on which the new meridian ε' lies.

Option (i): (The curve ε'' contains no ε_1-arcs and there is at least one ε''-tail starting in $\mathcal{A}_r$ with at least one intersection with $\widehat{V}$ in $\mathcal{A}_r$.) Since ε'' contains no ε_1 sub-arcs it does not pass above the the δ-tail in $\mathcal{A}_l$. If there are two adjacent δ sub-arcs along the left path in $\mathcal{A}_l$ one of which is the δ-tail in $\mathcal{A}_l$, as can be seen in Figure 48, these two δ sub-arcs give the $[\delta^-, \delta^+]$ blocking edge in $\Gamma(\delta, \varepsilon'')$. If there are no such adjacent δ sub-arcs then the left path in $\mathcal{A}_l$ is taken only by the δ-tail. In this case the $[\delta^-, \delta^+]$ edge is obtained by the segment of $\widehat{V}$ that intersects the δ-tail and continues upwards, passing to the left of Z^u and continuing to the left of Z^d until it meets δ again.

The $[\varepsilon''^-, \varepsilon''^+]$ blocking edge is obtained because of the existence, by the assumption, of an ε''-tail that intersects α to the right of Z^d. This segment of a component of α starting at ε''^- continues in $\mathcal{A}_l$ to the right Z^u in a downwards direction eventually meeting ε''^+ as δ takes the two short paths through $\mathcal{A}_l$. Thus we have the two blocking edges in $\Gamma(\delta, \varepsilon'')$.

Finally, the ε''-tail in the above paragraph intersects an α segment in $\mathcal{A}_r$ and after emerging from $\mathcal{R}^u$ turns right and intersects α again. Thus giving rise to the $[\alpha^-, \alpha^+]$ edge. There is also a δ-arc passing through the right path in $\mathcal{A}_r$ intersects β and continuing to the left path in $\mathcal{A}_l$ intersects β there as well. This gives the $[\beta^-, \beta^+]$ edge. The curve δ has not been modified throughout the so the complexity is greater than four so (V, W) is not a Heegaard splitting of S^3 by Theorem 1.3.10.

Option (ii): (The curve ε'' contains no tail which starts at $\mathcal{A}_r$, and there is at least one ε_1-arc.) It is possible, in this case, that an ε''-tail will start at the corner where

$\mathcal{A}_r$ meets $\mathcal{R}^u$ or anywhere on the top boundary of $\mathcal{R}^u$. If there is such an ε''-tail then there is another wave with respect to ε'' in $\mathcal{A}_r$ parallel to the ω-arc, as in Figure 48. Performing the wave move removes an ε_1-arc, and replaces one of the ε''-tails with another tail that starts at $Z^u \in J_l^u$ and has no intersections with $\widehat{V}$ before entering $\mathcal{R}^d$. Thus after perhaps, a finite number of such wave moves we obtain a curve ε''' which either has no ε_1-arcs, or has it's tails begin in $\mathcal{A}_l$ to the left of an α segment in $\mathcal{A}_l$. Now there are two possible cases:

(a) ε''' has at least two tails, or at least one ε_1-arc left.

(b) ε''' has a single tail and no ε_1-arcs.

Case ii(a): In this case we have the $[\varepsilon'''^-, \varepsilon'''^+]$ edge as Ψ meets $\widehat{V}$ and there are at least two ε''' arcs within Ψ. We also have the $[\delta^-, \delta^+]$ edge as we are either missing the ε_1-arcs (and can connect the δ-tail to the arc to its left in $\mathcal{A}_l$ as before), or there is an intersection with α to the right of the first tail of ε''' in $\mathcal{A}_l$ which connects the topmost δ arc in the right path in $\mathcal{A}_l$, passing through some vertical segments with no intersections in $\mathcal{A}_r$, to the bottommost arc in the right path in $\mathcal{A}_l$ which is also a δ arc. Thus we have the blocking edges with respect to $\Gamma(\delta, \varepsilon''')$.

If there are at least two α segments in $\mathcal{A}_l$ we have the $[\alpha^-, \alpha^+]$ edge from δ arcs taking the right path in $\mathcal{A}_l$ and the $[\beta^-, \beta^+]$ edge from δ arcs taking the left path in $\mathcal{A}_l$. Thus, unless there is a single segment of α in $\mathcal{A}_l$, we have all blocking edges for $\{\widehat{V}, \widehat{W}\}$. As the complexity is greater than four as above (V, W) is not a Heegaard splitting of S^3 by Theorem 1.3.10.

Assume therefore that there is a single segment of α in $\mathcal{A}_l$. We now have two cases marked by ii$(a)(*)$ and ii$(a)(**)$:

ii$(a)(*)$ The only δ-arc taking the left path in $\mathcal{A}_l$ is the δ-tail: There is a wave τ with respect to β, emanating from the bottom point of the rightmost β segment in $\mathcal{A}_r$. Perform the wave moves on τ and on parallel waves. The resulting curve β' is depicted in Figure 49. The resulting meridian $B' \subset V$ intersects $\delta = \partial D$ in a single point (along the δ-tail in $\mathcal{A}_l$).

Consider the curve κ depicted in Figure 49. It is composed of all the α segments in $\mathcal{A}_r$ and differs from α by changing the single α segment in $\mathcal{A}_l$ into a diagonal segment in $\mathcal{A}_l$. Since there is a single α segment in $\mathcal{A}_l$, its core $\mathfrak{a}_l$ is isotopic to a component of $\partial_- P$ (as the annulus $\mathcal{A}_l$ does not intersect γ). This implies that the knot K and the curve κ co-bound an annulus. Hence K can be isotoped to the curve $\kappa \subset \Sigma$, which does not intersect δ. The curves δ, β' and κ are depicted on Σ in Figure 50 for the case of a standard P. The meridian $B' \subset V$ intersects $\delta = \partial D$ in a single point. So we can isotope κ across D to remove the intersections $\kappa \cap \beta$. Attaching the disk D to V

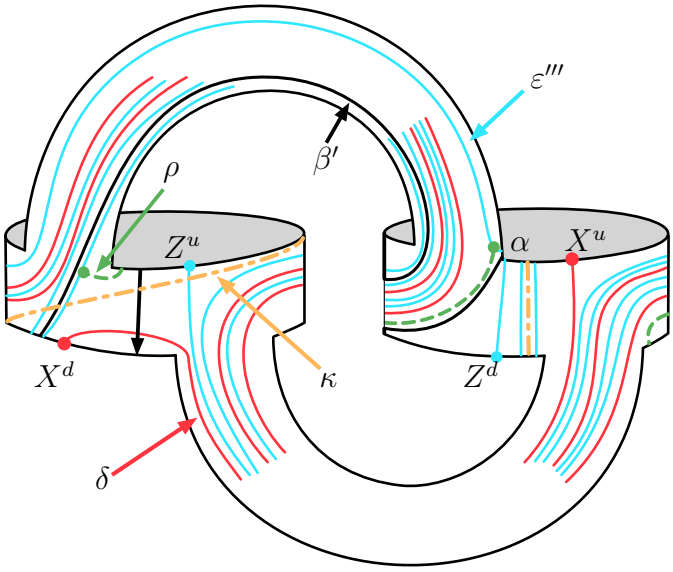

FIGURE 49. The resulting meridian β' and the wave ρ with respect to ε in Case $(*)$.

along $\partial D = \delta$ results in a solid torus so that κ is embedded in its boundary. Attaching D to V reduces the Heegaard splitting (V, W) of S^3 by the reducing pair (B', D) so we obtain a genus one Heegaard splitting of S^3. Thus κ is embedded in a standardly embedded torus in S^3 and K is a torus knot which is a Berge knot.

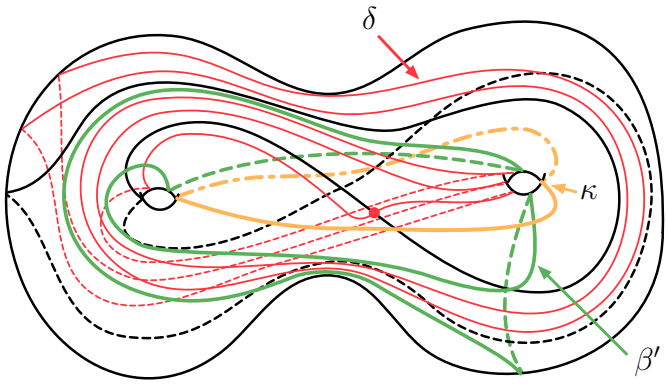

FIGURE 50. The meridional curve δ and the curve κ in Case ii$(a)(*)$ when P is standard.

ii$(a)(**)$ There is a δ-arc in addition to the tail the tail taking the left path in $\mathcal{A}_l$. There is a wave τ with respect to β as in Figure 51 and after performing a wave move on it and on parallel waves we obtain a meridian β'.

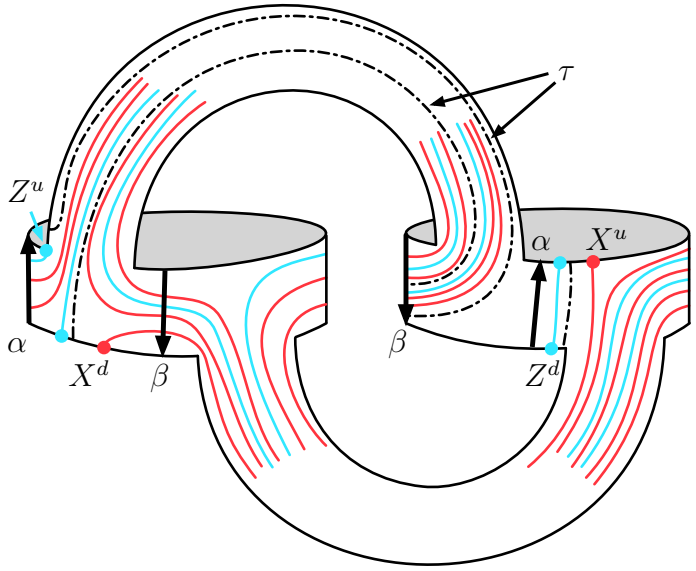

FIGURE 51. The wave τ with respect to β in ii$(a)(**)$.

We get the $[\delta^-, \delta^+]$ edge as follows: If there is no ε_1-arc, the δ-tail in $\mathcal{A}_l$ is adjacent to the δ sub-arc above it. The two curves might not intersect β' in $\mathcal{A}_l$ or $\mathcal{A}_r$. They continue parallel to each other into $\mathcal{A}_l$ and intersect the α segment there giving rise to the $[\delta^-, \delta^+]$ edge. If there is an ε_1-arc, the $[\delta^-, \delta^+]$ edge is given by a sub-arc of α, emanating from the topmost δ-arc in the right path in $\mathcal{A}_l$ to the right of Z^u, passing through the α segments in $\mathcal{A}_r$ and connecting to the bottommost δ arc in the right path in $\mathcal{A}_l$.

We obtain the $[\varepsilon'''^-, \varepsilon'''^+]$ edge as follows: If ε''' has an ε_1 sub-arc then there is no ε'''-tail starting to the left of Z^u in Figure 52. Thus the wave τ connects to the left of all the $\varepsilon''' \cap \partial_+ P$ near Z^u. So it continues to the left of all $\varepsilon''' \cap \partial_+ P$ near X^d. Hence there are at least two $\varepsilon''' \cap \beta$ points above the top endpoint of τ in $\mathcal{A}_r$. So we have the $[\varepsilon'''^-, \varepsilon'''^+]$ edge.

If there is no ε_1 type sub-arc in ε''' there are at least two ε''' tails (as we are in case ii(a)).

(I) Suppose ε''' has more than two tails. Then there are two adjacent tails either to the left of τ, in $\mathcal{R}^u$, in which case they meet a part of β in $\mathcal{A}_r$ that was not removed by the wave move, or there are two tails to the left of τ, in which case they continue into $\mathcal{R}^u$ after their intersections in $\mathcal{A}_r$ and intersect α in two adjacent points, thus we have the $[\varepsilon'''^-, \varepsilon'''^+]$ edge.

(II) Suppose ε''' has exactly two tails. Then Ψ must pass through either the right or the left path in $\mathcal{A}_l$, i.e. does not end the first time it returns to $\mathcal{A}_l$:

Assume in contradiction that Ψ ends the first time it returns to $\mathcal{A}_l$. Then we may perform a shortening of δ, along a shortcut ρ depicted in Figure 52. Each ρ wave move removes an arc from the endpoint of ρ next to X^d upwards, through $\mathcal{R}^u$, $\mathcal{A}_r$, $\mathcal{R}^d$ and $\mathcal{A}_l$ and $\mathcal{R}^u$ again where it meets the second endpoint of ρ. Thus it removes one intersection point with α. When all these wave moves are performed, there is a last sub-arc of δ intersecting α that was not removed by the wave moves. Now there is another wave ρ' parallel to ρ but extended from the endpoint of ρ near X^d through $\partial_+ P^u$ to the left of the β segment in $\mathcal{A}_l$, until it meets the bottommost δ sub-arc in $\mathcal{A}_r$. Thus, after the ρ' wave move, we arrive at a meridian δ' which does not intersect α, in contradiction to Lemma 1.3.3.

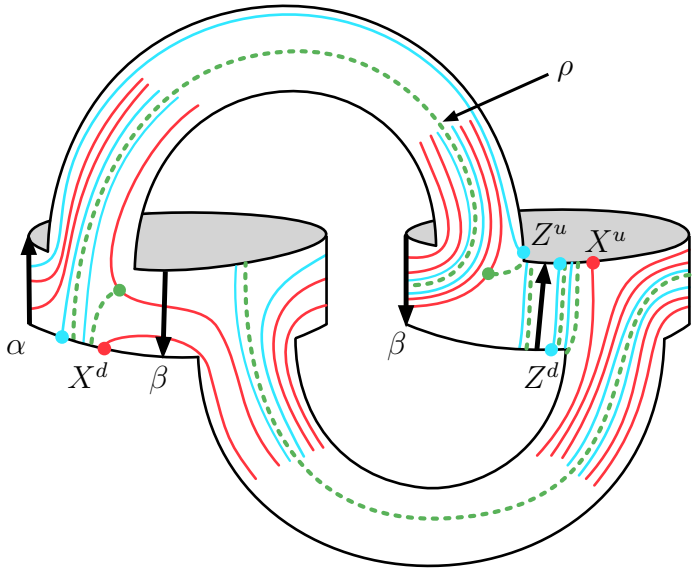

FIGURE 52. The shortcut ρ with respect to δ in Option (ii) Case (a), when ε'' has only two tails and Ψ does not pass through any path in $\mathcal{A}_l$.

Therefore the two tails, which are adjacent, must pass either through the left path in $\mathcal{A}_l$ and intersect β', as they intersect the part of β in $\mathcal{A}_r$ which is not removed. Or the two adjacent tails take the right path in $\mathcal{A}_l$ in which case they intersect α. Thus in both cases we have the $[\varepsilon'''^-, \varepsilon'''^+]$ edge.

If there is a sub-arc of δ or ε''' taking the right path in $\mathcal{A}_l$, and then meeting the part of β in $\mathcal{A}_r$ which was removed then we have the $[\alpha^-, \alpha^+]$ edge. If all the sub-arcs meeting the part of β in $\mathcal{A}_r$ which was removed come from the left path then the last τ wave has endpoints on β in $\mathcal{A}_l$ and the $[\alpha^-, \alpha^+]$ edge is given by the δ-head. Suppose then that both option above do not happen. Then the topmost ε'''-arc which meets the part of β in $\mathcal{A}_r$ which was removed, connects to Y^u. This implies that the last wave move performed was done on an arc τ' which is an extension of the original τ.

It has one endpoint on β under the δ-tail in $\mathcal{A}_l$. The arc extending τ at the other endpoint continues through $\partial_+ P$ at Y^u passes through $\mathcal{A}_r$ and emerges near X^d to the right of τ (as depicted in Figure 52). It connects to β in $\mathcal{A}_r$ above the top endpoint of τ. Thus performing a wave move on τ' removes all intersections of β' and δ which is a contradiction:

The Whitehead graph $\Gamma(\delta'', \varepsilon''')$ it is of type (iii) in Figure 3. Since δ'' intersects α once and does not intersect β'. We are guaranteed a wave with respect to ε''' (ε''' plays the role of V_1 in the figure). As long as the modified curve (ε''' after the wave moves) intersects α the graph $\Gamma(\delta'', \varepsilon''')$ is of type (iii). Continue to perform the guaranteed wave moves and this will stop when we obtain a meridian (instead of ε''') which does not intersect α. But this implies by Lemma 1.3.3 that K is a $(1,1)$- knot in contradiction. So this case cannot happen.

Remark 3.3.2. Note that any time we have the situation where one meridian in V intersects the knot K in a single point and that the other meridian in V does not intersect one of the two meridians in W we have a contradiction to Lemma 1.3.3 as explained in the paragraph above.

The topmost δ-arc in the right path in $\mathcal{A}_r$ passes through a part of β that was not removed, continues to the left path in $\mathcal{A}_l$, existing by assumption, yields the $[\beta'^-, \beta'^+]$ edge. As the complexity is greater than four so (V, W) is not a Heegaard splitting of S^3 by Theorem 1.3.10.

Case ii(b): In this case ε''' has a single tail and no ε_1-arcs. We claim that there is a ε''' sub-arc that takes the left path in $\mathcal{A}_l$. Assume in contradiction that there is no such arc. Assume that there is some number s , perhaps zero, of δ sub-arcs, except for the δ-tail taking the left path in $\mathcal{A}_l$. There is a sequence of s waves all denoted by ρ and depicted in Figure 53 with respect to δ. These wave exist because the s arcs plus the δ-tail continue through $\mathcal{R}^d$ around $\mathcal{A}_r$, through $\mathcal{R}^u$ and around $\mathcal{A}_l$. Thus there are $s+1$ δ-arcs next to the top endpoint of ρ. After performing these s wave moves there are no more δ sub-arcs taking the left path in $\mathcal{A}_l$. At this stage there is one more wave ρ' parallel to and to the left of the previous waves. The arc ρ' starts at the one remaining δ sub-arc at the top of the right path in $\mathcal{A}_l$ continues parallel to ρ and since there are no more δ sub-arcs and no ε_1-arcs ρ' continues to $\partial_+ P^u$ and connects to the bottommost δ-arc in $\mathcal{A}_r$. It meets $\mathfrak{a}_l$ (the core of $\mathcal{A}_l$) exactly once. After doing this wave move we obtain a meridional curve δ^* which intersects $\mathfrak{a}_l$ exactly once in contradiction to Corollary 2.4.7.

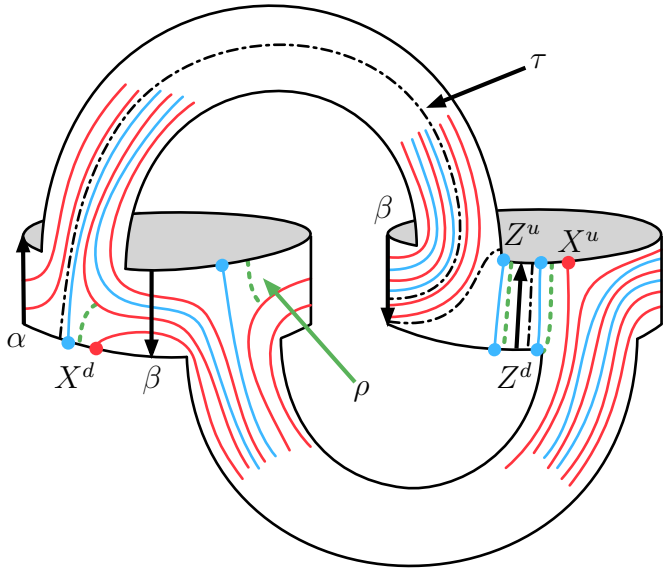

FIGURE 53. The wave ρ with respect to δ in Case (ii(b)) and the wave τ with respect to β.

Thus there is a ε''' sub-arc that takes the left path in $\mathcal{A}_l$. Let s be the number of δ sub-arcs taking the left path in $\mathcal{A}_l$ which are below the rightmost such ε''' sub-arc. Perform s wave moves along ρ on δ, obtaining a meridian δ' after which the lowest sub-arc in the left path in $\mathcal{A}_l$ is a ε''' sub-arc. Note that there are some number k of τ waves with respect to β (see Figure 53). This number k is equal to the number of β segments in $\mathcal{A}_r$. If all sub-arcs of δ', ε''' meeting β between the two endpoints of τ arrive from the left path in $\mathcal{A}_l$ then there is an additional such τ wave with endpoints on the β segment in $\mathcal{A}_l$. Perform all possible such wave moves to obtain a meridian β'.

There are two δ'-tails emanating next to X^d and entering $\mathcal{R}^d$ and continuing into $\mathcal{A}_r$. These adjacent δ' sub-arcs might intersect β' in $\mathcal{A}_l$ and even if they don't they will travel together through $\mathcal{A}_r$ and $\mathcal{R}^u$ to intersect α in $\mathcal{A}_l$. This will give the $[\delta^-, \delta'^+]$ edge. The ε'''-head meeting $\partial_+ P^d$ next to X^d is adjacent to an ε''' sub-arc to its left. These ε''' sub-arcs meet the original β in adjacent points. If these sub-arcs meet β on a segment which is not removed by the τ wave moves we have the $[\varepsilon'''^-, \varepsilon'''^+]$ edge.

If the top endpoint of τ is between the intersection points of the adjacent ε''' sub-arcs on β the if these two adjacent ε''' sub-arcs arrive together from either the right or left path in $\mathcal{A}_l$ they will intersect either an α or a β' segment and so will give the $[\varepsilon'''^-, \varepsilon'''^+]$ edge. If one arrives from the right path and the other arrives from the left path then there is a sub-arc of β' starting at the intersection point of ε''' above the top endpoint of τ and connecting it to the top intersection point on one of the β' segments which is also an intersection with ε'''. So we have the $[\varepsilon'''^-, \varepsilon'''^+]$ edge in this case as well.

Trace the topmost arc meeting the β segment in $\mathcal{A}_l$ through $\mathcal{R}^u$ back to the β segment in $\mathcal{A}_r$. The topmost intersection of β was not removed by the τ wave moves: If they were removed then there is a shortcut τ' with respect to β' parallel to τ elongated at the endpoints through $\mathcal{R}^u$. The shortening removes the remaining part of β in $\mathcal{A}_r$ and therefore the resulting meridian β'' of V does not intersect ε''' which is a contradiction by Remark 3.3.2. Thus the intersections survive in β' and thus we have the $[\beta'^-, \beta'^+]$ edge.

If we have performed k τ wave moves on β then there is a sub-arc of either δ' or ε''' which connects α in $\mathcal{A}_l$ through the part of β that was removed back to α. If we happened to perform $k+1$ τ wave moves on β then the δ'-head intersects α in the right path in $\mathcal{A}_l$ and continues through X^u into $\mathcal{A}_l$ then through $\mathcal{R}^d$, $\mathcal{A}_r$ and finally through $\mathcal{A}_l$ to intersect α. Thus we have the $[\alpha^-, \alpha^+]$ edge.

Since the complexity of all the systems involved is at least three these Heegaard splittings are not Heegaard splittings of S^3 by Theorem 1.3.10 so Option (ii) is ruled out.

Option (iii): The curve ε'' contains neither ε_1-arcs nor a tail starting in $\mathcal{A}_r$ with intersections with $\widehat{V}$ in $\mathcal{A}_r$. (Note that this case deals with ε'' as defined in Case (c) and Figure 48 and *not* with ε''' which is defined in Option (ii). In particular there is no tail emanating from the splitting point at the top of $\mathcal{A}_l$).

The argument splits into two cases, Option(iii)(a) ε'' has at least two tails, and Option(iii)(b) ε'' has a single tail.

Option(iii)(a): In this case the $[\varepsilon''^-, \varepsilon''^+]$ edge is given by any intersection with $\widehat{V}$ of Ψ. Note that Ψ contains the ε'' tails which are adjacent as they all emanate from $\partial_+ P^u$ in $\mathcal{A}_l$. The $[\delta^-, \delta^+]$ edge exists since there is no ε_1 arc in ε'' and thus the δ tail is adjacent to the δ-arc above it. Hence if there is more than one α segment in $\mathcal{A}_l$ then any arc taking the right path in $\mathcal{A}_l$ gives the $[\alpha^-, \alpha^+]$ edge and any arc taking the left path gives the $[\beta^-, \beta^+]$ edge. Since the complexity of the meridional system is greater than four we have a contradiction by Theorem 1.3.10 and (V, W) is not a Heegaard splitting for S^3.

Thus assume that there is a single α segment in $\mathcal{A}_l$. The left path in $\mathcal{A}_r$ does not intersect β and intersects k segments of α:

In this case there is a single arc along $\partial_+ P^u$ in $\mathcal{A}_l \cup \mathcal{R}^u$ from which the ε''-tails can emanate, to the right of the single α segment in $\mathcal{A}_l$. This is because in order to obtain ε'' we performed wave moves on ε'-tails as long as they had intersections with α in $\mathcal{A}_r$. This means that every vertical segment in ε'' is to the right of at least one α segment

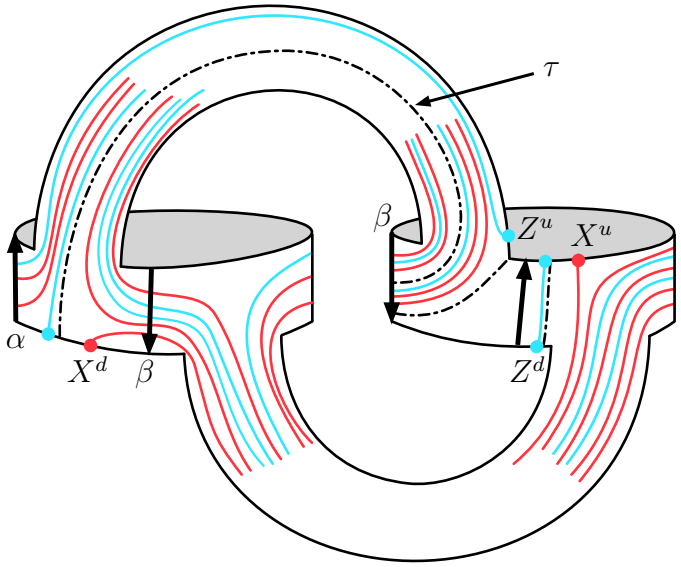

FIGURE 54. The wave τ with respect to β in Option (iii) Case (a).

in $\mathcal{A}_r$. This implies that we can have only one ε''-tail, as otherwise ε'' cannot close up. This contradicts the assumption in this case.

Option(iii)(b): In this case there is a wave η with respect to δ as in Figure 55. The bottommost arc in $\mathcal{A}_l$ in the right path is a δ-arc connecting to the η-wave in Figure 55. Let s denote the number of δ-arcs below the bottommost ε''-arc in the right path in $\mathcal{A}_l$. These arcs continue through $\mathcal{R}^d$ as the topmost arcs in the right path in $\mathcal{A}_r$, except for the δ-head. Thus we have $s-1$ δ-arcs to the left of the bottommost ε''-arc in R^u. These $s-1$ arcs become the topmost arcs in the left path in $\mathcal{A}_l$. To the right of these $s-1$ arcs we have either an ε''-arc (if ε'' passes through the left path in $\mathcal{A}_l$) or the δ-tail. The wave move along $\eta = \eta^1$ removes from $\delta = \delta^1$ the sub-arc starting at the top endpoint of η, adjacent to ε''. The resulting curve after $s-1$ wave moves along waves parallel to η is a curve δ'.

At this point the argument splits into two cases:

(1) ε'' takes only one path in $\mathcal{A}_l$.

(2) ε'' takes two paths in $\mathcal{A}_l$.

In case (1) assume ε'' takes the left path. Since ε'' does not take the right path $\mathcal{A}_l$ the ε''-tail emanating from Y^u has only δ'-arcs to its left. It has no δ' arcs on its right as those were eliminated by the wave moves. Hence the only δ sub-arc to the right of ε''-arcs in $\mathcal{R}^d$ is the δ'-tail which is the bottommost arc in $\mathcal{R}^d$. Thus the curve δ' consists of some arcs (heads and tails) starting and ending in intersection points with

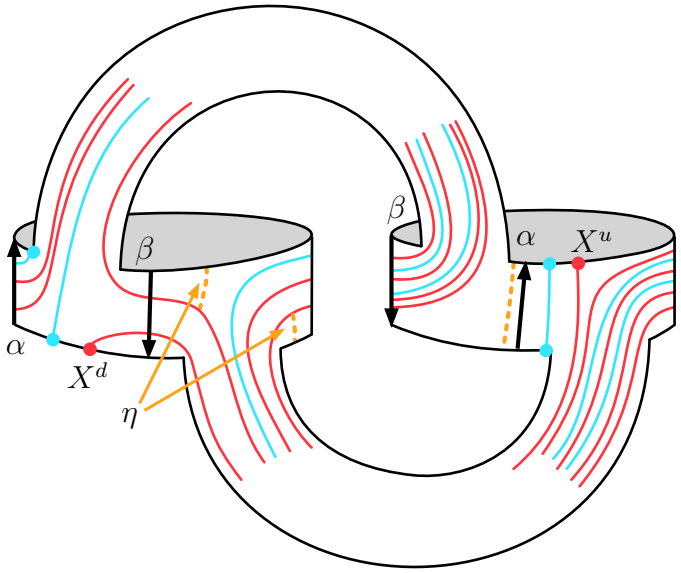

FIGURE 55. The wave η with respect to δ in Option (iii)(b). The α and β arrows in $\mathcal{A}_r$ each represent k segments of α or β, and so do the vertical sub-arcs of ε'' and η.

$\partial_+ P$ which *do not* intersect $\mathfrak{a}_l$, and a *single* arc (which is the continuation of the δ'-tail) that continues through $\mathcal{A}_l$ into $\mathcal{R}^d$, as in Figure 56.

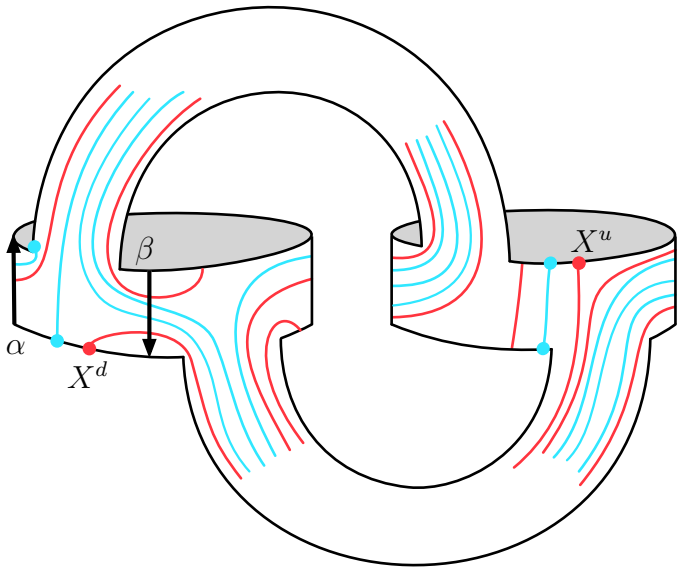

FIGURE 56. The resulting meridian δ', intersecting the core curve $\mathfrak{a}_l$ once.

Assume ε'' takes only the right path in $\mathcal{A}_l$. In this case there is an additional wave move on δ' along an arc parallel to η (as in Figure 55) with one of its endpoints on

the δ'-tail resulting in a meridional curve δ'' which intersects the core curve $\mathfrak{a}_l$ once in the single diagonal segment of $\delta'' \cap \mathcal{A}_l$. Thus in both cases we obtain a meridian intersecting $\mathfrak{a}_l$ in a single point which is ruled out by Corollary 2.4.7.

In case (2) ε'' takes both paths in $\mathcal{A}_l$. As all δ-arcs to the right of the ε''-tail at the top part of $\mathcal{A}_l$ have been eliminated by wave moves, there is an ε'' sub-arc adjacent to the ε''-tail. These two adjacent ε''-arcs intersect α in $\mathcal{A}_r$. Thus we obtain the $[\varepsilon''^-, \varepsilon''^+]$ edge in $\Gamma(\delta', \varepsilon'')$.

We also have the $[\delta'^-, \delta'^+]$ edge: The topmost intersection of the rightmost β segment in $\mathcal{A}_r$ is an intersection with δ'. It is connected by a sub-arc of β to the bottommost arc in $\mathcal{A}_r$ which is also a δ'-arc, giving the required edge. Hence if there is more than one α segment in $\mathcal{A}_l$ then any arc taking the right path in $\mathcal{A}_l$ gives the $[\alpha^-, \alpha^+]$ edge and any arc taking the left path gives the $[\beta^-, \beta^+]$ edge. Since the complexity of the meridional system is greater than four we have a contradiction by Theorem 1.3.10 and (V, W) is not a Heegaard splitting for S^3.

Thus assume that there is a single intersection with α in $\mathcal{A}_l$.

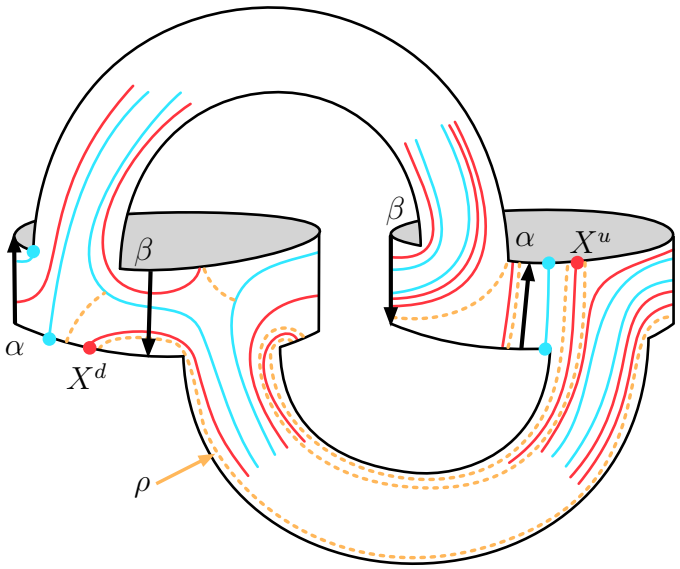

FIGURE 57. The resulting meridian δ' and the shortcut ρ with respect to ε'' for the case that that there is a single δ'-tail connecting to $\partial_+ P$ next to Z^u. If there are more than one δ'-tails the shortcut must pass once between each pair of tails.

In this case there is a shortcut ρ with respect to ε'', depicted in Figure 57. Perform the shortening to obtain a meridian ε'''.

At this point the topmost arc in the left path in $\mathcal{A}_l$ below the tails could either be a δ' arc or an ε''' arc. In any case, there is a wave τ with respect to β depicted in Figure 58. Perform the k wave moves along the τ waves to obtain a meridian β'.

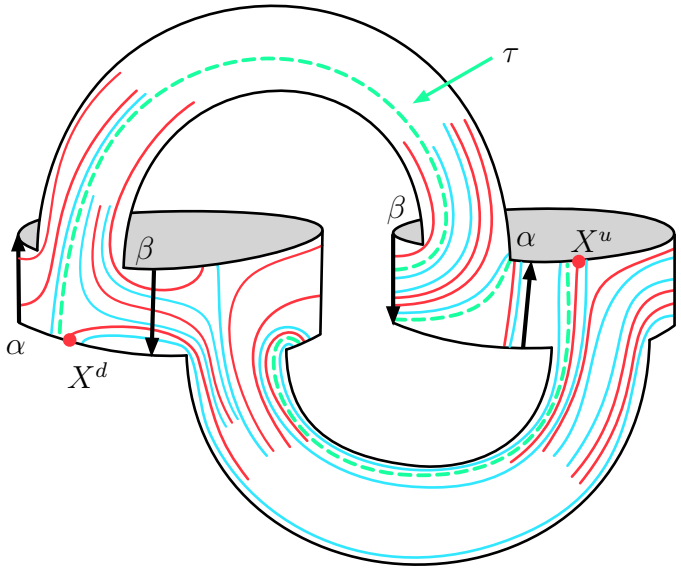

FIGURE 58. The wave τ with respect to β.

The ε'''-head which connects to $\partial_+ P^d$ to the left of X^d intersects β in $\mathcal{A}_r$ just below the top endpoint of τ cannot emanate from Z^u: If it does then ε''' is composed of this arc connecting Z^u to X^d and the shortcut ρ (depicted in Figure 57). Neither of these arcs intersect α in contradiction to Lemma 1.3.3. Note that if δ' has many heads meeting $\partial_+ P$ around Z^u the shortcut ρ will have many intersections with β'. Thus the ε'''-head must come from either the left or right path in $\mathcal{A}_l$.

Assume ε'''-head comes from the right path in $\mathcal{A}_l$. Then the topmost arc in the right path in $\mathcal{A}_l$ is a δ'-arc which meets α there. It continues to $\mathcal{A}_r$ and meets the β segments(s) there below the ε''' head, in a part of β that was thus removed by the τ wave moves. So it does not intersect β' and continues to meet α in $\mathcal{A}_l$. Hence we have the $[\alpha^-, \alpha^+]$ edge.

The leftmost δ'-head ending at Z^u meets β' in $\mathcal{A}_l$ and since it is the bottommost arc in $\mathcal{R}^u$ it meets the top part of β in $\mathcal{A}_r$ which survives the τ wave move so it also meets β' in $\mathcal{A}_r$ and gives the $[\beta'^-, \beta'^+]$ edge.

Note that the ε'''-head in Figure 58 ending at X^d which arrives from $\mathcal{R}^d$ has opposite orientations compared to the other ε'''-arcs intersecting β'. Note also that ε''' is tight since there is an intersection of β' with δ' on both sides of the intersection of this ε'''-head and β'. The β' segment in $\mathcal{A}_l$ contains both the $[\delta'^-, \varepsilon'''^+]$ and the $[\delta'^+, \varepsilon'''^+]$ edges.

So in this case we have all necessary blocking edges in $\Gamma(\alpha, \beta')$ and $\Gamma(\delta', \varepsilon''')$. Since the complexity of the meridional systems is greater than four we have a contradiction by Theorem 1.3.10 and (V, W) is not a Heegaard splitting for S^3.

Assume the ε'''-head arrives from the left path in $\mathcal{A}_r$. It passes through $\mathcal{A}_l$ and then meets $\partial_+ P$ next to X^d. In this case we have perform exactly $k+1$ wave moves along τ to obtain β'. Denote the number of δ'-tails emanating to the left of Z^u plus the δ'-tail emanating from X^u by x. (The number of tails to the left of X^d including is also equal to x.) Tracing the ε'''-head backwards from its endpoint to the left X^d into $\mathcal{R}^u$, denote the number of times it passes in $\mathcal{A}_r$ before it takes the right path in $\mathcal{A}_l$ for the first time and meets α by y. (It cannot connect to Z^u before it meets α.)

Now there are three cases: (1) $x < y$, (2) $x > y$ and (3) $x = y$

(1) $x < y$: We perform another wave move on β' along a wave η depicted in Figure 59. The η wave is an elongation of the τ wave. The wave τ removes the last intersection point of the ε'''-head with β in $\mathcal{A}_r$. Thus the η-wave removes the next intersection point (when tracing the ε'''-head backwards) with the rightmost β segment in $\mathcal{A}_r$. At the same time the η wave move eliminates the top part of the β segment in $\mathcal{A}_l$. This segment includes the intersection of the topmost δ'-tail, which turn right at Z^u, and the intersection with the ε'''-tail adjacent to it, if it exists (it exist when there is another δ' tail emanating from Z^u). If there is only one δ'-tail intersecting β' to begin with, there is no ε''' above it, and the wave η is shifted left on the right side of X^d as shown in Figure 60.

If $y > x+1$ we perform $x(k+1)$ τ wave moves. The wave moves result in a meridian β'' which does not intersect the δ'-tails, neither in $\mathcal{A}_l$ nor in $\mathcal{A}_r$. When $y = x+1$ we perform $x(k+1) - 1$ τ wave moves. When there is one δ'-tail left still intersecting the modified β', the elongation of the wave η is shifted left on the right side of X^d as above.

Next, if the topmost arc that is not a tail in the left path in $\mathcal{A}_l$ is a δ' arc, we further shorten δ' along the shortcut ζ depicted in Figure 61 and parallel ζ shortenings if they exist. The shortening results in a meridian δ'', so that the topmost arc in the left path in $\mathcal{A}_l$ that is not a tail is a ε''' arc: The s δ' arcs from the bottom of the right path in $\mathcal{A}_l$ all continue through $\mathcal{R}^d$, $\mathcal{A}_r$ and $\mathcal{R}^u$, until they arrive at the top of the left path in $\mathcal{A}_l$, where one of them connects to $\partial_+ P$ near Z^u. Thus there are $s-1$ δ' arcs in the top of the left path in $\mathcal{A}_l$, and these arcs all are removed by the wave move. Hence after the shortening the topmost arc in the left path in $\mathcal{A}_l$ that is not a tail is a ε''' arc.

Now there is a full system of blocking edges:

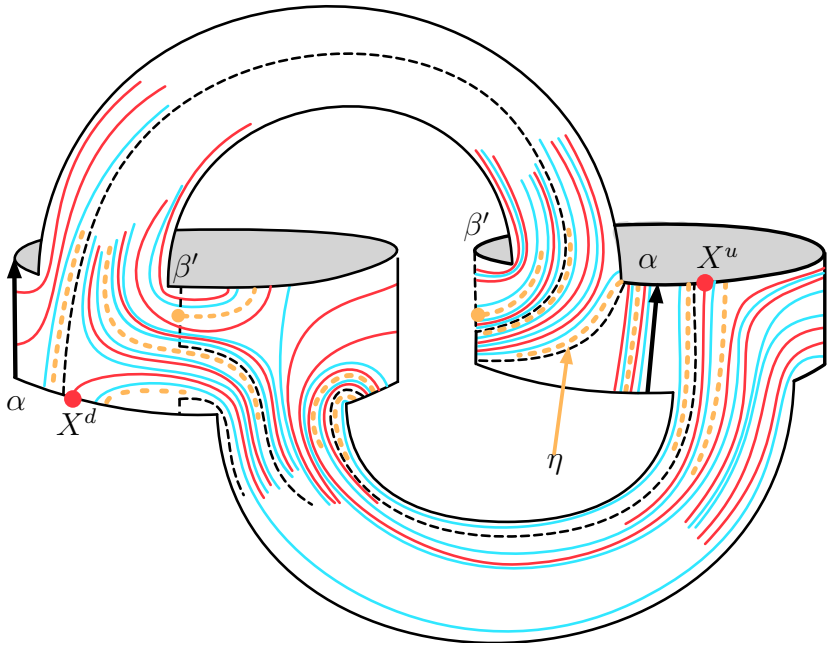

FIGURE 59. The wave η (the dotted curve), with respect to β' (dashed) in the case of more than one δ'-tail in $\mathcal{A}_l$. η connects to β' above the lowermost δ'- head.

Since $x < y$, ε'''-head still intersects β'' in $\mathcal{A}_r$ (If $y = x + 1$ the last η was shifted to the left and will meet β' in $\mathcal{A}_r$ below the ε'''-head). The ε'''-head is adjacent to another ε''' arcs on its left. Their intersection points with β are also intersection points with β''. Because they meet β below the tails arriving from $\mathcal{A}_l$ and above the endpoint of last 'η' wave (see Figure 60). This yields the $[\varepsilon'''^-, \varepsilon'''^+]$ edge. The $[\delta'^-, \delta'^+]$ or $[\delta''^-, \delta''^+]$ edge is given by the fact that the topmost and the bottommost intersections along the α segment in $\mathcal{A}_l$ are intersections with either δ' or δ'', (these intersection are with δ'-tails which are not removed by that shortening.) and α does not have intersections with δ' or ε''' in $\mathcal{A}_r$. So we have blocking edges in $\Gamma(\delta', \varepsilon''')$ or $\Gamma(\delta'', \varepsilon''')$.

If $y > x+1$ the bottommost arc in the right path in $\mathcal{A}_l$ is a δ' or δ'' arc that intersects α, continues through the δ'-tails in $\mathcal{R}^u$, that do not intersect β'', then continues through the top part of $\mathcal{R}^d$, meets X^u, continues from X^d as the bottommost arc in $\mathcal{R}^d$, and then the topmost arc in $\mathcal{R}^u$, all the while not intersecting β'', and meets β again in $\mathcal{A}_l$, yielding the $[\alpha^-, \alpha^+]$ edge. When $y = x + 1$ the bottommost arc in the right path in$\mathcal{A}_l$ is a δ' or δ'' arc. Tracing this arc backwards from its intersection with α does not meet β'' (the intersection are below the intersection of the ε'''-head). This arc continues parallel to the ε'''-head and when the ε'''-head takes the the right path in $\mathcal{A}_l$ so does the arc and meets α. Thus giving the $[\alpha^-, \alpha^+]$ edge in this case as well.

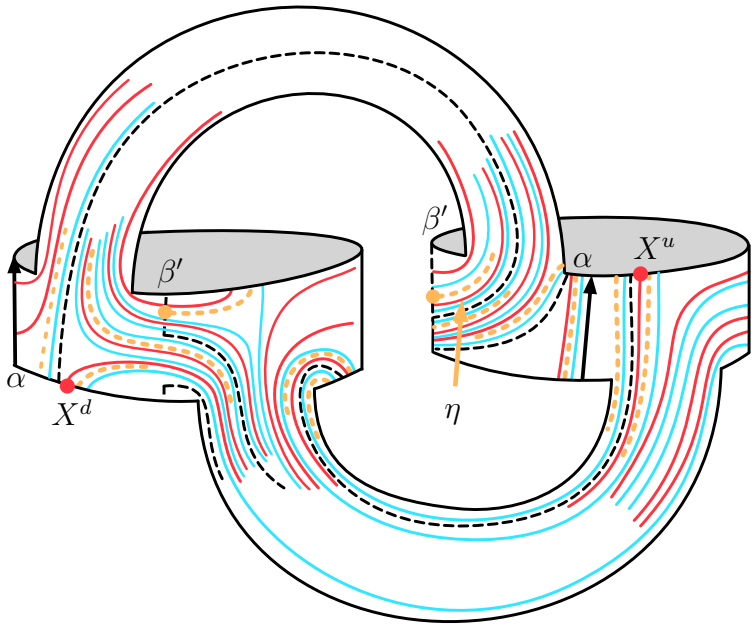

FIGURE 60. The wave η (the dotted curve), with respect to β' (dashed), in the case of only one δ-tail in $\mathcal{A}_l$. Note some of the dashed arcs are actually several parallel arcs of β', as every wave move performed adds an arc parallel to each previous wave.

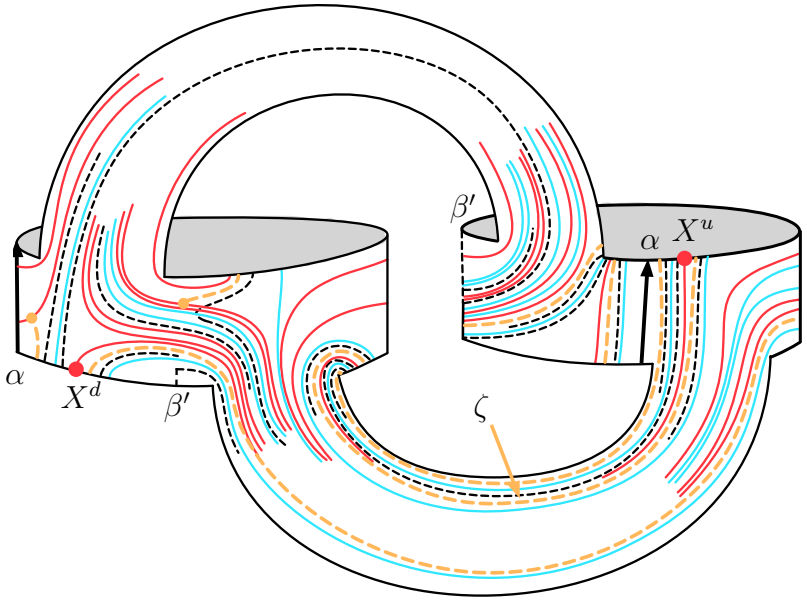

FIGURE 61. The shortcut ζ with respect to δ', given by connecting the thick arrows through the tails.

The $[\beta''^-, \beta''^+]$ edge is given by the ε'''-arc to the right of the ε'''-tail emanating downwards from Z^u: Its intersection with β' in $\mathcal{A}_l$ is not removed by the wave moves. Tracing it backwards it intersects β'' again in $\mathcal{A}_r$ as it is below all δ'-tails. So we have blocking edges in $\Gamma(\alpha, \beta'')$. Since the complexity of the meridional systems is greater than four we have a contradiction by Theorem 1.3.10 and (V, W) is not a Heegaard splitting for S^3.

(2) $x > y$: The wave moves have eliminated all intersections of ε'''-head and β on way to obtaining β'', however there are still intersections of δ'-tails with β''.

Tracing ε''' backwards starting at the ε'''-head in $\mathcal{A}_l$, it continues not meeting β'', until meets α^- in $\mathcal{A}_l$. Starting at the same ε'''-head and tracing ε''' forwards, it continues through ε'''-tails it meets β''^- at some point. This yields the $[\alpha^-, \beta''^-]$ edge. The bottommost δ'-arc in $\mathcal{A}_l$ connects α^- to β''^+ (in $\mathcal{A}_r$) giving the $[\alpha^-, \beta''^+]$ edge. Thus we have the blocking edges in $\Gamma(\alpha, \beta'')$.

The meridian ε''' intersects α, by Lemma 1.3.3 and the topmost arc in $\mathcal{A}_l$ is a δ' arc. Hence α contains a sub-arc connecting δ'^- to ε'''^+ giving the $[\delta^-, \varepsilon'''^+]$ edge. Since there is least one intersection between β'' with the ε'''-tails and above it there is an intersection between β'' and a δ'-tail, β'' contains a sub-arc connecting δ'^+ to ε'''^+. (As the ε'''^+-tails and δ'-tails meet α'' with opposite orientations.) The intersection of ε''' and β'' is tight as between any two such intersection points with opposite orientations there is and intersection point of β'' with δ'. We thus have the $[\delta'^+, \varepsilon'''^+]$ edge. So we have blocking edges in $\Gamma(\delta', \varepsilon''')$ as well. Since the complexity of the meridional systems is greater than four we have a contradiction by Theorem 1.3.10 and (V, W) is not a Heegaard splitting for S^3.

(3) $x = y$: Perform the wave moves as before. In this case the τ and η wave moves, with respect to β, remove all intersections with the tails, except a single intersection with the bottommost δ'-tail (on the leftmost β segment in $\mathcal{A}_r$).

If the topmost arc in the left path in $\mathcal{A}_l$ is a δ' arc perform the shortening of δ' as in Figure 61. This shortening is done, say r times, until the topmost arc in the left path in $\mathcal{A}_l$ is an ε''' arc. There are now two adjacent ε'''-arcs starting at Z^u and continuing into $\mathcal{R}_d$. It follows that the bottommost arc in the left path in $\mathcal{A}_l$ is an ε''' arc as well, as this is the only point at which these two arcs can split. Tracing back the ε'''-head and the ε''' arc adjacent to it on the left, the two arcs wind x times through $\mathcal{R}_u$, $\mathcal{A}_r$ and $\mathcal{R}^d$. After that they both turn to the right path in $\mathcal{A}_l$ (they cannot split as the topmost arc in the right path is a δ'' arc, as it is the continuation of the δ tail) and meet α there.

Therefore, the $[\varepsilon'''^-, \varepsilon'''^+]$ edge is given by a sub-arc of α. The $[\delta''^-, \delta''^+]$ edge is also given by a sub-arc of α, as the topmost and bottommost arcs intersecting α in $\mathcal{A}_l$ are δ'' arcs (or δ' if we did not shorten δ'). Thus we have a pair of blocking edges in $\Gamma(\delta', \varepsilon''')$ or $\Gamma(\delta'', \varepsilon''')$.

Consider the topmost arc, which is a δ'' arc, in the right path in $\mathcal{A}_l$. It spirals, parallel to ε'''-head, as in Figure 62, through parts of β that have been removed, until it reaches α again. This yields the $[\beta^-, \beta^+]$ edge.

Next, consider the topmost arc in the left path in $\mathcal{A}_l$. It passes immediately beneath the ε''' and δ' or δ'' tails. Thus its intersection with β in $\mathcal{A}_l$ has not been removed by the wave moves and this arc intersects β'' there. Tracing the same arc backwards into $\mathcal{A}_r$, it again passes immediately beneath all tails and thus intersects β'' in $\mathcal{A}_r$ as well. This yields the $[\beta''^-, \beta''^+]$ edge. Thus we have the blocking edges in $\Gamma(\alpha, \beta'')$. Since the complexity of the meridional systems is greater than four we have a contradiction by Theorem 1.3.10 and (V, W) is not a Heegaard splitting for S^3.

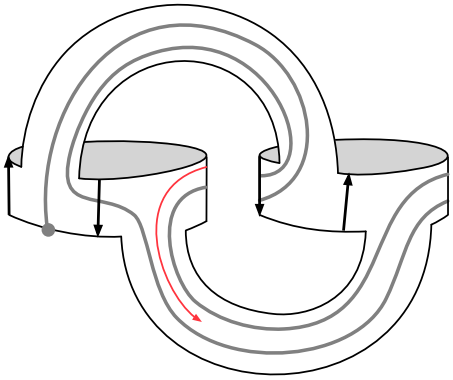

FIGURE 62. Each intersection of the topmost δ' (or δ'') arc in $\mathcal{A}_l$ with β is below an intersection with ε'''-head.

As none of the options (i), (ii) or (iii) can occur, the proof is complete. □

Lemma 3.3.3. *If K is not a Berge knot then the Heegaard splitting $\{V, W\}$ cannot be a Heegaard splitting of S^3 when the curve δ takes a single path in $\mathcal{A}_r$ and two paths in $\mathcal{A}_l$ and when ε takes a long path in $\mathcal{A}_r$.*

Proof. As before $\varepsilon = m\varepsilon_1 + n\varepsilon_2$, see Lemma 3.1.4. In this case the wave ω will be along the arc ω as depicted in Figure 63. This specific arc is convenient as the resulting meridian is tight.

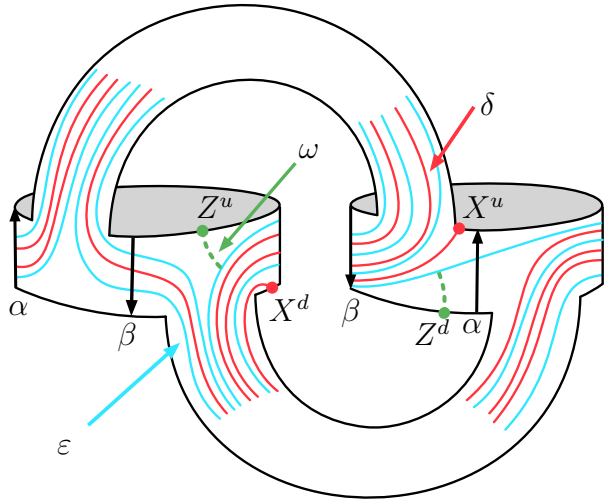

FIGURE 63. The wave ω with resect to ε.

Case (a): $m = n = 1$. In this case there is a wave η depicted in Figure 64 with respect to δ intersecting $\partial_+ P$ once. This a contradiction to the minimality of δ, see Proposition 1.3.14. So this case cannot happen.

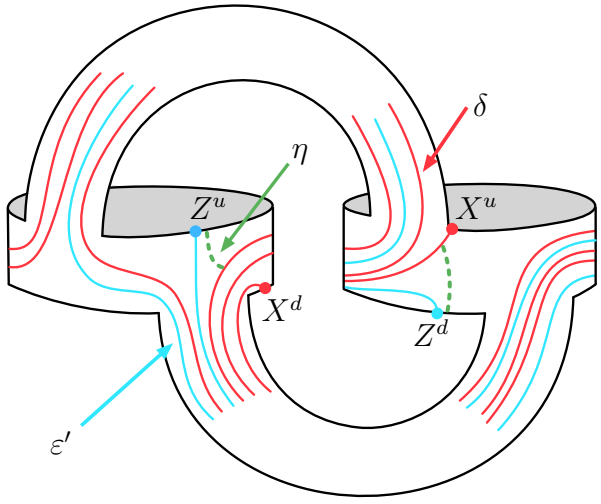

FIGURE 64. The shortcut η with resect to δ in the case $m = n = 1$.

Case (b): $m > n$. In this case after the ω wave moves on ε there are still ε_1-arcs in ε'. Thus ε' has a sub-arc connecting α^+ to β^+, see Figure 63, giving the $[\alpha^+, \beta^+]$ edge. Any arc taking the right path in $\mathcal{A}_l$ connects α^- in $\mathcal{A}_l$ to β^+ in $\mathcal{A}_r$, giving the $[\alpha^-, \beta^+]$ edge. Thus we have blocking edges in $\Gamma(\alpha, \beta)$.

After the wave moves the bottommost arc in $\mathcal{A}_l$ is a δ arc. Thus α will connect δ^- in $\mathcal{A}_l$ to ε'^-, giving the $[\delta^-, \varepsilon'^-]$ edge. There is a β segment in $\mathcal{A}_l$ which connects δ^+ to ε'^-, giving the $[\delta^+, \varepsilon'^-]$ edge. Thus we have blocking edges in $\Gamma(\delta, \varepsilon')$. Since the complexity of the meridional systems is greater than four we have a contradiction by Theorem 1.3.10 and (V, W) is not a Heegaard splitting for S^3.

Case (c): $m < n$. In this case there is an additional wave ρ with respect to ε', depicted in Figure 65. The wave ρ connects the $n - m$ arcs of type ε_2, that remain after the ω wave moves, which connect the ε_2 sub-arcs to the ε_1 sub-arcs (see Figure 64), with the m tails in $\mathcal{A}_r$ that were created by the ω wave moves. Denote the resulting meridional curve by ε''.

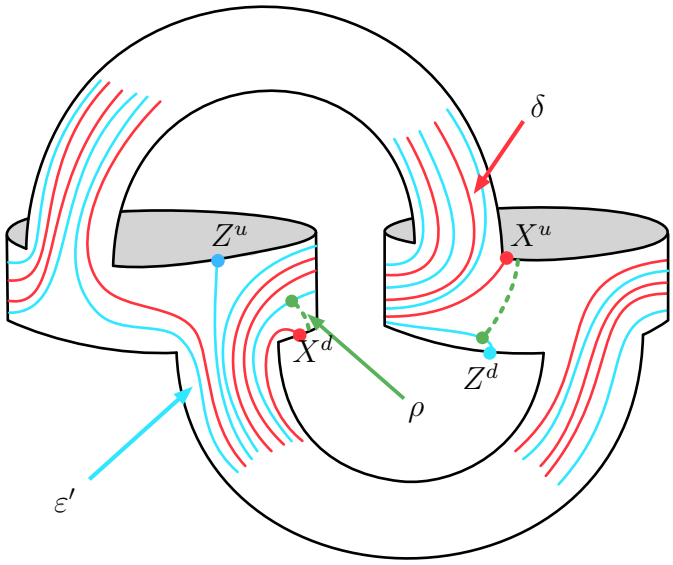

FIGURE 65. The shortcut ρ with resect to ε' in the case $m < n$.

$n > 2m$: In this case ε'' contains no tail ending at Z^d. We perform a wave move with respect to β, along the wave τ depicted in Figure 66. There exists another wave parallel to τ as long as all arcs meeting β in the sub-segment removed by the previous τ wave move arrive from the same β segment (parallel to each other). Perform all such wave moves and denote the resulting meridional curve by β'.

We now have blocking edges with respect to both sides: All the sub-arcs of ε'' and δ' which meet β along the part of the β segment in $\mathcal{A}_r$, removed by the first τ wave move, arrive from α^-. This includes the ε'' heads emanating from Z^u, as when tracing them backwards they continue to vertical segments in $\mathcal{A}_r$ which then emerge in $\mathcal{A}_l$ to the right of X^d and meet α^-. By our assumption we have performed the wave moves until some of the above sub-arcs do not meet the same β segment. The only way these

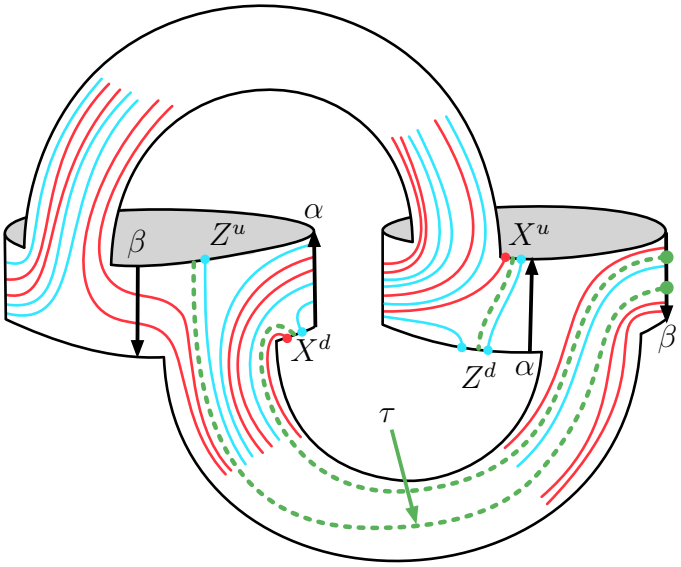

FIGURE 66. The shortcut τ with resect to β in the case $n > 2m$.

sub-arcs can become non-parallel (so some of them do not meet β) is if they split into two paths in $\mathcal{A}_l$, or if some of them connect to $\partial_+ P$. In order to connect to $\partial_+ P$ a ε'' sub-arc must meet α first. A δ sub-arc which meets $\partial_+ P$ is the δ head connecting to X^u. If this δ head met the sub-segment removed from β by τ, there are also ε'' such sub-arcs taking the right path in $\mathcal{A}_l$ and these meet α. This is because the rightmost arc in the segment removed by τ is an ε'' sub-arc. Thus there is at least one arc which met the removed β segment which now continues to meet α again. Such an arc gives rise to the $[\alpha^-, \alpha^+]$ edge. The intersections of the topmost δ sub-arc in the right path in $\mathcal{A}_r$ with β was not removed by the wave moves, and neither was its next intersection with β in $\mathcal{A}_r$ or $\mathcal{A}_l$. This yields the $[\beta'^-, \beta'^+]$ edge. Thus we have blocking edges in $\Gamma(\alpha, \beta')$.

The topmost intersection along the β segment in $\mathcal{A}_l$ and the bottom intersection along the rightmost β segment in $\mathcal{A}_r$ are both intersections with δ. Neither were removed by the τ wave moves and thus there is a sub-arc of β' connecting these two intersection points and yielding the $[\delta^-, \delta^+]$ edge. There are at least two ε'' arcs intersecting the bottom part of the α segment in $\mathcal{A}_l$m which give the $[\varepsilon''^-, \varepsilon''^+]$ edge. Thus we have the blocking edges in $\Gamma(\delta, \varepsilon'')$. Since the complexity of the meridional systems is greater than four we have a contradiction by Theorem 1.3.10 and (V, W) is not a Heegaard splitting for S^3.

$\underline{n < 2m}$: In this case there is a wave τ with respect to β, depicted in Figure 67. The bottom endpoint of τ lies between the intersections of the leftmost β segment in $\mathcal{A}_l$

with the ε'' tails emanating from Z^u. Let x denote the number of ε''-tails at the bottom of $\mathcal{R}^d$ connecting to Z^d in $\mathcal{A}_l$. The ω wave moves create m such ε'-tails and the ρ wave moves turn $n-m$ such ε'-tails into vertical segments. Hence $x = 2m-n$. Let y denote the number of ε''-tails connecting to the right of X^d in $\mathcal{A}_l$ these were created by doing wave moves on ρ so $y = n-m$. The wave τ has x tails below it and y tails above it in $\mathcal{R}^d$.

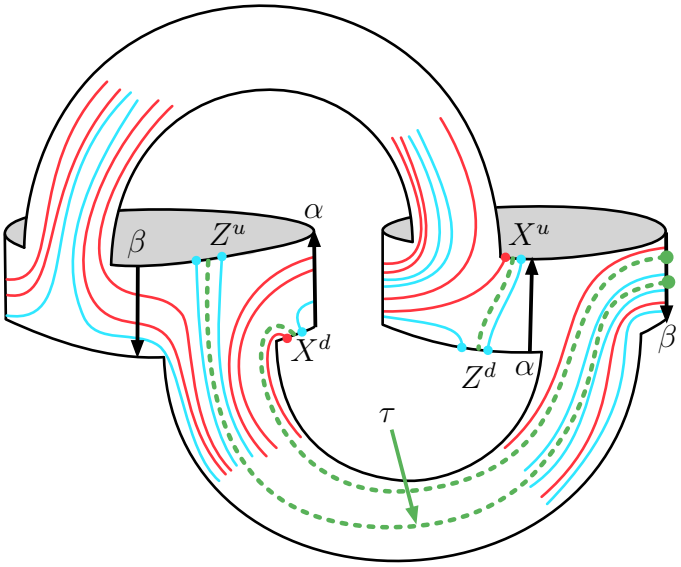

FIGURE 67. The shortcut τ with resect to β in the case $n < 2m$.

$(*)$ If $y > x$, or if the adjacent ε'' tails emanating from Z^u meet α before they split in two different directions in $\mathcal{A}_l$ we have blocking edges with respect to V and W:

All ε''-tails emanating from Z^u to the right of τ, have all their intersection points with β removed by the τ wave moves. At least one of these tails continues to meet α^+ by the assumption (If the tails reach the splitting point, only x out of these y ε'' tails continue to meet β in $\mathcal{A}_l$. The rest $y-x$ tails turn to the right and meet α there). When tracing this tail backwards from Z^u it continues through a vertical segment in $\mathcal{A}_r$ and emanates from X^d, turning right to meet α^-. This gives the $[\alpha^-, \alpha^+]$ edge. The $[\beta'^-, \beta'^+]$ edge is given as before by the δ-tail, which continues through the topmost intersections with the β segments in $\mathcal{A}_r$ and $\mathcal{A}_l$, which have not been removed. Thus we have all blocking edges in $\Gamma(\alpha, \beta')$.

Since $y > x$ there are $y > 1$ intersections with ε'' along the bottom part of the α segment in $\mathcal{A}_l$. This yields the $[\varepsilon''^-, \varepsilon''^+]$ edge. The bottom part of each β segment, including the intersections with the ε''-tails and the δ-arcs directly above them, has not been removed. The topmost arc in $\mathcal{R}^u$ is a δ-arc and tracing it backwards from the

β segment in $\mathcal{A}_l$ it becomes adjacent to the δ-head, and both arcs meet the rightmost β segment in $\mathcal{A}_r$ in the bottom part of the segment which was not removed. This β segment gives the $[\delta^-, \delta^+]$ edge. Thus we have the blocking edges in $\Gamma(\delta, \varepsilon'')$. Since the complexity of the meridional systems is greater than four we have a contradiction by Theorem 1.3.10 and (V, W) is not a Heegaard splitting for S^3.

$(**)$ Assume $x > y$ and that the adjacent ε'' tails emanating from Z^u do *not* meet α before they split in two different directions in $\mathcal{A}_l$. In this case the last $k+1$ (k is the number of α segments in $\mathcal{A}_r$) τ wave move are elongation of τ with their bottom endpoint between the x ε'' tails. So the wave moves remove the bottom part of the β segments in $\mathcal{A}_l$ and $\mathcal{A}_r$.

Suppose there are at least two δ sub-arcs taking the right path in $\mathcal{A}_l$. These arcs start on α and continue through the parts that have been removed from β, until the topmost one of them connects to X^u. There is at least one additional such arc adjacent to it which continues at the top of $\mathcal{R}^u$. This arc turns right in $\mathcal{A}_l$ and meets α again. This gives the $[\alpha^-, \alpha^+]$ edge. The $[\beta'^-, \beta'^+]$ edge is given by the δ-tail, which continues to connect the topmost intersections with the β segments in $\mathcal{A}_r$ and $\mathcal{A}_l$, (which have not been removed). Thus we have all blocking edges in $\Gamma(\alpha, \beta')$.

Below the bottom endpoint of τ on the β segment in $\mathcal{A}_r$ there are $x \geq 2$ intersections of β with ε''. These intersections are not removed by the τ wave move. As subsequent τ waves connect to the β segments with a δ intersection above their top endpoint, these intersection point are not removed. Thus, there is a sub-arc of β' yielding the $[\varepsilon''^-, \varepsilon''^+]$ edge.The sub-arcs of δ intersecting α are all adjacent, as ε'' intersects only the bottom part of α. This α segment yields the $[\delta^-, \delta^+]$ edge. Thus we have the blocking edges in $\Gamma(\delta, \varepsilon'')$. Since the complexity of the meridional systems is greater than four we have a contradiction by Theorem 1.3.10 and (V, W) is not a Heegaard splitting for S^3.

Suppose there is a single δ sub-arc taking the right path in $\mathcal{A}_l$. In this case $|\delta \cap \alpha| = 1$ which is a contradiction by Lemma 1.3.3.

$(***)$ Assume $x = y$ and that the adjacent ε'' tails emanating from Z^u do *not* meet α before they split in two different directions in $\mathcal{A}_l$. As $\gcd(m, n) = 1$, $x = 2m - n$ and $y = n - m$ it follows that $\gcd(x, y) = 1$ as well. Note this implies $x = 1$ and $y = 1$. There is a *shortcut* ρ with respect to δ as in Figure 68. One endpoint of ρ connects to the bottommost δ segment in the right path in $\mathcal{A}_l$ above X^d. It has a ε''-tail to its right and a δ-tail to its left. So the wave move results in a meridian continuing left from the endpoint of ρ, into $\mathcal{R}^d$ (as its other side is isotopic to ε''). Note that ρ does not intersect α and thus the shortening in ρ removes at least one intersection of δ with α.

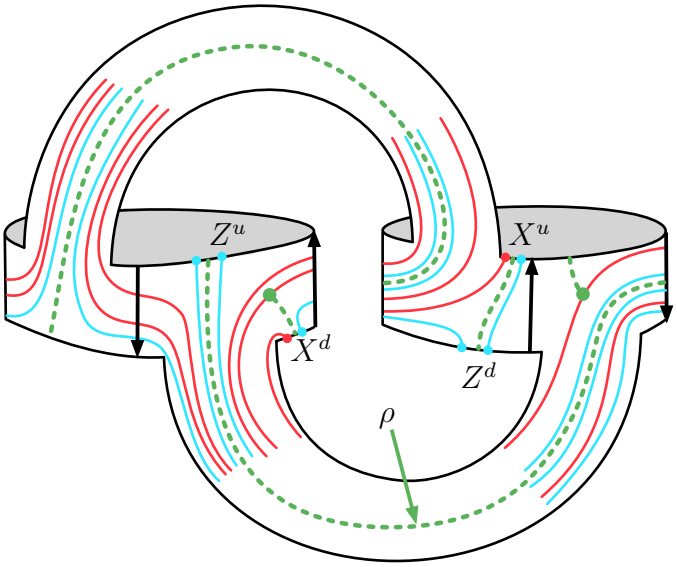

FIGURE 68. The shortcut ρ with resect to δ in the case $n < 2m$ and $x = y$.

The other endpoint of ρ is on the topmost δ sub-arc in $\mathcal{A}_r$. Suppose there are s δ-arcs taking the right path in $\mathcal{A}_l$. All these arcs, together with the δ-tail, become the $s+1$ adjacent arcs at the top of $\mathcal{A}_r$. The part of δ removed by a ρ wave move, starting at the top of $\mathcal{A}_r$ is on the bottom of $\mathcal{R}^u$ and after taking the left path in $\mathcal{A}_r$ is on the right of ε'' through all its length. Thus, none of the other s arcs have been affected by the wave move. Hence after we perform s wave moves along ρ we obtain a meridian δ' that does not intersect α. This is a contradiction to Lemma 1.3.3.

$\underline{n = 2m}$: This implies $m = 1$ and $n = 2$. The curve ε' in this case has one tail reaching Z^d and one ε_2 arc. The curve ε'' has neither ε_2 arcs nor tails reaching Z^d, and is depicted in Figure 69.

There is a wave ρ with respect to δ. By the same consideration as above, we perform s ρ wave moves, where s is the number of δ arcs taking the right path in $\mathcal{A}_l$, and reach a meridian δ' that does not intersect α. This is again a contradiction to Lemma 1.3.3. □

3.4. One path in $\mathcal{A}_l$ and one path in $\mathcal{A}_r$

In this section we rule out the last remaining case namely when δ takes only two paths one path in $\mathcal{A}_l$ and one path in $\mathcal{A}_r$.

Lemma 3.4.1. *If K is not a Berge knot then (V, W) is not a Heegaard splitting of S^3 when the curve δ takes two paths, one in each annulus $\mathcal{A}_r$ and $\mathcal{A}_l$.*

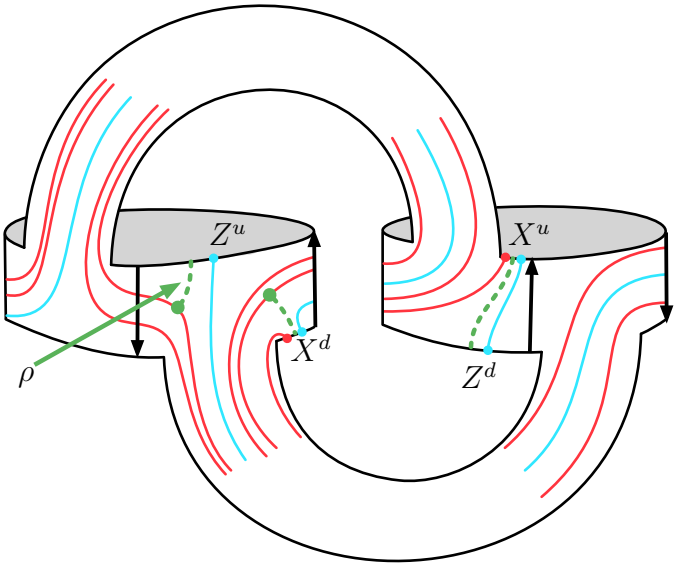

FIGURE 69. The shortcut ρ with resect to δ in the case $n = 2m$.

Proof. Assume in contradiction that δ takes one path in $\mathcal{A}_l$ and one in $\mathcal{A}_r$.

By Lemma 3.1.1 both paths are short. By the symmetries in Remark 2.2.1 we can assume that δ takes a right short path in $\mathcal{A}_r$. The segments of the meridians in $\widehat{V}$ which intersect right path in $\mathcal{A}_r$ and the left path in $\mathcal{A}_l$ all belong to the same meridian as P is admissible, by Lemma 2.4.5. If δ takes the left short path in $\mathcal{A}_l$ δ does not intersect the other meridian in contradiction to Lemma 1.3.3.

If the δ head is the leftmost arc in $\mathcal{R}^d$, the point X^d is located between W_{ll} and W_{lr} (as in Lemma 2.4.5). It follows that the δ tail must turn right and is the rightmost arc in $\mathcal{R}^d$ (as otherwise the tail must connect to X^u without going through $\mathcal{R}^u$). This implies that δ takes the left path in $\mathcal{A}_r$ which is ruled out in the above paragraph.

Assume therefore that the δ head is the rightmost arc in $\mathcal{R}^d$ (and ε takes a long path in $\mathcal{A}_r$, see Figure 70), and that δ takes the right short path in $\mathcal{A}_l$. Let r denote the number of α segments in $\mathcal{A}_r$, and l denote the number of α segments in $\mathcal{A}_l$.

If $r > l$ then the location of X^d (which is r segments to the left of Y^d) will be contained in $\mathcal{A}_r$. In this case there is a sub-arc of α (The meridian to the right of X^u and X^d intersects δ less times than the meridian on their left so it must be α) connecting δ^- to itself and intersecting $\partial_+ P$ once (to the left of Y^u). If this α segment does not intersect ε we have a contradiction to Proposition 1.3.14 (2). If it does intersect ε choose an innermost such segment. If it intersects ε with conflicting orientations then we have wave moves with respect to ε. After performing all such wave moves we can assume assume that all intersections points with ε are consistently oriented. Hence this

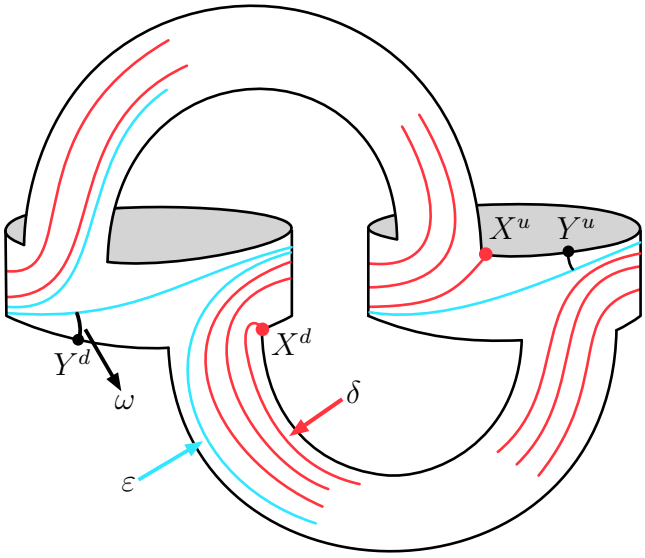

FIGURE 70. The configuration of δ and ε when ε takes a long path through $\mathcal{A}_l$, and the wave ω with respect to ε.

segment gives the $[\delta^-, \varepsilon^+]$ and $[\delta^-, \varepsilon^-]$ edges in $\Gamma(\delta, \varepsilon)$. The δ-tail connects α^+ to β^+ in $\mathcal{A}_r$ giving the $[\alpha^+, \beta^+]$ edge. The $[\alpha^+, \beta^-]$ edge is obtained by the continuation of the δ-tail connecting β^- in $\mathcal{A}_r$ to α^+ in $\mathcal{A}_l$, giving the blocking edges in $\Gamma(\alpha, \beta)$. Since the complexity of the meridional systems is greater than four we have a contradiction by Theorem 1.3.10 and (V, W) is not a Heegaard splitting for S^3.

Thus we can assume that $r \leq l$.There are now two cases depending on whether ε takes a long path in $\mathcal{A}_l$ or two short paths.

Assume first ε takes a long path through $\mathcal{A}_l$ as well as through $\mathcal{A}_r$ as in Figure 70. Let n be the number of ε_2 arcs and m the number of ε_1 arcs as in Figure 34 (ii). There is wave ω with respect to εwhich is depicted in Figure 70. After performing each of the first $\min\{m, n\}$ ω wave moves, the resulting curve is not tight. The intersection of ε^i, the modified ε at the i-th iteration, with $\partial_+ P$ (located at the intersection of ω and $\partial_+ P$) must be slid to the right, passing r segments of $\widehat{V}$ to reach the corner of $\mathcal{R}^u$ and $\mathcal{A}_r$. The next wave moves (existing if $m > n$) result in a tight curve. Denote the resulting curve by ε'.

If $r < l$ then after all the ω wave moves and the tightening there are sub-arcs of ε' intersecting a $\widehat{V}$ segment in $\mathcal{A}_l$ with opposite orientations. Now the exact same argument as for $r > l$ results in blocking edges with respect to both sides and (V, W) is not a Heegaard splitting for S^3.

Therefore we may assume $r = l$. This implies that $r = l = 1$ and P is standard as explained in the proof of Lemma reflem:SoLong in the paragraph just above Case (1).

In this case there is a closed curve κ that does not intersect δ, depicted in Figure 71. The curve κ is exactly the curve depicted in Figures 49 and 50 and the knot K and the curve κ co-bound an annulus. Hence as in the proof of ii(a)$(*)$ in Case(c) of Lemma 3.3.1, K can be isotoped to the curve $\kappa \subset \Sigma$, which does not intersect δ. There is a wave η with respect to β, also depicted in Figure 71. The wave move results in a meridian $B' \subset V$ intersecting $\delta = \partial D$ in a single point. So we can isotope κ across D to remove the intersections $\kappa \cap \beta$. Attaching the disk D to V along $\partial D = \delta$ results in a solid torus so that κ is embedded in its boundary. Attaching D to V equivalent to reducing the Heegaard splitting (V, W) of S^3 by the reducing pair (B', D) so we obtain a genus one Heegaard splitting of S^3. Thus κ is embedded in a standardly embedded torus in S^3 and K is a torus knot. Thus K is on the Berge list.

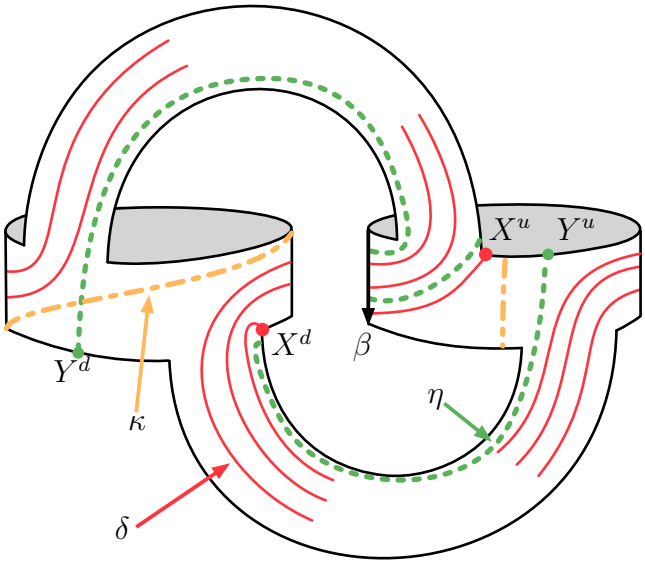

FIGURE 71. The wave η with respect to β and the closed curve κ.

Finally, assume ε takes the two short paths through $\mathcal{A}_l$. Let n be the number of ε_2 arcs and m the number of ε_1 arcs as in Figure 34 (i). The wave ω in this case is depicted in Figure 72.

The wave ω has one endpoint on the topmost arc of the $m + n$ ε sub-arcs crossing α from left to right in $\mathcal{A}_r$, and its other endpoint is on the bottommost arc of the n sub-arcs of type ε_2 in the right path in in $\mathcal{A}_l$. Thus, there are n possible ω wave moves and there are $m \geq 1$ sub-arcs still crossing α from left to right in the resulting meridian ε'.

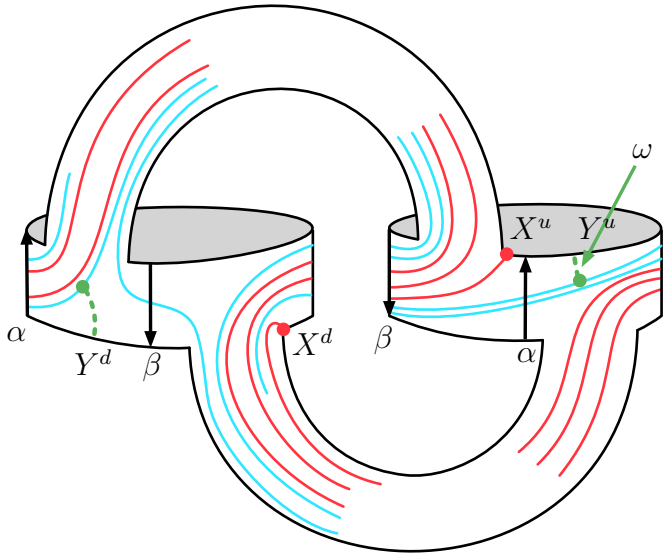

FIGURE 72. The configuration of δ and ε when ε takes two short paths through $\mathcal{A}_l$, and the wave ω with respect to ε.

Any one arc of these m sub-arcs connects α^+ to β^+ in $\mathcal{A}_r$ giving the $[\alpha^+, \beta^+]$ edge. Any sub-arc of δ connects β^- in $\mathcal{A}_r$ to α^+ in $\mathcal{A}_l$ giving the $[\alpha^+, \beta^-]$ edge. Thus we have the blocking edges in $\Gamma(\alpha, \beta)$. The α segment in $\mathcal{A}_r$ connects ε'^- to δ^- as there are no ε_2 sub-arcs in ε'. There is a sub-arc of β in $\mathcal{A}_r$ connecting ε'^- to δ^+. We thus have both blocking edges $[\delta^+, \varepsilon'^-,]$ and $[\delta^-, \varepsilon'^-]$ in $\Gamma(\delta, \varepsilon')$. Since the complexity of the meridional systems is greater than four we have a contradiction by Theorem 1.3.10 and (V, W) is not a Heegaard splitting for S^3. □

3.5. The Proof

Proposition 3.5.1. *The Heegaard splitting $\{V, W\}$ cannot be a Heegaard splitting of S^3 unless K is either a Berge knot or a $(1, 1)$ knot.*

Proof. We start with the meridian systems $\widehat{V}$, chosen in Lemma 2.5.3, and $\widehat{W} = \{\delta, \varepsilon'\}$, chosen in 3.1.4, for the Heegaard diagram. By Lemma 3.1.5 the statement of the proposition holds when δ takes all paths, by Lemma 3.2.1 and 3.3.1 it holds for a δ curve that takes exactly three paths and by Lemma 3.4.1 it holds for a δ that takes only two paths i.e., a single path in each of $\mathcal{A}_r$ and $\mathcal{A}_l$. □

Proof of Theorem 0.0.4. If K is a non-hyperbolic knot then it is known by [17], [5], [25] and [27], that it is a Berge knot. If $K \subset S^3$ is a hyperbolic tunnel number one knot

$S^3 \setminus \mathcal{N}(K)$ has a genus two Heegaard splitting (U, W) with $\partial(S^3 \setminus \mathcal{N}(K)) \subset U$ and Heegaard surface Σ. Let V be the handlebody obtained by ∞-Dehn surgery on K so (V, W) is a Heegaard splitting for S^3. Since K admits an integer surgery which results in a Lens space, the Heegaard splitting (V, W) contains a (P_N, D) reducing pair.

If $N = 1$ then P_N is an annulus and by Proposition 1.1.7 the knot K is doubly primitive and we are done. Assume therefore, that $N \geq 2$. By Theorem 2.4.3 the planar surface P_N is admissible so we can apply Proposition 3.5.1 to show that this can happen only if K is either a $(1, 1)$ knot, or it is on the Berge list. If K is a Berge knot then K^* is a $(1, 1)$ knot in the lens space and the proof is complete. □

References

[1] K. Baker, E. Grigsby, M. Hedden, *Grid diagrams for lens spaces and combinatorial knot Floer homology*, Int. Math. Res. Not. IMRN, (10):Art. ID rnm024, 39, 2008.

[2] K. Baker, C. Gordon, J. Luecke, *Bridge number, Heegaard genus and non integral Dehn surgery*, Trans. Amer. Math. Soc. 367 , no. 8, (2015), 5753 - 5830. arXiv:1202.0263v1 [math:GT]

[3] J. Berge, *Some knots with surgeries yielding lens spaces*, Unpublished manuscript (1990).

[4] J. Berge, *The simple closed curves in genus two Heegaard surfaces of S^3 which are double-primitives*, Unpublished manuscript, 2010.

[5] S. Bleiler, R. Litherland, *Lens spaces and Dehn surgery*, Proc. Amer. Math. Soc. 107 (1989), 1127 - 1131.

[6] F. Bonahon, J.P. Otal, *Scindements de Heegaard des espaces lenticulaire's*, Ann. Sci. Ec. Norm. Super. 16 (1983), 451 - 466 .

[7] R. S. Bowman, S. Taylor, A. Zupan, *Bridge Spectra of Twisted Torus Knots*, Int. Math. Res. Notices 16 (2015), 7336-7356.

[8] M. Culler, C. Gordon, J. Luecke, P. Shalen, *Dehn surgery on knots*, Annals of Mathematics 125 (1987), 237 - 300.

[9] D. Gabai, *Foliations and topology of 3-manifolds III*, J. Diff. Geom. 26 (1987), 479 - 536.

[10] D. Gabai, *Surgery on Knots in Solid tori*, Topology Vol. 28, No.1, (1989), 1 - 6.

[11] J. Greene, *The lens space realization problem*, Annals of Mathematics, vol. 177, no. 2, (2013), 449 - 511.

[12] C. Gordon, *Dehn Filling: a Survey*, Knot Theory, Banach Center Publications Vol 42, Warsaw (1998), 129 - 144.

[13] C. Gordon, J. Luecke, *Knots are determined by their complements*, J. Amer. Math. Soc. 2 (1989), 371 - 415.

[14] T. Homma, M. Ochiai, M, Takahashi *An algorithm for recognizing S^3 in manifolds with Heegaard splitting of genus two*, Osaka J. Math. 17 (1980), 625 - 648.

[15] R. C. Kirby, *Problems in Low Dimensional Topology,*
Geometric topology (Athens, GA, 1993), (R Kirby, editor), AMS/IP Stud. Adv. Math. 2, Amer. Math. Soc., Providence, RI (1997), 35 - 473.

[16] K. Morimoto, M. Sakuma, *On unknotting tunnels for knots.*
Math. Ann.289, (1991) 143 - 167.

[17] L. Moser, *Elementary surgery along a torus knot*,
Pacific J. Math. 38 (1971), 737 - 745.

[18] M. Ochiai, *Heegaard-Diagrams and Whitehead-Graphs*,
Math. Sem. Notes of Kobe Univ. 7 (1979), 573 - 590.

[19] P. Ozsvath, Z. Szabo, *On knot Floer homology and lens space surgeries*,
Topology,44(6) (2005). 1281 - 1300.

[20] J. Rasmussen, *Lens space surgeries and L-space homology spheres*,
arXiv:0710.2531, 2007.

[21] T. Saito, *A note on lens space surgeries: orders of fundamental groups versus Seifert genera*,
J. Knot Theory Ramifications 20 (2011), no. 4, 617 - 624. arXiv:0907.2554v1 [math.GT]

[22] M. Tange, *Lens spaces given from L-space homology 3-spheres*,
Experiment. Math., 18(3) (2009), 285 - 301.

[23] M. Tange, *A complete list of lens spaces constructed by Dehn surgery I*,
arXiv:1005.3512, (2010).

[24] W. Thurston, *The Geometry and Topology of Three-Manifolds*,
1980 Princeton lecture notes on geometric structures on 3-manifolds.

[25] S. Wang, *Cyclic surgery on knots*,
Proc. Amer. Math. Soc. 107 (1989), 1091 - 1094.

[26] M. Williams, *Lens space surgeries & primitive/Seifert type constructions*,
arXivv 0713.1797 v1 [math.GT] 2007.

[27] Y. Q. Wu, *Cyclic surgery and satellite knots*,
Topology Appl. 36 (1990), 205 - 208.

Department of Mathematics, Technion, Haifa, 32000 Israel
E-mail address: ymoriah@tx.technion.ac.il

Department of Mathematics, Tata Institute for Fundamental Research, Mumbai, India
E-mail address: tali@math.tifr.res.in